On some Variational Principles in Discrete Differential Geometry

Jan Techter

January 15, 2015

Masterarbeit im Studiengang
Mathematik

zur Erlangung des akademischen Grades
Master of Science

eingereicht an der
TU Berlin

Erstgutachter:	**Prof. Dr. Alexander I. Bobenko**
Zweitgutachter:	**Prof. Dr. Boris Springborn**

Abstract

The focus lies on introducing some exemplary variational principles in discrete differential geometry. We characterize some specific discrete objects as critical points of a suitable functional. The work is intended to be suitable as an introductory text to the topics at hand. Most sections are preceded by a condensed version of the corresponding smooth theory, which is presented in a way fitting the following discretization scheme.

The first part treats discrete curves.
After introducing discrete curves with emphasis on discrete arc length parametrized curves, we discuss some notions of discrete curvature from osculating circles. The focus of the first part lies on discrete elastica. We explain the characterization of smooth and discrete elastic curves

- as critical points of a bending energy
- by the corresponding Euler-Lagrange equations
- in terms of the evolution under the Heisenberg flow

as well as the Kirchhoff analogy. After discussing the generalization to isotropic elastic rods in the smooth case, we state the idea of the corresponding discretization.
On the way we introduce the discrete tangent flow, the discrete Heisenberg flow and the quaternionic description of Euclidean motions, rotating frames and the Lagrange top.

The second part treats discrete surfaces.
We introduce the notion of discrete surfaces from the point of view of topology (abstract discrete surfaces), metric geometry (piecewise flat surfaces) and Euclidean geometry (polyhedral surfaces). We introduce the discrete cotan Laplace operator of a simplicial surface and more general of a geodesic triangulation of a piecewise flat surface as coming in a natural way from considering the Dirichlet energy of piecewise affine functions.
A proof for the characterization of Delaunay triangulations of a piecewise flat surface in terms of a local edge property is given. This implies an angle criterion identical to the planar case. We show how to construct the Delaunay tessellation of a piecewise flat surface by means of an edge-flip algorithm from any given start triangulation. The intrinsic notion of the Delaunay triangulation enables us to define the discrete Laplace-Beltrami operator of a piecewise flat surface.
For both discrete Laplace operators of a simplicial surface –the extrinsic cotan Laplace operator and the intrinsic Laplace-Beltrami operator– we discuss discrete minimal surfaces as an application. Both notions come with a construction algorithm.

In the appendix we discuss the Heisenberg magnet model as an example of a physical system involving the Heisenberg flow.

German Abstract

Der Fokus der Arbeit liegt auf der Beschreibung einiger examplarischer Variationsprinzipien in der diskreten Differentialgeometrie. Wir charakterisieren bestimmte diskrete Objekte als kritische Punkte eines geeigneten Funktionals. Die Arbeit soll dabei als einführender Text in die behandelten Themen geeignet sein. Den meisten Kapiteln geht eine komprimierte Version der entsprechenden glatten Theorie veraus, die auf die darauffolgende Diskretisierung zugeschnitten ist.

Der erste Abschnitt behandelt diskrete Kurven.
Nach Einführung diskreter Kurven, mit Schwerpunkt auf diskreten nach Bogenlänge parametrisierten Kurven, werden mehrere Möglichkeiten der Definition von oskulierenden Kreisen behandelt, die jeweils zu verschiedenen diskreten Krümmungen führen. Im Zentrum des ersten Abschnittes stehen diskrete Elastika. Wir beschreiben die Charakterisierung von glatten und diskreten elastischen Kurven

- als kritische Punkte einer Biegeenergie
- durch die entsprechenden Euler-Lagrange-Gleichungen
- durch die Evolution unter dem Heisenberg-Fluss

sowie die Kirchhoff-Analogie. Nach der Behandlung von glatten elastischen Stäben wird die Idee einer entsprechenden Diskretisierung genannt. Auf dem Weg werden der diskrete Tangential-Fluss, der diskrete Heiseberg-Fluss und die quaternionische Beschreibung Euklidischer Bewegungen, rotierender Rahmen und dem Lagrange-Kreisel eingeführt.

Der zweite Abschnitt behandelt diskrete Flächen.
Wir betrachten diskrete Fächen vom Standpunkt der Topologie (abstrakte diskrete Flächen), der metrischen Geometrie (stückweise flache Flächen) und der Euklidischen Geometrie (polyedrische Flächen). Die Dirichlet-Energie von stückweise affinen Funktionen auf einer siplizialen Fläche und allgemeiner auf einer geodätischen Triangulierung einer stückweise flachen Fläche führt zur Definition des diskreten cotan Laplace-Operators.
Wir führen einen Beweis zur Charakterisiering von Delaunay-Triangulierungen einer stückweise flachen Fläche mit Hilfe einer lokalen Kanten-Eigenschaft. Dies impliziert ein Winkelkriterium, das identisch zum planaren Fall ist. Wir zeigen wie man die Delaunay-Tesselierung einer stückweise flachen Fläche mit Hilfe eines Kanten-Flip-Algorithmus aus einer beliebigen Start-Triangulierung erzeugen kann. Die intrinsische Natur der Delaunay-Tesselierung ermöglicht die Definition eines diskreten Laplace-Beltrami-Operators einer stückweise flachen Fläche.
Als Anwendung beider diskreter Laplace-Operatoren einer simplizialen Fläche (dem extrinsischen cotan Laplace-Operator und dem intrinsischen Laplace-Beltrami-Operator) besprechen wir Definitionen von diskreten Minimalflächen und zugehörige Konstruktionsalgorithmen.

Im Anhang findet sich eine Besprechung des Heisenberg-Magnet-Modells als Beispiel eines physikalischen Systems, das den Heisenberg-Fluss enthält.

Hiermit erkläre ich, dass ich die vorliegende Arbeit selbstständig und eigenhändig sowie ohne unerlaubte fremde Hilfe und ausschließlich unter Verwendung der aufgeführten Quellen und Hilfsmittel angefertigt habe.

Berlin, den .....

General References

This thesis comprises topics based on the lecture *Geometry 2* held by Alexander Bobenko in the Sommersemester 2014 at TU Berlin. All chapters are partially based on [Bob14] as well as personal communication with Alexander Bobenko and Boris Springborn. Additionally the following references considerably influenced this work:

- Part I is partially based on oral and hand-written lore from previous similar lectures held by Alexander Bobenko and Boris Springborn. Some influence might also be found in [Hof08].
- Section 3.4 has been influenced by the chapter on rigid bodies in [Arn89].
- Section 4.2 has been influenced by discussing the topic with Thilo Rörig and Lara Skuppin as well as reading [FW99].
- The construction in Section 7.2 of the Delaunay tessellation from the Voronoi tessellation on a piecewise flat surface contains ideas from [MS91].
- Section 7.3 contains additional notions from [BS07].
- The continuous Heisenberg chain in Section A is introduced from a naive discrete model as in [Tur81] and further discussed following [FT87].

Contents

Part I
Discrete Curves

1 Curves and curvature

1.1 Basic definitions

Definition 1.1 (smooth curves)**.** Let $I \subset \mathbb{R}$ be a finite or infinite interval. Then a *smooth curve* in $\mathbb{R}^N$ is a map

$$\gamma : I \to \mathbb{R}^N$$

such that all derivatives γ', γ'',... exist.
The *length* of a smooth curve γ is defined by

$$L(\gamma) \coloneqq \int_I \|\gamma'(x)\| \, \mathrm{d}x.$$

γ is called *regular* if $\|\gamma'(x)\| > 0$ for all $x \in I$.
For a regular curve γ the (unit) *tangent vector* at $x \in I$ is defined by

$$T(x) \coloneqq \frac{\gamma'(x)}{\|\gamma'(x)\|}.$$

γ is called *arc length parametrized* if $\|\gamma'(x)\| = 1$ for all $x \in I$.

Remark 1.1.

- Any arc length parametrized curve is regular and any regular curve can be parametrized by arc length. We usually denote the arc length parameter of a curve by s.
- The length of an arc length parametrized curve is given by $L(\gamma) = |I|$.
- We defined curves as 'parametrized curves'. But we are also interested in quantities that are invariant under reparametrization and Euclidean transformations, i.e. well-defined on equivalence classes representing the 'shape of a curve'.

Definition 1.2 (discrete curves)**.** Let $I \subset \mathbb{Z}$ be a finite or infinite interval. Then a *discrete curve* in $\mathbb{R}^N$ is a map

$$\gamma : I \to \mathbb{R}^N.$$

For a discrete curve γ we define the *vertex difference vector* at the edge $(k, k+1)$ with $k, k+1 \in I$ by

$$\Delta\gamma_k \coloneqq \gamma_{k+1} - \gamma_k,$$

and its *length* by

$$L(\gamma) \coloneqq \sum_{k,k+1 \in I} \|\gamma_{k+1} - \gamma_k\| .$$

If any two successive points of γ are different, i.e. $\|\Delta\gamma_k\| > 0$ we can define the (unit) *tangent vector* at the edge $(k, k+1)$ with $k, k+1 \in I$ by

$$T_k := \frac{\gamma_{k+1} - \gamma_k}{\|\gamma_{k+1} - \gamma_k\|}.$$

We further define

$$\begin{aligned} \gamma \textit{ regular} &:\Leftrightarrow \text{ any three successive points } \gamma_{k-1}, \gamma_k, \gamma_{k+1} \\ &\quad\ \text{ are different for all } k-1, k, k+1 \in I \\ \gamma \textit{ arc length parametrized} &:\Leftrightarrow \|\gamma_{k+1} - \gamma_k\| = 1 \text{ for all } k \in I \end{aligned}$$

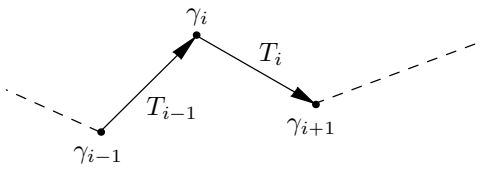

Figure 1.1. Part of a discrete arc length parametrized curve.

Remark 1.2.

- The vertex difference vectors $\Delta\gamma_k$ and tangent vectors T_k are naturally defined on edges rather than vertices despite the notation.
- For a discrete arc length parametrized curve γ the tangent and vertex difference vectors coincide

  $$T_k = \Delta\gamma_k = \gamma_{k+1} - \gamma_k.$$

  It is regular if and only if two successive tangent vectors T_{k-1} and T_k are not anti-parallel.
- The definition of regularity is more than is needed to define edge tangent vectors. But we will see that it allows to have a well defined discrete tangent flow at vertices as well.
- For plane curves it will be sometimes convenient to identify $\mathbb{R}^2 \cong \mathbb{C}$ and for space curves $\mathbb{R}^3 \cong \mathrm{Im}\mathbb{H}$

1.2 On the smooth limit

Consider a discrete curve $\gamma : \mathbb{Z} \to \mathbb{R}^N$. To obtain a continuous limit we introduce a small parameter $\varepsilon > 0$ and replace the lattice $\mathbb{Z}$ by

$$\mathcal{B}^\varepsilon := \varepsilon\mathbb{Z}$$

for $\varepsilon > 0$ and $\mathcal{B}^0 := \mathbb{R}$. So the discrete curve is replaced by a family

$$\gamma^\varepsilon : \mathcal{B}^\varepsilon \to \mathbb{R}^N.$$

In the limit $\varepsilon \to 0$ the vertices $\varepsilon k \in \varepsilon\mathbb{Z}$ become points $x \in \mathbb{R}$.[1]

We will not concern ourselves with the question of convergence of the curve itself but are more interested whether we can recover the smooth quantities –like tangent vectors and arc length– from the corresponding discrete definitions. Suppose that γ^ε possesses a smooth limit

$$\gamma^\varepsilon \to \gamma \quad (\varepsilon \to 0).$$

or alternatively start with the smooth curve and define the family of discrete curves by sampling. Then we can investigate how properties from the discrete case transfer to the smooth case in the following way:

- Take some local discrete quantity depending on some vertex $k \in \mathbb{Z}$ and its neighbors.
- Replace $k \in \mathbb{Z}$ by a point $x \in \mathbb{R}$, $k-1$ by $x-\varepsilon$, $k+1$ by $x+\varepsilon$, ...
- Investigate the limit $\varepsilon \to 0$, e.g. by applying Taylor's theorem at $\varepsilon = 0$.

The discrete unit tangent vectors $T_k = \frac{\gamma_{k+1}-\gamma_k}{\|\gamma_{k+1}-\gamma_k\|}$ become smooth unit tangent vectors $T = \frac{\gamma'(x)}{\|\gamma'(x)\|}$:

$$\begin{aligned} T_k &= \frac{\gamma(x+\varepsilon)-\gamma(x)}{\|\gamma(x+\varepsilon)-\gamma(x)\|} = \frac{\gamma'(x)\varepsilon + o(\varepsilon)}{\|\gamma'(x)\varepsilon + o(\varepsilon)\|} \\ &= \frac{\gamma'(x)+o(1)}{\|\gamma'(x)\|+o(1)} \to \frac{\gamma'(x)}{\|\gamma'(x)\|}. \end{aligned}$$

If we consider the (non-unit) vertex differences $\Delta\gamma_k = \gamma_{k+1} - \gamma_k$ we have to scale appropriately to obtain the tangent vector $\gamma'(x)$ in the limit. Indeed

$$\frac{1}{\varepsilon}(\gamma_{k+1}-\gamma_k) = \frac{1}{\varepsilon}(\gamma'(x)\varepsilon + o(\varepsilon)) \to \gamma'(x).$$

Starting with a discrete arc length parametrized curve for $\varepsilon = 1$, i.e. $\|\Delta\gamma_k\| = 1$, we take all curves of the family γ^ε to have vertex differences of constant length, i.e. $\|\Delta\gamma^\varepsilon_{\varepsilon k}\| = \varepsilon$ for all $\varepsilon > 0$, $k \in \mathbb{Z}$. Then the smooth limit is also arc length parametrized:

$$\|\gamma'(x)\| \leftarrow \frac{1}{\varepsilon}\|\gamma_{k+1}-\gamma_k\| = \frac{\varepsilon}{\varepsilon} = 1.$$

In the arc length parametrized case the tangent vectors T_k are equal to the vertex differences $\Delta\gamma_k$. But while scaling down the lattice size by ε we get

$$T_k = \frac{\Delta\gamma_k}{\varepsilon},$$

due to the normalization of T_k.

[1] Depending on the situation it might be more convenient to consider a refinement of the lattice, like $\frac{1}{2^k}\mathbb{Z}$. The procedure described above is convenient for the investigation of local properties around 0.

Let us investigate sum and difference of two neighboring tangent vectors T_k and T_{k-1} in the smooth limit. In this limit the angle between the vectors tends to 0.

$$\begin{aligned}
T_k + T_{k-1} &= \frac{1}{\varepsilon}(\Delta\gamma_k + \Delta\gamma_{k-1}) \\
&= \frac{1}{\varepsilon}(\gamma(x+\varepsilon) - \gamma(x-\varepsilon)) \\
&= \frac{1}{\varepsilon}(\gamma(x) + \varepsilon\gamma'(x) - \gamma(x) + \varepsilon\gamma'(x) + o(\varepsilon)) \\
&= 2\gamma'(x) + o(1). \\
T_k - T_{k-1} &= \frac{1}{\varepsilon}(\Delta\gamma_k - \Delta\gamma_{k-1}) \\
&= \frac{1}{\varepsilon}(\gamma(x+\varepsilon) - 2\gamma(x) + \gamma(x-\varepsilon)) \\
&= \frac{1}{\varepsilon}\left(\varepsilon\gamma'(x) + \frac{1}{2}\varepsilon^2\gamma''(x) - \varepsilon\gamma'(x) + \frac{1}{2}\varepsilon^2\gamma''(x) + o(\varepsilon^2)\right) \\
&= \varepsilon\gamma''(x) + o(\varepsilon).
\end{aligned}$$

So to approximate the second derivative of the curve we have to scale the difference of the tangent vectors by $\frac{1}{\varepsilon}$.

1.3 Discrete curvature from osculating circles

Definition 1.3 (curvature of smooth curves)**.** Let $\gamma : I \to \mathbb{R}^N$ be a smooth curve parametrized by arc length. Then the curvature of γ at $s \in I$ is

$$\kappa(s) \coloneqq \left\|\gamma''(s)\right\|.$$

This definition extends to any smooth regular curve upon reparametrization by arc length.

Remark 1.3.

- The *osculating circle* at $s \in I$ is the unique circle best approximating γ at $\gamma(s)$. It can for example be obtained
  - as the arc length parametrized circle through $\gamma(s)$ agreeing with γ up to second order.
  - by a limiting procedure of circles through three distinct points on γ going to $\gamma(s)$.
  - as the circle among all tangent circles at $\gamma(s)$ for which the distance to γ in normal direction decays the least.

  Let $R(s) > 0$ be the radius of the osculating circle. Then the curvature of γ at $s \in I$ is the reciprocal
  $$\kappa(s) = \frac{1}{R(s)}.$$
- If $\gamma''(s) \neq 0$ the osculating circle lies in the *osculating plane* which is the plane spanned by $\gamma'(s)$ and $\gamma''(s)$.
  If $\gamma''(s) = 0$ it degenerates to a line and $\kappa(s) = 0$.

- Let $\gamma : I \to \mathbb{R}^2$ be a plane curve parametrized by arc length. Then we can define a signed curvature $\kappa_\pm(s)$ of γ at $s \in I$ by

$$T'(s) = \kappa_\pm(s)N(s),$$

where $T(s) = \gamma'(s)$ and $N(s) \coloneqq iT(s)$ is $T(s)$ rotated by $\frac{\pi}{2}$.

We consider three possibilities of defining osculating circles in the discrete case leading to different notions of discrete curvature. Let $\gamma : I \to \mathbb{R}^N$ be a discrete curve. We define

$$\varphi_k \coloneqq \measuredangle(\Delta\gamma_k, \Delta\gamma_{k-1}) = \measuredangle(T_k, T_{k-1}) \in [0, \pi].$$

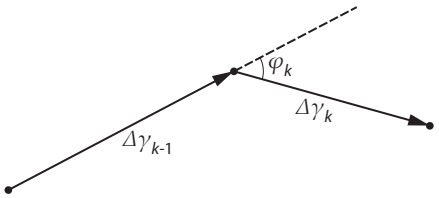

Figure 1.2. Turning angle at a vertex of a discrete curve.

For planar curves $\gamma : I \to \mathbb{R}^2$ we can define the angle φ_k to be in $[-\pi, \pi]$.

1.3.1 Vertex osculating circle

Definition 1.4 (vertex osculating circle)**.** The *vertex osculating circle* at a vertex k is the circle through γ_k and its two neighbors γ_{k-1} and γ_{k+1}.

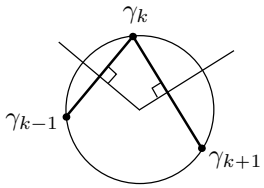

Figure 1.3. Vertex osculating circle as the circle through three neighboring vertices.

Its center is given by the intersection of the two bisecting lines of the adjacent difference vectors $\Delta\gamma_k$ and $\Delta\gamma_{k-1}$. The radius is given by $\|\gamma_{k+1} - \gamma_{k-1}\| = 2R_k \sin\varphi_k$ which leads to the curvature

$$\kappa_k = \frac{2\sin\varphi_k}{\|\gamma_{k+1} - \gamma_{k-1}\|}.$$

Note that for planar curves with $\varphi_k \in [-\pi, \pi]$ this leads to a signed curvature where the sign corresponds to the expected behavior from the smooth case.

Remark 1.4. For discrete arc length parametrized curves we find

- $T_k - T_{k-1}$ is perpendicular to the circle at γ_k. So $T_k + T_{k-1}$ is tangent to the vertex osculating circle.
- The curvature is bounded from above by 2 since the radius of the vertex osculating circle is always greater than $\frac{1}{2}$ in this case.

1.3.2 Edge osculating circle

The edge osculating circle can only be defined for planar curves since we need any three consecutive edges to be planar.

Definition 1.5 (edge osculating circle)**.** Let γ be a planar discrete curve. Then the *edge osculating circle* of γ at the edge $(k, k+1)$ is the oriented circle which touches the lines through the three successive edges $\Delta\gamma_{k-1}$, $\Delta\gamma_k$ and $\Delta\gamma_{k+1}$ such that the orientation of the circle at the touching points matches the orientation of the lines (which are oriented by the direction of the corresponding edges).

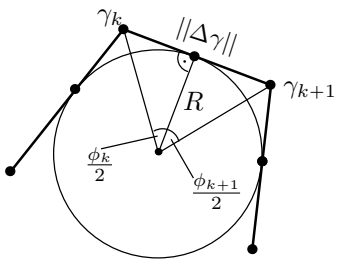

Figure 1.4. Edge osculating circle as the circle touching three consecutive edges.

The edge osculating circle is uniquely determined as long as the three consecutive edges are of different directions. Even if the curve is non-convex.

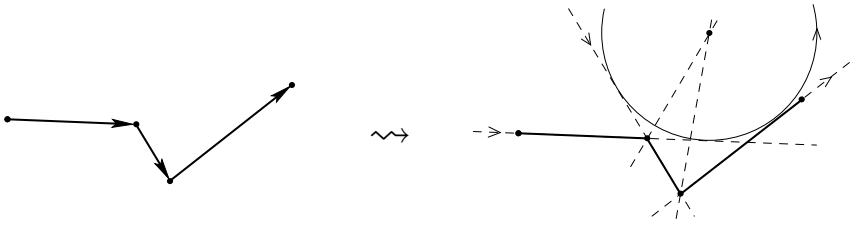

Figure 1.5. Edge osculating circle for a non-convex discrete curve.

Its center is the intersection of the two angular bisectors of the three consecutive edges. The radius is given by $\|\Delta\gamma_k\| = R_k(\tan\frac{\varphi_k}{2} + \tan\frac{\varphi_{k+1}}{2})$. This leads to the curvature

$$\kappa_k = \frac{\tan\frac{\varphi_k}{2} + \tan\frac{\varphi_{k+1}}{2}}{\|\Delta\gamma_k\|}.$$

It is unbounded from above even for arc length parametrized curves but has the disadvantages of being not as local as the previous definition,[2] while only being applicable to planar curves.

1.3.3 Osculating circle for arc length parametrized curves

For arc length parametrized discrete curves we can achieve the locality of the first and the unboundedness of the second definition by taking the circle touching two consecutive edges in their midpoints. This works in any dimension.

Definition 1.6 (osculating circle for arclength parametrized curves)**.** Let $\gamma : I \to \mathbb{R}^N$ be a discrete arc length parametrized curve. Then we define the *osculating circle* at vertex k to be the circle touching the two edges T_{k-1} and T_k in its midpoints.

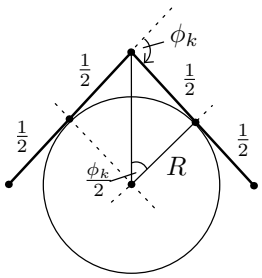

Figure 1.6. Osculating circle for a discrete arc length parametrized curve.

The center is given by the intersection of the bisecting lines of the two edges while we find for the radius $2R_k \tan \frac{\varphi_k}{2} = 1$ which leads to the following definition of curvature

$$\kappa_k = 2 \tan \frac{\varphi_k}{2}. \tag{1.1}$$

Note that it is zero at straight vertices and goes to infinity at non-regular vertices.

[2] It is defined at edges while depending on the neighboring edges which makes it involve a total of four consecutive points.

2 Flows on curves

2.1 Flows on smooth curves

2.1.1 Local geometric flows

We want to describe the motion of a curve $\gamma : I \to \mathbb{R}^N$ in space by applying some vector field v. In general v might depend on the whole curve, i.e. be some vector field on some domain in the space of curves. If v depends only locally on γ, i.e. only on a small neighborhood at each point of the curve, we call the generated flow a *local flow*. This is the case if the evolution process of γ under the flow generated by v can be described by a differential equation

$$\partial_t \gamma = v\left(\gamma, \gamma', \gamma'', \dots\right). \tag{2.1}$$

A one-parameter family of curves

$$\gamma : I \times J \to \mathbb{R}^N$$

which is a solution of (2.1) in the sense that

$$\partial_t \gamma(s,t) = v\left(\gamma(s,t), \gamma'(s,t), \gamma''(s,t), \dots\right) =: v(s,t)$$

for all $(s,t) \in I \times J$ is called the *evolution of the curve* $\gamma_0(s) = \gamma(s,0)$ under the flow given by v.
For this particular initial curve γ_0 the vector field v becomes a one-parameter family of vector fields along the parametrization

$$v : I \times J \to \mathbb{R}^N$$

and (2.1) becomes

$$\partial_t \gamma(s,t) = v(s,t).$$

The map

$$\Phi : (t, \gamma) \mapsto \Phi_t \gamma,$$

where $\Phi_t \gamma(s) \coloneqq \gamma(s,t)$ is the evolution of γ is called the *curve flow* given by v. Note that in general Φ might not be well defined due to lack of existence and uniqueness of solutions of (2.1) for arbitrary γ_0.

Additionally one might want the flow to be *geometric*, i.e. only depend on the shape of the curve. For this it should be invariant with respect to

- Euclidean motions,[3]
- reparametrization of the curve.

The flow is then well defined on the corresponding equivalence classes of parametrized curves.

Example 2.1 (planar geometric flow)**.** For planar curves these two conditions can be realized by the ansatz:

$$v = v(\kappa, \kappa', \kappa'', \dots) = \alpha(\kappa, \kappa', \kappa'', \dots)T + \beta(\kappa, \kappa', \kappa'', \dots)N. \tag{2.2}$$

[3] Or more general, invariant with respect to the action of some other Lie group.

2.1.2 Arc length preserving flows

Now we restrict our attention to flows that preserve the arc length parametrization, i.e.

$$\partial_t \left\|\gamma'\right\| = 0. \tag{2.3}$$

If we think of the curve as a one-dimensional distribution of mass, (2.3) means that the density along the curve does not change under the action of the flow. In particular the length of the curve is preserved.

Example 2.2 (planar geometric flow preserving arc length)**.** Using the ansatz (2.2) for a planar geometric flow and starting out with an arc length parametrization we obtain

$$\partial_t \gamma' = \alpha' T + \alpha T' + \beta' N + \beta N' = (\alpha' - \kappa\beta)T + (\kappa\alpha + \beta')N,$$

where we used $T' = \kappa N$ and $N' = -\kappa T$. Under this condition (2.3) becomes

$$0 = \frac{1}{2}\partial_t \langle \gamma', \gamma' \rangle = \langle \partial_t \gamma', \gamma' \rangle = \alpha' - \kappa\beta.$$

The solution $\alpha = 1$, $\beta = 0$ leads to the *tangent flow*

$$\partial_t \gamma = T,$$

while $\alpha = \frac{1}{2}\kappa^2$, $\beta = \kappa'$ leads to the *modified Korteweg-deVries flow* (mKdV flow)

$$\partial_t \gamma = \frac{1}{2}\kappa^2 T + \kappa' N.$$

The curvature κ of curves evolving under the mKdV flow changes as

$$\begin{aligned} \partial_t \kappa &= \partial_t \langle T', N \rangle = \langle \partial_t T', N \rangle = (\kappa\alpha + \beta')' \\ &= \frac{3}{2}\kappa^2 \kappa' + \kappa''', \end{aligned}$$

which is the *mKdV equation*.

Example 2.3 (arc length preserving tangent flow)**.** Consider a curve flow on curves in $\mathbb{R}^N$ in tangent direction

$$\partial_t \gamma = \alpha T.$$

Closed curves and infinite curves are invariant with respect to such a flow. In general the flow just induces a reparametrization of the curve. It is arc length preserving if and only if α is constant along the curve at any time, i.e. $\alpha = \alpha(t)$. The normalized version $\alpha = 1$ acts as

$$\Phi_t \gamma(s) = \gamma(t, s) = \gamma(0, s + t) = \gamma(s + t).$$

Example 2.4 (Heisenberg flow)**.** For arc length parametrized curves in $\mathbb{R}^3$ consider the *Heisenberg flow*[4]

$$\partial_t \gamma = \gamma'' \times \gamma'. \tag{2.4}$$

[4]The Heisenberg flow is also known as the *smoke ring flow* or *Hashimoto flow*.

Using a Frenet frame T, N, B we obtain

$$\partial_t \gamma = T' \times T = \kappa N \times T = -\kappa B.$$

So the Heisenberg flow is always acting in binormal direction and is therefore arc length preserving.
The tangent vector evolves under the Heisenberg flow as

$$\partial_t T = (\gamma'' \times \gamma')' = \gamma''' \times \gamma' = T'' \times T.$$

2.2 Flows on discrete arc length parametrized curves

For $I \coloneqq [0, \dots, n] \subset \mathbb{Z}$ finite interval, $I = \mathbb{Z}_n \coloneqq \mathbb{Z}/n\mathbb{Z}$ and $I = \mathbb{Z}$ we define the space

$$\mathcal{C}_I \coloneqq \{\gamma : I \to \mathbb{R}^N\}$$

of finite, finite closed and infinite curves respectively. Note that in the finite case $\mathcal{C}_I \cong (\mathbb{R}^N)^n$. By $\mathcal{C}_I^{\text{reg}}$ and $\mathcal{C}_I^{\text{arc}}$ we denote the corresponding submanifolds of regular and arc length parametrized curves.

A *flow of discrete curves* is given by a vector field

$$v : \mathcal{C}_I \to \mathrm{T}\mathcal{C}_I, \quad \gamma \mapsto v[\gamma] \in \mathrm{T}_\gamma \mathcal{C}_I,$$

or on some submanifold $U \subset \mathcal{C}_I$. In the finite case we have $\mathrm{T}_\gamma \mathcal{C}_I = (\mathbb{R}^N)^n$. So v gives a direction in $\mathbb{R}^N$ at every vertex k which possibly depends on the whole curve γ. We state this relation as

$$v_k[\gamma] \in \mathbb{R}^N.$$

For a given initial curve $\gamma : I \to \mathbb{R}^N$ the vector field v on $\mathcal{C}_I$ becomes a one-parameter family of vector fields along the parametrization of the curve

$$v : I \times J \to \mathbb{R}^N,$$

where $J \subset \mathbb{R}$ is an open interval. The action of the flow leads to a continuous deformation of the curve $\gamma_k = \gamma_k(0)$

$$\gamma : I \times J \to \mathbb{R}^N$$

satisfying

$$\partial_t \gamma_k(t) = v_k(t).$$

In the following we restrict our attention to inner vertices only. The advantage is that we have to define vector fields only on inner vertices. This restriction is realized by examining closed and infinite curves, i.e. $I = \mathbb{Z}_n$ or $I = \mathbb{Z}$.
As in the smooth case we focus on local geometric flows on $\mathcal{C}_I^{\text{arc}}$. In the discrete case we interpret these conditions as follows.

arc length preserving To preserve arc length parametrization, i.e. make γ stay in $\mathcal{C}_I^{\text{arc}}$ the flow must satisfy[5]

$$\begin{aligned} & 0 = \partial_t \left\| \Delta \gamma_k \right\| \\ \Leftrightarrow \; & 0 = \langle \partial_t \Delta \gamma_k, T_k \rangle = \langle \partial_t \gamma_{k+1} - \partial_t \gamma_k, T_k \rangle = \langle v_{k+1} - v_k, T_k \rangle. \end{aligned} \tag{2.5}$$

[5]This means we want the vector field v to be defined on the submanifold $\mathcal{C}_I^{\text{arc}}$ of $\mathcal{C}_I$, i.e. make sure that $v[\gamma] \in \mathrm{T}_\gamma \mathcal{C}_I^{\text{arc}} \subset \mathrm{T}_\gamma \mathcal{C}_I$.

Decomposing the vector field at the vertex k into its parts along the tangent plane $\operatorname{span}\{T_k, T_{k-1}\}$ and its orthogonal complement we see that this only imposes constraints on the former.

local flow By a *local flow* we mean a flow which at every vertex k only depends on the curve at the adjacent vertices[6], i.e. γ_{k-1}, γ_k, γ_{k+1}:

$$v_k[\gamma] = v(\gamma_{k-1}, \gamma_k, \gamma_{k+1}).$$

geometric Since we do not consider reparametrizations in the discrete case a *geometric flow* is a flow which is just invariant with respect to Euclidean transformations, i.e. translations and rotations.
On the level of the vector field this means that for $R \in \mathrm{SO}(N)$, $a \in \mathbb{R}^N$

$$v_k[R\gamma + a] = Rv_k[\gamma].$$

Let us break down these conditions a little bit further in the case of local flows on $\mathcal{C}_I^{\mathrm{arc}}$.

translation invariance For a local flow given by the vector field v translation invariance means that for any $a \in \mathbb{R}^N$

$$v(\gamma_{k-1} + a, \gamma_k + a, \gamma_{k+1} + a) = v(\gamma_{k-1}, \gamma_k, \gamma_{k+1}),$$

which can also be expressed the following way: For any given direction $b \in \mathbb{S}^{N-1}$

$$\frac{\mathrm{d}}{\mathrm{d}\varepsilon}\bigg|_{\varepsilon=0} v(\gamma_{k-1} + \varepsilon b, \gamma_k + \varepsilon b, \gamma_{k+1} + \varepsilon b) = 0.$$

For a flow on $\mathcal{C}_I^{\mathrm{arc}}$ we can rewrite a local vector field to be a function of the form $v_k = v_k(\gamma_k, T_k, T_{k-1})$. For this we get

$$0 = \frac{\mathrm{d}}{\mathrm{d}\varepsilon}\bigg|_{\varepsilon=0} v(\gamma_k + \varepsilon b, T_k, T_{k-1}) = \frac{\partial v_k}{\partial \gamma_k} \cdot b$$

for all $b \in \mathbb{S}^{N-1}$, i.e. v must not explicitly depend on γ_k and therefore be of the form

$$v_k = v(T_k, T_{k-1}). \tag{2.6}$$

rotation invariance For a local translation invariant vector field (2.6) on $\mathcal{C}_I^{\mathrm{arc}}$ this means that for any rotation $R \in \mathrm{SO}(N)$

$$v(RT_k, RT_{k-1}) = Rv(T_k, T_{k-1}).$$

We consider this further in the three dimensional case. At every vertex[7] k we can take $T_k, T_{k-1}, T_k \times T_{k-1}$ as a rotation invariant basis.[8]

[6] By this we mean in particular that v depends on the adjacent vertices "equally" at every vertex.

[7] At least at regular, non-straight vertices.

[8] In this context T_k, T_{k-1} have to be interpreted as vector fields on $\mathcal{C}_I$. The cross product of two rotation invariant vector fields is rotation invariant. So we get three rotation invariant vector fields which define a basis of $\mathrm{T}_\gamma \mathcal{C}_I = (\mathbb{R}^3)^n$ for any curve γ, i.e. a basis of $\mathbb{R}^3$ at every vertex k.
Note that this in general is not an orthonormal basis. Such a basis could be obtained by taking $\frac{T_k+T_{k-1}}{\|T_k+T_{k-1}\|}, \frac{T_k-T_{k-1}}{\|T_k-T_{k-1}\|}, \frac{T_k\times T_{k-1}}{\|T_k\times T_{k-1}\|}$.

Expressing v in this basis we get

$$v_k(T_k, T_{k-1}) = \alpha_1(T_k, T_{k-1})T_k + \alpha_2(T_k, T_{k-1})T_{k-1} + \alpha_3(T_k, T_{k-1})T_k \times T_{k-1}, \tag{2.7}$$

and see that rotation invariance is equivalent to the invariance of the scalar components α_i:

$$\alpha_i(RT_k, RT_{k-1}) = \alpha_i(T_k, T_{k-1}). \tag{2.8}$$

2.2.1 Tangent flow

Since tangent vectors of a discrete arc length parametrized curve γ live on edges it is not instantly clear what the tangent direction at a vertex k should be. If we want it to depend only on the neighboring tangent vectors an obvious symmetric choice would be[9]

$$T_k + T_{k-1}.$$

If we set a local flow on $\mathcal{C}_I^{\text{arc}}$ to be parallel to $T_k + T_{k+1}$ it is already uniquely determined –up to a constant– and turns out to be geometric.

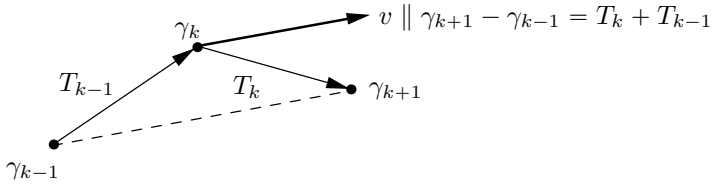

Figure 2.1. Tangent flow on a discrete arc length parametrized curve.

Proposition 2.1 (discrete tangent flow)**.** *The* discrete tangent flow[10]

$$\partial_x \gamma_k = v_k \coloneqq \frac{T_k + T_{k-1}}{1 + \langle T_k, T_{k-1} \rangle}$$

is up to a multiplicative constant the only discrete local curve flow in tangent direction $T_k + T_{k-1}$ which preserves arc length parametrization.
It is geometric.

Proof. Let us start with a general flow in tangent direction

$$v_k = \alpha_k(T_k + T_{k-1}),$$

where $\alpha_k = \alpha_k[\gamma]$ might depend on the curve in any way.
Now we impose arc length preservation. From (2.5) we know that

$$\begin{aligned}
& 0 = \partial_t \|\Delta\gamma_k\| \\
\Leftrightarrow \quad & 0 = \langle v_{k+1} - v_k, T_k \rangle \\
& = \langle \alpha_{k+1}(T_{k+1} + T_k) - \alpha_k(T_k + T_{k-1}), T_k \rangle \\
& = \alpha_{k+1}(\langle T_{k+1}, T_k \rangle + 1) - \underbrace{\alpha_k(\langle T_k, T_{k-1} \rangle + 1)}_{=: c_k} \\
\Leftrightarrow \quad & c_{k+1} = c_k
\end{aligned}$$

[9] Note that this is only a well-defined direction on regular vertices.
[10] Note that x is the flow parameter of the tangent flow here.

for all $k \in I$. So $c_k = c_k[\gamma] =: c[\gamma]$ is constant in k and therefore

$$\alpha_k[\gamma] = \frac{c[\gamma]}{1 + \langle T_k, T_{k-1} \rangle},$$

where this constant might still depend on γ.
Now the locality of the flow ensures that c is the same for any curve γ.[11]
The flow is geometric since it is of the translation invariant form

$$v_k[\gamma] = \alpha(T_k, T_{k-1})(T_k + T_{k-1}),$$

where $\alpha(T_k, T_{k-1}) = \frac{1}{1+\langle T_k, T_{k-1} \rangle}$ is rotation invariant. □

Remark 2.1.

- Since $1 + \langle T_k, T_{k-1} \rangle \to \infty$ as $T_k \to -T_{k-1}$ it is only well-defined at regular vertices.
- Comparing with the smooth tangent flow on arc length parametrized curves which is $\partial_x \gamma = \gamma'$ gives rise to the definition of the *vertex tangent vector* at the vertex k of an arc length parametrized curve[12] to be

  $$\frac{T_k + T_{k-1}}{1 + \langle T_k, T_{k-1} \rangle}.$$

  Note that

  $$1 + \langle T_k, T_{k-1} \rangle = \frac{1}{2} \left\| T_k + T_{k-1} \right\|^2.$$

  So the vertex tangent vectors are not of constant length

  $$\left\| \frac{T_k + T_{k-1}}{1 + \langle T_k, T_{k-1} \rangle} \right\| = \frac{2}{\| T_k + T_{k-1} \|}.$$

- For the discrete tangent-flow v

$v[\gamma]$ is a translation	$\Leftrightarrow$	γ is a straight zig-zag curve
$v[\gamma]$ is a rotation	$\Leftrightarrow$	γ is a circular zig-zag curve.

  Note that the first case includes straight lines and the second regular polygons as special cases.

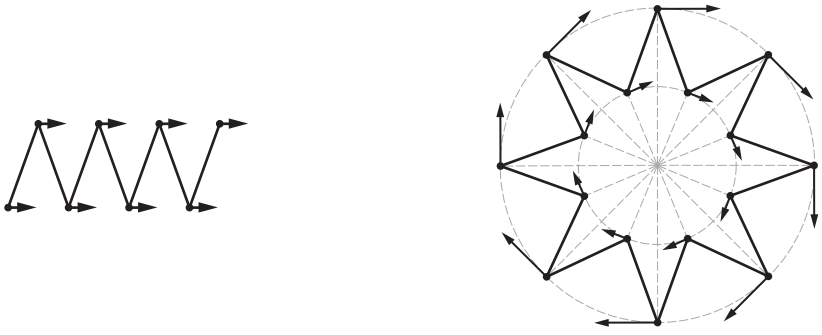

Figure 2.2. Discrete tangent flow. Straight zig-zag curves evolve by a translation. Circular zig-zag curves evolve by a rotation.

[11] ∂_x local $\Rightarrow c[\gamma] = c(\gamma_{k-1}, \gamma_k, \gamma_{k+1})$ with the same value for every k.
[12] This can be generalized to general discrete curves as can be seen in [Hof08].

- We investigate the smooth limit where we refine the lattice $\varepsilon\mathbb{Z} \to \mathbb{R}$ as $\varepsilon \to 0$ as discussed in Section 1.2. We set $\|\Delta\gamma_k\| = \varepsilon$ and therefore $T_k = \frac{\Delta\gamma_k}{\varepsilon}$. Replacing $k \in \mathbb{Z}$ by $x = \varepsilon k \in \mathbb{R}$ we have

$$T_k + T_{k-1} = 2\gamma'(x) + o(1)$$

and

$$1 + \langle T_k, T_{k-1}\rangle = \frac{1}{2}\|T_k + T_{k-1}\|^2 = 2\|\gamma'(x)\| + o(1) = 2 + o(1)$$

since the smooth limit is arc length parametrized, i.e. $\|\gamma'(x)\| = 1$. So

$$\frac{T_k + T_{k+1}}{1 + \langle T_k, T_{k-1}\rangle} = \frac{2\gamma'(x) + o(1)}{2 + o(1)} \to \gamma'(x),$$

which is the smooth tangent flow of an arc length parametrized curve as introduced in Section 2.1.

2.2.2 Heisenberg flow

We now consider curves in $\mathbb{R}^3$ and a flow in binormal direction $T_k \times T_{k-1}$. Any flow in binormal direction is arc length preserving.[13] So this property does not distinguish any of these flows as for the flows in tangent direction. But there is only one that commutes with the tangent flow.

Proposition 2.2 (discrete Heisenberg flow)**.** *The* discrete Heisenberg flow

$$\partial_t\gamma_k = w_k \coloneqq \frac{T_k \times T_{k-1}}{1 + \langle T_k, T_{k-1}\rangle} \tag{2.9}$$

is up to a multiplicative constant the only discrete local curve flow in binormal direction $T_k \times T_{k-1}$ which commutes with the tangent flow.
It is geometric and preserves arc length parametrization.

Remark 2.2.

- Commuting flows (infinitely many) is a characteristic feature of integrable systems.
- Two flows given by v and w commute if they can be integrated simultaneously. This means for some initial curve γ there is some local two-parameter variation

$$\begin{aligned}\gamma\colon (-\varepsilon,\varepsilon)\times(-\varepsilon,\varepsilon) &\to \mathcal{C}_I^{\mathrm{arc}}\\ (x,t) &\mapsto \gamma(x,t)\end{aligned}$$

satisfying

$$\begin{cases}\partial_x\gamma_k &= v_k\\ \partial_t\gamma_k &= w_k.\end{cases}$$

A necessary and sufficient condition for this is

$$\partial_x\partial_t\gamma_k = \partial_t\partial_x\gamma_k,$$

[13] See for example (2.5).

formally meaning that the derivatives ∂_x, $\partial_t \in \mathrm{T}_\gamma \mathcal{C}_I^{\mathrm{arc}}$ on $\mathcal{C}_I^{\mathrm{arc}}$ identified with the vector fields v, w at the point γ commute, i.e.

$$0 = [\partial_x, \partial_t] \in \mathrm{T}_\gamma \mathcal{C}_I^{\mathrm{arc}}.$$

Proof. We start with a general flow in binormal direction

$$\partial_t \gamma = w_k = \beta_k (T_k \times T_{k-1}),$$

where $\beta_k = \beta_k[\gamma]$.

($\Rightarrow$) We have to show that, if w commutes with the tangent flow

$$\partial_x \gamma = v_k = \frac{T_k + T_{k-1}}{1 + \langle T_k, T_{k-1} \rangle},$$

it has to be the Heisenberg flow, where x is the flow parameter of the tangent flow and t is the flow parameter of our ansatz.

$$\begin{aligned}
\partial_x \partial_t \gamma &= \partial_x w_k \\
&= \partial_x \left(\beta_k T_k \times T_{k-1} \right) \\
&= \beta_k \left(\partial_x T_k \times T_{k-1} + T_k \times \partial_x T_{k-1} \right) \\
&\quad + \left(\partial_x \beta_k \right) T_k \times T_{k-1} \\
&= \beta_k \left[(v_{k+1} - v_k) \times T_{k-1} + T_k \times (v_k - v_{k-1}) \right] \\
&\quad + \left(\partial_x \beta_k \right) T_k \times T_{k-1} \\
&= \beta_k \Bigg[\left(\frac{T_{k+1} + T_k}{1 + \langle T_{k+1}, T_k \rangle} - \frac{T_k + T_{k-1}}{1 + \langle T_k, T_{k-1} \rangle} \right) \times T_{k-1} \\
&\quad + T_k \times \left(\frac{T_k + T_{k-1}}{1 + \langle T_k, T_{k-1} \rangle} - \frac{T_{k-1} + T_{k-2}}{1 + \langle T_{k-1}, T_{k-2} \rangle} \right) \Bigg] \\
&\quad + \left(\partial_x \beta_k \right) T_k \times T_{k-1}.
\end{aligned}$$

So in particular

$$\langle \partial_x \partial_t \gamma, T_k \rangle = \beta_k \frac{\langle T_{k+1} \times T_{k-1}, T_k \rangle}{1 + \langle T_{k+1}, T_k \rangle}. \tag{2.10}$$

On the other hand

$$\begin{aligned}
\partial_t\partial_x\gamma &= \partial_t v_k \\
&= \partial_t\left(\frac{T_k + T_{k-1}}{1+\langle T_k, T_{k-1}\rangle}\right) \\
&= \frac{1}{1+\langle T_k, T_{k-1}\rangle}\partial_t\left(T_k + T_{k+1}\right) + \partial_t\left(\frac{1}{1+\langle T_k, T_{k-1}\rangle}\right)(T_k + T_{k+1}) \\
&= \frac{1}{1+\langle T_k, T_{k-1}\rangle}\left(w_{k+1} - w_{k-1}\right) \\
&\quad - \frac{1}{(1+\langle T_k, T_{k-1}\rangle)^2}\Big(\langle w_{k+1} - w_k, T_{k-1}\rangle + \langle T_k, w_k - w_{k-1}\rangle\Big)(T_k + T_{k-1}) \\
&= \frac{1}{1+\langle T_k, T_{k-1}\rangle}\Big(\beta_{k+1}T_{k+1}\times T_k - \beta_{k-1}T_{k-1}\times T_{k-2}\Big) \\
&\quad - \frac{1}{(1+\langle T_k, T_{k-1}\rangle)^2}\Big(\beta_{k+1}\langle T_{k+1}\times T_k, T_{k-1}\rangle \\
&\quad - \beta_{k-1}\langle T_k, T_{k-1}\times T_{k-2}\rangle\Big)(T_k + T_{k-1}).
\end{aligned}$$

In particular

$$\langle \partial_t\partial_x\gamma, T_k\rangle = -\beta_{k+1}\frac{\langle T_{k+1}\times T_k, T_{k-1}\rangle}{1+\langle T_k, T_{k-1}\rangle}. \tag{2.11}$$

Comparing (2.10) and (2.11) we get

$$\begin{aligned}
&\frac{\beta_k}{1+\langle T_{k+1}, T_k\rangle} = \frac{\beta_{k+1}}{1+\langle T_k, T_{k-1}\rangle} \\
\Leftrightarrow\quad &\beta_k(1+\langle T_k, T_{k-1}\rangle) = \beta_{k+1}(1+\langle T_{k+1}, T_k\rangle)
\end{aligned}$$

for all $k \in I$ which is equivalent to

$$\beta_k[\gamma] = \frac{c[\gamma]}{1+\langle T_k, T_{k-1}\rangle},$$

where c is some constant depending on the curve γ. Imposing the locality of w eliminates this dependence.

($\Leftarrow$) A similar –but even longer– calculation shows that the obtained Heisenberg flow actually does commute with the tangent flow. After calculating $\partial_x\partial_t\gamma$ and $\partial_t\partial_x\gamma$ one can compare the scalar products with T_k, T_{k-1} and $T_k \times T_{k-1}$ respectively.

We still have to show that the Heisenberg flow is geometric and arc length preserving.
Similar to the tangent flow it is of the translation invariant form

$$w_k[\gamma] = \beta(T_k, T_{k-1})T_k \times T_{k-1},$$

where β is rotation invariant. Since $T_k \times T_{k-1}$ is a rotation invariant vector field the Heisenberg flow is geometric.
It always lies in the orthogonal complement of $\operatorname{span}\{T_k, T_{k-1}\}$ and therefore is arc length preserving. □

Remark 2.3. We investigate the smooth limit using the method described in Section 1.2. Setting $x = \varepsilon k$ we have[14]

$$\begin{aligned} T_k \times T_{k-1} &= T(x) \times T(x-\varepsilon) \\ &= T(x) \times (T(x) - \varepsilon T'(x) + o(\varepsilon)) \\ &= \varepsilon T'(x) \times T(x) + o(\varepsilon) \end{aligned}$$

and

$$1 + \langle T_k, T_{k-1} \rangle = 2 + o(1).$$

Rescaling the time by replacing $t \to \frac{\varepsilon t}{2}$ we obtain the smooth limit

$$\partial_\tau \gamma = T' \times T. \tag{2.12}$$

This results in the following equation of motion for T

$$\partial_t T(x) = T'' \times T, \tag{2.13}$$

which is the continuous Heisenberg magnetic chain as described in Section A. This is an integrable system as is the discretization obtained from (2.9) which yields

$$\begin{aligned} \partial_t T_k &= \frac{T_{k+1} \times T_k}{1 + \langle T_{k+1}, T_k \rangle} - \frac{T_k \times T_{k-1}}{1 + \langle T_k, T_{k-1} \rangle} \\ &= \left(\frac{T_{k+1}}{1 + \langle T_{k+1}, T_k \rangle} + \frac{T_{k-1}}{1 + \langle T_k, T_{k-1} \rangle} \right) \times T_k. \end{aligned} \tag{2.14}$$

[14] Which might be seen immediately from $T_k \times T_{k-1} = (T_k - T_{k-1}) \times T_{k-1}$.

3 Elastica

3.1 Smooth elastic curves

We consider variations of curves γ in $\mathbb{R}^3$ with fixed endpoints, fixed end directions and fixed length.

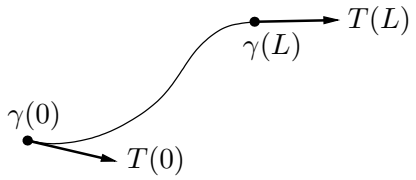

Figure 3.1. Curve with fixed endpoints and fixed end tangent vectors.

We represent each curve by its arc length parametrization $\gamma : [0, L] \to \mathbb{R}^3$ with $T \coloneqq \gamma' : [0, L] \to \mathbb{S}^2$. Then admissible variations have to

- fix $\gamma(0)$, $\gamma(L) \in \mathbb{R}^3$,
- fix $T(0)$, $T(L) \in \mathbb{S}^2$,
- preserve the arc length parametrization, i.e. $\|T(s)\| = 1$,
  in particular this implies that the length of γ is preserved.

We define the bending energy of γ to be

$$\mathcal{E}[\gamma] \coloneqq \int_0^L \kappa(s)^2 \mathrm{d}s = \int_0^L \langle T', T' \rangle \mathrm{d}s = \mathcal{E}[T],$$

where $\kappa = \|\gamma''\|^2 = \|T'\|^2$ is the curvature of γ.

Remark 3.1. Note that the bending energy is invariant w.r.t. Euclidean motions.

Definition 3.1 (Bernoulli's elastica)**.** An *elastic curve* is a critical point γ of the bending energy $\mathcal{E}$ under the described admissible variations.

The tangent vector $T : [0, L] \to \mathbb{S}^2$ uniquely determines the curve γ up to translations. We note that fixed $\gamma(0)$, $\gamma(L) \in \mathbb{R}^3$ implies

$$\int_0^L T(s) \mathrm{d}s = \gamma(L) - \gamma(0).$$

So if we reformulate the problem of finding critical points of the bending energy $\mathcal{E}[T]$ only in terms of $T : [0, L] \to \mathbb{S}^2$, we have to impose this additional constraint. Admissible variations of T have to

- fix $T(0)$, $T(L) \in \mathbb{S}^2$,
- satisfy $\int_0^L T(s) \mathrm{d}s = const. \in \mathbb{R}^3$,
- preserve $\|T(s)\| = 1$ for all $s \in [0, L]$.

Basic fact from the calculus of variations: Lagrange-multipliers. *The critical points of the functional*

$$\mathcal{S}[q] = \int_0^L \mathcal{L}(q(s), q'(s))\mathrm{d}s$$

on the space of smooth functions $q : [0, L] \to \mathbb{R}^3$ *under the variations preserving the constraints*

$$F_i = \int_0^L f_i(q, q')\mathrm{d}s = c_i \in \mathbb{R}, \qquad i = 1, \dots, N$$

are the critical points of the functional

$$\mathcal{S}_\lambda \coloneqq \mathcal{S} + \sum_{i=1}^{N} \lambda_i F_i$$

with some constants λ_i *(*Lagrange-Multipliers*).*
These constants are determined from the conditions $F_i = c_i,\ i = 1, \dots, N$.

Basic fact from Lagrangian mechanics: Hamilton's principle of least action. *The trajectory* $q(t)$ *of a mechanical system with potential energy* $\mathcal{U}$ *and kinetic energy* $\mathcal{T}$ *is critical for the* action functional

$$\mathcal{S}[q] \coloneqq \int_{t_1}^{t_2} \mathcal{L}(q(t), q'(t))\mathrm{d}t$$

with the Lagrangian $\mathcal{L} \coloneqq \mathcal{T} - \mathcal{U}$.

Implementing the constraint $\int_0^L T(s)\mathrm{d}s = const. \in \mathbb{R}^3$ into the functional via Lagrange-multiplicators, we obtain the following physical interpretation.

Theorem 3.1 (Kirchhoff analogy for elastic curves)**.** *An arc length parametrized curve* $\gamma : [0, L] \to \mathbb{R}^3$ *is an elastic curve if and only if its tangent vector* $T \coloneqq \gamma' : [0, L] \to \mathbb{S}^2$ *describes the evolution of the axis of a spherical pendulum.*
The arc length parameter of the curve coincides with the time parameter of the pendulum.

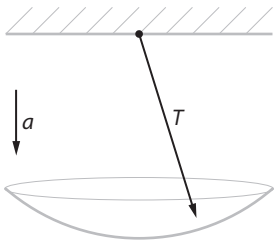

Figure 3.2. Spherical pendulum T with gravitational vector a.

Proof. The extrema of the functional

$$\mathcal{E}_a[T] \coloneqq \int_0^L \left(\langle T', T'\rangle + 2\langle a, T\rangle\right) \mathrm{d}s,$$

where $a \in \mathbb{R}^3$ and $T : [0, L] \to \mathbb{S}^2$ can be interpreted in two different ways:

(1) Extrema of the bending energy

$$\mathcal{E} = \int_0^L \kappa^2 \mathrm{d}s = \int_0^L \langle T', T' \rangle \mathrm{d}s$$

for variations with fixed endpoints under the constraint $\int_0^L T \mathrm{d}s = const. \in \mathbb{R}^3$. Here $a = (a_1, a_2, a_3)$ are treated as Lagrange-multipliers

$$\sum_{i=1}^3 \lambda_i F_i = \sum_{i=1}^3 a_i \int_0^L T_i(s) \mathrm{d}s = \int_0^L \langle a, T \rangle \mathrm{d}s.$$

(2) Extrema of the action functional with Lagrangian $\mathcal{L} = \mathcal{T} - \mathcal{U}$ where $\mathcal{T} = \langle T', T' \rangle, \mathcal{U} = -\langle a, T \rangle$ are the kinetic and potential energy of the spherical pendulum.
Here $a \in \mathbb{R}^3$ is the gravitational vector.

□

Remark 3.2.

- Planar elastica were first classified by Euler.
  The tangent vector describes the motion of a planar pendulum. The only closed elastica in the plane are the circle and Euler's elastic eight.

Figure 3.3. Some planar elastic curves.

- Elastica in $\mathbb{R}^N$ are reduced to elastica in $\mathbb{R}^3$.
  They always lie in the 3-dimensional space

$$\mathrm{span}\{\gamma(L) - \gamma(0), T(0), T(L)\}.$$

  Similarly the spherical pendulum in $\mathbb{S}^{N-1}$ always lies in the 2-dimensional space

$$\mathbb{S}^{N-1} \cap \mathrm{span}\{a, T(0), T'(0)\}.$$

Basic fact from calculus of variations: Euler-Lagrange equations. *$q : [0, L] \to \mathbb{R}^3$ is a critical point of the functional $\mathcal{S}[q] = \int_0^L \mathcal{L}(q(s), q'(s)) \mathrm{d}s$ under variations with fixed endpoints $q(0)$, $q(L)$ if and only if*

$$\frac{\mathrm{d}}{\mathrm{d}s} \nabla_{q'} \mathcal{L} - \nabla_q \mathcal{L} = 0.$$

We can implement the remaining constraint $\|T\| = 1$ into the functional using a "continuous Lagrange-multiplier":

$$\mathcal{E}_{(a,c)}[T] \coloneqq \int_0^L \left(\langle T', T' \rangle + c(s)(\langle T, T \rangle - 1) + 2\langle a, T \rangle \right) \mathrm{d}s.$$

From this we obtain the Euler-Lagrange equations for elastic curves.

Theorem 3.2 (Euler-Lagrange equations for elastic curves)**.** *An arc length parametrized curve $\gamma : [0, L] \to \mathbb{R}^3$ is an elastic curve if and only if*

$$\gamma'' \times \gamma' = a \times \gamma + b$$

for some $a, b \in \mathbb{R}^3$,
or equivalently if and only if its tangent vector $T : [0, L] \to \mathbb{S}^2$ satisfies

$$T'' \times T = a \times T$$

for some $a \in \mathbb{R}^3$.

Proof. The equation for γ can be obtained from the equation for T by integration, using $(\gamma'' \times \gamma')' = T'' \times T$.
With

$$\mathcal{L}(T, T') \coloneqq \frac{1}{2}\langle T', T' \rangle + \frac{1}{2}c(s)(\langle T, T \rangle - 1) + \langle a, T \rangle$$

we obtain

$$\begin{aligned} \frac{\mathrm{d}}{\mathrm{d}s}\nabla_{T'}\mathcal{L} = \nabla_T \mathcal{L} \;&\Leftrightarrow\; T'' = c(s)T + a \\ &\Leftrightarrow T'' \times T = a \times T, \end{aligned}$$

where we applied the cross-product with T. □

Remark 3.3. We recognize the left-hand side of the Euler-Lagrange equations as the Heisenberg flow (2.4) (acting on γ and T respectively) while the right-hand side describes an infinitesimal Euclidean motion.

Corollary 3.3. *A curve γ is an elastic curve if and only if the Heisenberg flow preserves its form, i.e. under the action of the Heisenberg flow the curve evolves by an Euclidean motion.*

Proof. That $v \mapsto a \times v + b$ is the infinitesimal generator of an Euclidean motion is best be seen using the quaternionic description of Euclidean motions, which is described in the following section. □

3.2 Quaternions and Euclidean Motions

The *quaternionic algebra* $\mathbb{H}$ is a 4-dimensional generalization of the complex numbers. It can be constructed the following way.

Let $\mathbb{H}$ be a real 4-dimensional vector space $\mathbb{R}^4$ where we denote the standard basis by $\{\mathbb{1}, \mathbb{i}, \mathbb{j}, \mathbb{k}\}$. So a general quaternion $q \in \mathbb{H}$ can be written as

$$q = q_0\mathbb{1} + q_1\mathbb{i} + q_2\mathbb{j} + q_3\mathbb{k}$$

with $q_i \in \mathbb{R}$.

We define a multiplication on $\mathbb{H}$ by prescribing it on the basis vectors. By distributivity it uniquely extends to all quaternions. For this the following relations are sufficient:

$$\mathbb{i}^2 = \mathbb{j}^2 = \mathbb{k}^2 = \mathbb{ijk} = -\mathbb{1}. \tag{3.1}$$

Associativity then fixes the multiplication for all combinations of basis vectors.

$$\begin{aligned}\mathbb{i}\mathbb{j} &= -\mathbb{j}\mathbb{i} = \mathbb{k}\\ \mathbb{j}\mathbb{k} &= -\mathbb{k}\mathbb{j} = \mathbb{i}\\ \mathbb{k}\mathbb{i} &= -\mathbb{i}\mathbb{k} = \mathbb{j}\end{aligned}$$

This also implies skew symmetry and therefore *non-commutativity* of the quaternionic multiplication. On the other hand we see that $\mathbb{1}$ commutes with everything, which is why we can identify the first component of the quaternions with the real numbers where $\mathbb{1} = 1$. Eventually we write

$$q = q_0 + q_1\mathbb{i} + q_2\mathbb{j} + q_3\mathbb{k}$$

with $q_i \in \mathbb{R}$.
The quaternionic multiplication extends the scalar multiplication of the vector space.

We denote the *real and imaginary part*[15] of $q \in \mathbb{H}$ by

$$\begin{aligned}\mathrm{Re}q &\coloneqq q_0 = q_0 1 = q_0\mathbb{1}\\ \mathrm{Im}q &\coloneqq q_1\mathbb{i} + q_2\mathbb{j} + q_3\mathbb{k}\end{aligned}$$

and the *conjugated quaternion* by

$$\overline{q} \coloneqq \mathrm{Re}q - \mathrm{Im}q.$$

Like in the complex case we define the absolute value of an quaternion $q \in \mathbb{H}$ by

$$|q|^2 \coloneqq q\overline{q} = \overline{q}q = q_0^2 + q_1^2 + q_2^2 + q_3^2$$

which turns out to be the same as the Euclidean distance in $\mathbb{R}^4$.

Quaternionic conjugation and absolute value give us means to define an inverse[16] for $q \in \mathbb{H}$, $q \neq 0$:

$$q^{-1} \coloneqq \frac{\overline{q}}{|q|^2}.$$

We see that the quaternionic multiplication induces a group structure on the following subsets of $\mathbb{H}$:

$$\begin{aligned}\mathbb{H}_* &\coloneqq \mathbb{H}\backslash\{0\}\\ \mathbb{H}_1 &\coloneqq \{q \in \mathbb{H} \mid |q| = 1\} \ \textit{unitary quaternions}\end{aligned}$$

3.2.1 Euclidean motions in $\mathbb{R}^3$

The set

$$\mathrm{Im}\mathbb{H} \coloneqq \{q \in \mathbb{H} \mid \mathrm{Re}q = 0\}$$

of *imaginary quaternions* is a 3-dimensional vector space which we identify with $\mathbb{R}^3$:

$$v_1\mathbb{i} + v_2\mathbb{j} + v_3\mathbb{k} \in \mathrm{Im}\mathbb{H} \Leftrightarrow (v_1, v_2, v_3) \in \mathbb{R}^3$$

This leads to the following geometric interpretation of multiplication of two imaginary quaternions.

[15] Note that the imaginary part includes the basis vectors unlike in the complex case.

[16] It is meaningful to write this as a fraction, since $|q|^2$ is real and therefore real invertible while commuting with every quaternion.

Lemma 3.4. *Let $v, w \in \mathrm{Im}\mathbb{H}$. Then*

$$vw = -\underbrace{\langle v, w\rangle}_{\in\mathbb{R}} + \underbrace{v \times w}_{\in \mathrm{Im}\mathbb{H}} \in \mathbb{H}.$$

Proof.

$$\begin{aligned}&(v_1\mathbb{i} + v_2\mathbb{j} + v_3\mathbb{k})(w_1\mathbb{i} + w_2\mathbb{j} + w_3\mathbb{k})\\ &= -v_1w_1 - v_2w_2 - v_3w_3 + (v_2w_3 - v_3w_2)\mathbb{i} + (v_3w_1 - v_1w_3)\mathbb{j} + (v_1w_2 - v_2w_1)\mathbb{k}.\end{aligned}$$

□

So we get the cross product and the scalar product of $v, w \in \mathrm{Im}\mathbb{H}$ in terms of commutator and anti-commutator.

$$\begin{aligned}v \times w &= \frac{1}{2}(vw - wv) =: \frac{1}{2}[v, w]\\ \langle v, w\rangle &= -\frac{1}{2}(vw + wv)\end{aligned}$$

In particular, two imaginary non-vanishing quaternions $v, w \neq 0$ are parallel if and only if they commute, and they are perpendicular if and only if they anti-commute:

$$\begin{aligned}vw - wv = 0 &\Leftrightarrow v \times w = 0 \Leftrightarrow v \parallel w\\ vw + wv = 0 &\Leftrightarrow \langle v, w\rangle = 0 \Leftrightarrow v \perp w\end{aligned}$$

Lemma 3.5. *Unitary quaternions $q \in \mathbb{H}_1$ can be parametrized as*

$$q = \cos\alpha + (\sin\alpha)n,$$

where $n \in \mathrm{Im}\mathbb{H}$ with $|n| = 1$ and $\alpha \in [0, \pi]$.

Proof. For $q \in \mathbb{H}_1$ we can write $\mathrm{Re}q = q_0 \in \mathbb{R}$ and $\mathrm{Im}q = cn$ with $c \geqslant 0$, $n \in \mathrm{Im}\mathbb{H}$, $|n| = 1$. Then

$$1 = |q|^2 = (q_0 + cn)(q_0 - cn) = q_0^2 + c^2$$

which can be parametrized as

$$\begin{aligned}q_0 &= \cos\alpha\\ c &= \sin\alpha\end{aligned}$$

with $\alpha \in [0, \pi]$. □

Remark 3.4. This parametrization is a double covering since

$$q(-\alpha, -n) = q(\alpha, n).$$

Proposition 3.6 (quaternionic rotation in $\mathbb{R}^3$)**.** *For $q \in \mathbb{H}_1$, $q = \cos\alpha + (\sin\alpha)n$, $n \in \mathrm{Im}\mathbb{H}$, $|n| = 1$, $\alpha \in [0, \pi]$ the map $\mathcal{R}_q : \mathbb{R}^3 \to \mathbb{R}^3$ given by*

$$\mathcal{R}_q(v) \coloneqq qvq^{-1}$$

is a rotation about the axis n by the angle 2α.[17]

[17] Instead of $q \in \mathbb{H}_1$ one can take $q \in \mathbb{H}_*$, since the absolute value of q cancels in qvq^{-1}.

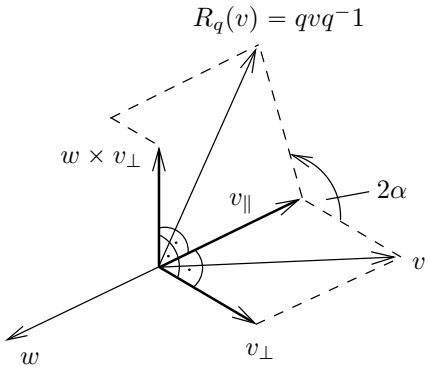

Figure 3.4. Decomposition of a vector v into its part along the rotation axis and along the orthogonal complement.

Proof. Decompose $v \in \mathrm{Im}\mathbb{H}$ into the part parallel and the part perpendicular to n, i.e.

$$v = v_\parallel + v_\perp,$$

where $v_\parallel w = w v_\parallel$ and $v_\perp w = -w v_\perp$. Then

$$\begin{aligned} q v_\parallel q^{-1} &= v_\parallel \\ q v_\perp q^{-1} &= (\cos\alpha + (\sin\alpha)n) v_\perp (\cos\alpha - (\sin\alpha)n) \\ &= (\cos^2\alpha - \sin^2\alpha 2(\cos\alpha\sin\alpha)n) v_\perp \\ &= (\cos 2\alpha) v_\perp + (\sin 2\alpha) w \times v_\perp. \end{aligned}$$

□

Remark 3.5. The map $\mathbb{H}_1 \to \mathrm{SO}(3), \quad q \mapsto \mathcal{R}_q$ is a double covering of $\mathrm{SO}(3)$ since

$$\mathcal{R}_{-q} = \mathcal{R}_q.$$

Multiplication of unitary quaternions corresponds to the composition of rotations

$$\mathcal{R}_{q_2 q_1} = \mathcal{R}_{q_2} \circ \mathcal{R}_{q_1},$$

i.e. multiplication in $\mathrm{SO}(3)$.

An *Euclidean motion* is a composition of rotation and translation:

$$v \mapsto q v q^{-1} + p, \quad v \in \mathrm{Im}\mathbb{H},$$

where $q \in \mathbb{H}_1$, $p \in \mathrm{Im}\mathbb{H}$. Consider an *Euclidean flow*

$$\Phi_t(v) = q(t) v q(t)^{-1} + p(t), \quad t \in \mathbb{R}.$$

The infinitesimal generator of this flow

$$\varphi_t(\Phi_t(v)) \coloneqq \frac{\mathrm{d}}{\mathrm{d}t}\Phi_t(v)$$

gives a time-dependent vector field which is called an *infinitesimal Euclidean motion*.

Corollary 3.7 (Infinitesimal Euclidean motions)**.** *Infinitesimal Euclidean motions are vector fields of the form*

$$v \mapsto \frac{1}{2}[a, v] + b = a \times v + b, \quad v \in \mathrm{Im}\mathbb{H},$$

where $a, b \in \mathrm{Im}\mathbb{H}$ are called the angular and translational velocity.

Proof. We have to compute the time derivative of an Euclidean flow

$$\begin{aligned}\frac{\mathrm{d}}{\mathrm{d}t}\Phi_t(v) &= (q(t)vq(t)^{-1})' + p'(t)\\ &= q'vq^{-1} - qv(q^{-1})' + p'\\ &= q'vq^{-1} - qvq^{-1}q'q^{-1} + p'\\ &= [q'q^{-1}, \Phi_t(v)] + p' - [q'q^{-1}, p]\\ &= \frac{1}{2}[a(t), \Phi_t(v)] + b(t),\end{aligned}$$

where we set $a(t) \coloneqq 2q'(t)q^{-1}(t) \in \mathrm{Im}\mathbb{H}$ and $b(t) \coloneqq p'(t) - \frac{1}{2}[a(t), p(t)] \in \mathrm{Im}\mathbb{H}$. □

Conversely, given a one-parameter family of infinitesimal Euclidean motions

$$\varphi_t(v) = a(t) \times v + b(t),$$

there exists an essentially unique corresponding one-parameter family of Euclidean motions $\Phi_t(v)$ which is the flow generated by $\varphi_t(v)$.
It can be obtained by integrating the quaternionic linear differential equations

$$\begin{aligned}q' &= \frac{1}{2}aq\\ p' &= b + \frac{1}{2}[a, p].\end{aligned}$$

This completes the proof of Corollary 3.3.

3.3 Discrete elastic curves

We consider discrete arc length parametrized curves

$$\gamma : I \to \mathbb{R}^3, \quad T_k = \gamma_{k+1} - \gamma_k, \quad |T_k| = 1.$$

What is the proper bending energy for discrete elastica?

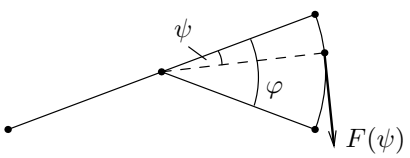

Figure 3.5. Bending energy as the integral of the bending force.

Assume that the bending force at an inner vertex $k \in I$ (depending on the bending angle φ_k) is proportional to the curvature

$$\kappa_k = 2 \tan \frac{\varphi_k}{2}$$

we defined for discrete arc length parametrized curves.
Then we obtain the corresponding local energy at vertex k

$$\begin{aligned}\int_0^{\varphi_k} \kappa(\psi) \mathrm{d}\psi &= 2 \int_0^{\varphi_k} \tan \frac{\psi}{2} \mathrm{d}\psi = -4 \log \cos \frac{\psi}{2} \Big|_0^{\varphi_k} = -4 \log \cos \frac{\varphi_k}{2} \\ &= -2 \log \cos^2 \frac{\varphi_k}{2} = 2 \log \left(1 + \tan^2 \frac{\varphi_k}{2}\right) = 2 \log \left(1 + \frac{\kappa_k^2}{4}\right).\end{aligned}$$

We define the local bending energy

$$\mathcal{E}_k \coloneqq \log \left(1 + \frac{\kappa_k^2}{4}\right).$$

With

$$\frac{1}{2} \left\| T_k + T_{k-1} \right\|^2 = 1 + \langle T_k, T_{k-1} \rangle = 1 + \cos \varphi_k = 2 \cos^2 \frac{\varphi_k}{2}$$

we find alternate expressions

$$\mathcal{E}_k = -\log \left(1 + \langle T_k, T_{k-1} \rangle\right) + \log 2 = -log \left\| T_k + T_{k-1} \right\|^2 + \log 4.$$

Remark 3.6.

- The discrete local bending energy is invariant under Euclidean transformations.
- In the smooth limit we have $\varphi_k \to 0$ and therefore $\kappa_k \to 0$. We find that

  $$\mathcal{E}_k = \log \left(1 + \frac{\kappa_k^2}{4}\right) = \frac{\kappa_k^2}{4} + o(\kappa^2)$$

  is quadratic in the curvature.
- At singular vertices we have $\varphi_k \to \pi$ and therefore $\kappa_k \to \infty$. We obtain

  $$\mathcal{E}_k = \log \left(1 + \frac{\kappa_k^2}{4}\right) \to \infty.$$

  So discrete elastic curves are regular.

For finite curves with $I = [0, n]$ we consider variations of the total energy on $\mathcal{C}_I^{\mathrm{arc}}$

$$\sum_{k=1}^{n-1} \mathcal{E}_k,$$

where the sum goes over all "inner vertices" of I.
Admissible variations should fix end points and end tangent vectors and preserve the arc length.

Definition 3.2 (Discrete elastic curve)**.** A discrete arc length parametrized curve $\gamma : I \to \mathbb{R}^3$, $I = [0, n] \subset \mathbb{Z}$ with tangent vector $T : I \to \mathbb{R}^3$, $T_k = \gamma_{k+1} - \gamma_k$ is called *discrete elastic curve* if it is a critical point of the functional

$$\mathcal{E}[\gamma] \coloneqq \sum_{k=1}^{n-1} \log\left(1 + \frac{\kappa_k^2}{4}\right) \sim \sum_{k=1}^{n-1} \log\left(1 + \langle T_k, T_{k-1}\rangle\right) \sim \sum_{k=1}^{n-1} \log \|T_k + T_{k-1}\|$$

under variations on $\mathcal{C}_I^{\text{arc}}$ with fixed $\gamma_0, \gamma_n, T_0, T_{n-1}$, where $\kappa_k = 2\tan\frac{\varphi_k}{2}$ is the discrete curvature. The $\sim$ denotes equivalent functionals, i.e. functionals which have the same critical points.

Remark 3.7.

- Closed arc length parametrized curves $I = \mathbb{Z}_{n-1}$ can be treated as a special case of $I = [0, n]$ with $\gamma_0 = \gamma_{n-1}, \gamma_1 = \gamma_n$ and therefore $T_{n-1} = T_0$.

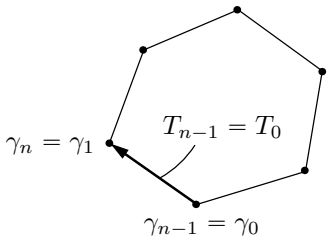

Figure 3.6. Closed elastic curves as a special case.

  We note that factorizing by Euclidean motions we can get rid of any fixed points and directions in this case.

- Factorizing by translations we reformulate the variational problem in terms of $T : I \to \mathbb{R}^3$ only. Admissible variations of T have to
  - fix $T_0, T_{n-1} \in \mathbb{S}^2$,
  - satisfy $\sum_{k=0}^{n-1} T_k = \gamma_n - \gamma_0 \in \mathbb{R}^3$,
  - preserve $\|T_k\| = 1$ for $i = 0, \dots, n-1$.
- Functionals are functions of many variables in the discrete case. Applying that $T_0, T_{n-1} \in \mathbb{S}^2$ are fixed,

$$\mathcal{E}[T] = \mathcal{E}(T_0, \dots, T_{n-1}) = \mathcal{E}(T_1, \dots, T_{n-2})$$

  is a function of $3(n-2)$ variables which has to be varied under the constraints
  - $\sum_{k=1}^{n-2} T_k = const. \in \mathbb{R}^3$,
  - $\|T_k\| = 1$ for $i = 1, \dots, n-2$.

Theorem 3.8 (Euler-Lagrange equations for discrete elastic curve)**.** *A discrete arc length parametrized curve $\gamma : I \to \mathbb{R}^3$, $I = [0, n] \subset \mathbb{Z}$ is a discrete elastic curve if and only if there exists $a, b \in \mathbb{R}^3$ such that*

$$\frac{T_k \times T_{k-1}}{1 + \langle T_k, T_{k+1}\rangle} = a \times \gamma_k + b, \qquad k = 1, \dots, n-1,$$

where $T_k = \gamma_{k+1} - \gamma_k$.

Proof. We want to derive equations for the critical points of

$$\mathcal{E}(T_1, \dots, T_{n-2}) = \sum_{k=1}^{n-1} \log\left(1 + \langle T_k, T_{k-1}\rangle\right)$$

under the constraints

- $\sum_{k=1}^{n-2} T_k = const. \in \mathbb{R}^3$,
- $\|T_k\| = 1$ for $k = 1, \dots, n-2$.

We implement these constraints using Lagrange-multipliers $c_k \in \mathbb{R}, k = 1, \dots, n-2$ and $a = (a_1, a_2, a_3) \in \mathbb{R}^3$, and obtain

$$\mathcal{E}_\lambda \coloneqq \sum_{k=1}^{n-1} \log\left(1 + \langle T_k, T_{k-1}\rangle\right) - \sum_{k=1}^{n-2} \left(c_k \langle T_k, T_k\rangle + \langle a, T_k\rangle\right).$$

The corresponding Euler-Lagrange equations are

$$\nabla_{T_k} \mathcal{E}_\lambda = 0, \qquad k = 1 \dots, n-2.$$

Using $\nabla_{T_k}\langle T_k, a\rangle = b$ and $\nabla_{T_k}\langle T_k, T_k\rangle = 2T_k$, we find for $k = 1, \dots, n-2$

$$\nabla_{T_k} \mathcal{E}_\lambda = \frac{T_{k-1}}{1 + \langle T_k, T_{k-1}\rangle} + \frac{T_{k+1}}{1 + \langle T_{k+1}, T_k\rangle} - 2c_k T_k - a = 0. \tag{3.2}$$

Taking the cross-product with T_k, we obtain

$$\frac{T_{k+1} \times T_k}{1 + \langle T_{k+1}, T_k\rangle} - \frac{T_{k-1} \times T_k}{1 + \langle T_k, T_{k-1}\rangle} = a \times T_k = a \times (\gamma_{k+1} - \gamma_k), \tag{3.3}$$

which is equivalent to

$$\frac{T_k \times T_{k-1}}{1 + \langle T_k, T_{k+1}\rangle} - a \times \gamma_k = b = const. \in \mathbb{R}^3.$$

Noting that (3.2) and (3.3) are equivalent, we obtain the claim. □

Remark 3.8.

- If we identify the left-hand side of the Euler-Lagrange equations as the discrete Heisenberg flow, which we denote by ∂_t, we have shown

$$\begin{aligned} \gamma \text{ discrete elastica } &\Leftrightarrow \partial_t \gamma_k = a \times \gamma_k + b \\ &\Leftrightarrow \partial_t T_k = a \times T_k, \end{aligned}$$

  where the second line are the equivalent equations in terms of the tangent vector which are written down explicitly in (3.3).

- Recalling the smooth limit of the Heisenberg flow (2.12) and (2.13), we obtain for the smooth limit of the Euler-Lagrange equations

$$\begin{aligned} T' \times T = a \times \gamma + b &\Leftrightarrow \gamma'' \times \gamma' = a \times \gamma + b \\ &\Leftrightarrow T'' \times T = a \times T, \end{aligned}$$

  which are the Euler-Lagrange equations for smooth elastic curves as stated in Theorem 3.2.

Corollary 3.9. *A discrete arc length parametrized curve is a discrete elastic curve if and only if the Heisenberg flow preserves its form, i.e. under the action of the Heisenberg flow the curve evolves by an Euclidean motion.*

Proof. Same as in the smooth case. □

Definition 3.3 (discrete spherical pendulum)**.** A *discrete spherical pendulum* is a mechanical system on $\mathbb{S}^2$ with discrete time and Lagrangian

$$\mathcal{L}_k \coloneqq \log\left(1 + \langle T_k, T_{k-1}\rangle\right) - \langle a, T_k\rangle$$

with some $a \in \mathbb{R}^3$. This means that the trajectories $T : I \to \mathbb{S}^2$ are critical points of the action functional $\mathcal{S} = \sum_k \mathcal{L}_k$.

Remark 3.9. The terms $\mathcal{T}_k \coloneqq \log\left(1 + \langle T_k, T_{k-1}\rangle\right)$ and $\mathcal{U}_k \coloneqq \langle a, T_k\rangle$ are interpreted as kinetic and potential energies of the pendulum with gravitation vector a. In the smooth limit

$$\begin{aligned}\mathcal{U}_k &\to \langle a, T\rangle,\\ \mathcal{T}_k &\sim \log\left(1 + \frac{\kappa_k}{4}\right) = \frac{\kappa_k^2}{4} + o(\kappa_k^2),\end{aligned}$$

where $\kappa_k \to \|T'\|$. So in the smooth limit the kinetic energy is quadratic in the velocity.

From this definition we immediately obtain a discrete analog of Theorem 3.1.

Theorem 3.10 (Kirchhoff analogy for discrete elastic curves)**.** *A discrete arc length parametrized curve $\gamma : I \to \mathbb{R}^3$ is a discrete elastic curve if and only if its tangent vector $T_k = \gamma_{k+1} - \gamma_k$ describes the evolution of a discrete spherical pendulum.*

Proof. Analogous to the proof of Theorem 3.1. □

3.4 Moving frames and framed curves

Let $T, N, B : I \to \mathbb{R}^3$ be three smooth maps such that $T(s), N(s), B(s)$ is an orthonormal basis for any $s \in I$, i.e. the matrix $\mathcal{R}(s) \coloneqq (T(s), N(s), B(s)) \in \mathrm{SO}(3)$. We can think of it as a coordinate frame fixed inside a rigid body which rotates around some fixed point. In this interpretation we call (T, N, B) the *body frame*.

Definition 3.4 (moving frame)**.** Let $I \subset \mathbb{R}$ be an interval. A *moving frame* is a differentiable map

$$\mathcal{R} : I \to \mathrm{SO}(3).$$

This is a special case of an Euclidean motion where the rotation $\mathcal{R}$ describes the movement of the frame with respect to the stationary coordinate system (e_1, e_2, e_3):

$$T = \mathcal{R}e_1, \quad N = \mathcal{R}e_2, \quad B = \mathcal{R}e_3.$$

On the other hand $\mathcal{R}$ is the coordinate transformation mapping points

$$X = X_1 e_1 + X_2 e_2 + X_3 e_3$$

in the rotating body frame to points

$$x(s) = X_1 T(s) + X_2 N(s) + X_3 B(s) = x_1(s) e_1 + x_2(s) e_2 + x_3(s) e_3$$

in the stationary coordinate system by

$$x = \mathcal{R} X.$$

We usually suppose the frame to be aligned with the fixed coordinate system for $s = 0$, i.e. $\mathcal{R}(0) = \mathrm{id}_{\mathbb{R}^3}$.

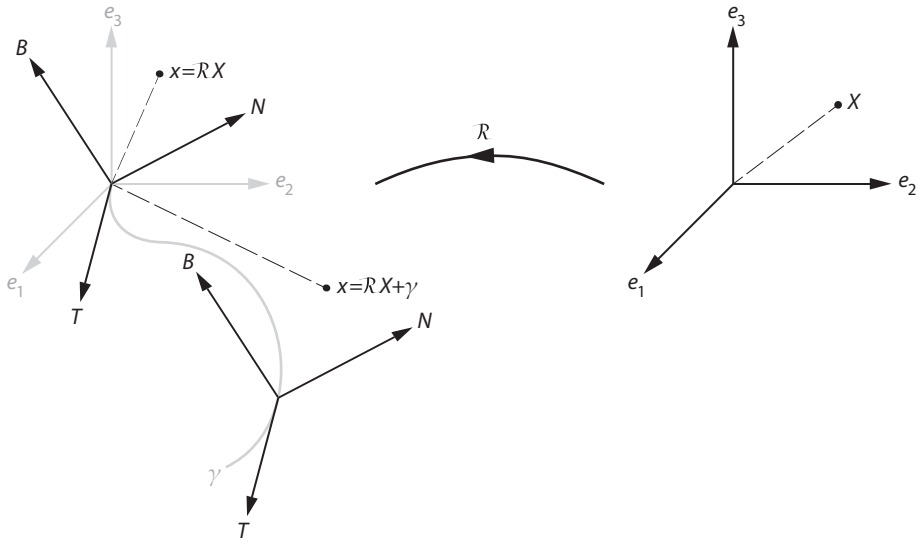

Figure 3.7. $\mathcal{R}$ describes the rotation of a moving frame. It is the coordinate transformations from the rotating coordinate system to a stationary coordinate system. The translational part along the corresponding framed curve can be obtained by integration.

Curvatures κ_1, κ_2 and torsion τ of a frame $\mathcal{R} = (T, N, B)$ are defined as

$$\begin{aligned} \kappa_1 &\coloneqq \langle T', N \rangle \\ \kappa_2 &\coloneqq \langle T', B \rangle \\ \tau &\coloneqq \langle N', B \rangle. \end{aligned}$$

Remark 3.10. A moving frame can be recovered from the differentiable data $\kappa_1, \kappa_2, \tau : [0, L] \to \mathbb{R}$ up to rotation using the *frame equations*

$$\begin{pmatrix} T \\ N \\ B \end{pmatrix}' = \underbrace{\begin{pmatrix} 0 & \kappa_1 & \kappa_2 \\ -\kappa_1 & 0 & \tau \\ -\kappa_2 & -\tau & 0 \end{pmatrix}}_{=A} \begin{pmatrix} T \\ N \\ B \end{pmatrix}. \tag{3.4}$$

Definition 3.5 (framed curve)**.** A *framed curve* is given by an arc length parametrized curve $\gamma : I \to \mathbb{R}^3$, $T \coloneqq \gamma'$ together with a unit normal field $N : I \to \mathbb{S}^2$, i.e. $\langle N, T\rangle = 0$.

A framed curve is carrying a moving frame $\mathcal{R} : I \to \mathrm{SO}(3)$, $\mathcal{R} \coloneqq (T, N, B)$, where $B \coloneqq T \times N$. Vice versa, given an orthonormal frame we can recover the curve γ (up to translation) by integration of T.
So framed curves and moving frames are in one-to-one correspondence.
The curvature $\kappa \coloneqq \|\gamma''\| = \|T'\|$ of the curve γ satisfies

$$\kappa^2 = \kappa_1^2 + \kappa_2^2.$$

for any frame.

Remark 3.11. The transformation $x = \mathcal{R}X$ captures only the rotation of the frame, not the translation along the curve. The coordinates in the moving frame –as it moves along the curve– are given by

$$x(s) = \mathcal{R}(s)X + \gamma(s),$$

where $\gamma = \int T$.

Using $\mathbb{H}_1$ as a double covering of $\mathrm{SO}(3)$ we apply the quaternionic description for Euclidean motions. We identify $\mathcal{R} : I \to \mathrm{SO}(3)$ with[18]

$$\Phi : I \to \mathbb{H}_1,$$

i.e.

$$\mathcal{R} \in \mathrm{SO}(3) \text{ acts on } X \in \mathbb{R}^3 \text{ by } x = \mathcal{R}X$$

becomes

$$\Phi \in \mathbb{H}_1 \text{ acts on } X \in \mathrm{Im}\mathbb{H} \text{ by } x = \Phi X \Phi^{-1}.$$

Then the movement of some static point $X = X_1\mathbb{i} + X_2\mathbb{j} + X_3\mathbb{k} \in \mathrm{Im}\mathbb{H}$ in the rotating frame as it is seen in the stationary frame is described by the differential equation

$$\begin{aligned} x' &= \Phi' X \Phi^{-1} - \Phi X \Phi^{-1}\Phi'\Phi^{-1} \\ &= [\Phi'\Phi^{-1}, x] = \frac{1}{2}[\omega, x] = \omega \times x, \end{aligned}$$

where $\omega \coloneqq 2\Phi'\Phi^{-1}$, i.e.

$$\Phi' = \frac{1}{2}\omega\Phi. \tag{3.5}$$

Here, ω is called the *angular velocity* in the stationary frame. In the rotating frame the angular velocity is seen as Ω where $\omega = \Phi\Omega\Phi^{-1}$, i.e. $\Omega = 2\Phi^{-1}\Phi'$. The movement of the frame in terms of Ω can be expressed as

$$\Phi' = \frac{1}{2}\Phi\Omega. \tag{3.6}$$

[18]Note that Φ is not the Euclidean flow as before, but the quaternion –denoted by q before– corresponding to the rotation of the flow.

Remark 3.12. In this form it corresponds directly to (3.4). Indeed,

$$\begin{aligned}(3.4) &\Leftrightarrow (T,N,B)'^T = A(T,N,B)^T\\ &\Leftrightarrow \mathcal{R}'^T = A\mathcal{R}^T\\ &\Leftrightarrow \mathcal{R}' = \mathcal{R}A^T.\end{aligned}$$

The components κ_1, κ_2, τ of $A \in \mathrm{so}(3)$ correspond to the components of $\Omega \in \mathrm{Im}\mathbb{H}$ as we will see below.

For the basis vectors of the frame

$$T, N, B : I \to \mathrm{Im}\mathbb{H}$$

we have

$$T = \Phi \mathbb{i} \Phi^{-1}, \quad N = \Phi \mathbb{j} \Phi^{-1}, \quad B = \Phi \mathbb{k} \Phi^{-1},$$

which becomes

$$\begin{aligned}T' &= \frac{1}{2}[\omega, T] = \omega \times T\\ N' &= \frac{1}{2}[\omega, N] = \omega \times N\\ B' &= \frac{1}{2}[\omega, B] = \omega \times B\end{aligned} \tag{3.7}$$

upon differentiation. From here we obtain

$$\begin{aligned}\kappa_1 &= \langle T', N\rangle = \langle \omega \times T, N\rangle = \langle T \times N, \omega\rangle = \langle B, \omega\rangle = \langle e_3, \Omega\rangle\\ \kappa_2 &= \langle T', B\rangle = \langle \omega \times T, B\rangle = \langle T \times B, \omega\rangle = -\langle N, \omega\rangle = -\langle e_2, \Omega\rangle\\ \tau &= \langle N', B\rangle = \langle \omega \times N, B\rangle = \langle N \times B, \omega\rangle = \langle T, \omega\rangle = \langle e_1, \Omega\rangle.\end{aligned}$$

Remark 3.13. (3.4), (3.5), (3.6), (3.7) are equivalent versions of the frame equations using different choices within the identifications

$$\mathrm{SO}(3) \;\leftrightarrow\; \mathbb{H}_1, \quad \mathbb{R}^3 \;\leftrightarrow\; \mathrm{so}(3) \;\leftrightarrow\; \mathrm{Im}\mathbb{H}$$

or different coordinate systems to express the angular velocity. They describe the relation between the rotating motion and its angular velocity as the infinitesimal generator.

3.4.1 The Lagrange top

The *Lagrange top* is a rigid body with a symmetry axis that rotates around a fixed point on its symmetry axis in a homogeneous gravitational field. Let $\Phi \cong (T, N, B) : I \to \mathrm{SO}(3)$ be the rotating frame fixed within the body such that T is aligned with the axis of symmetry. In this body frame the tensor of inertia is diagonal and looks like

$$J = \begin{pmatrix}\alpha & 0 & 0\\ 0 & 1 & 0\\ 0 & 0 & 1\end{pmatrix}$$

with some $\alpha > 0$. The kinetic energy of the Lagrange-top is

$$\begin{aligned}\mathcal{T} = \langle \Omega, J\Omega\rangle &= \alpha\langle e_1, \Omega\rangle^2 + \langle e_2, \Omega\rangle^2 + \langle e_3, \Omega\rangle^2\\ &= \alpha\langle T, \omega\rangle^2 + \langle N, \omega\rangle^2 + \langle B, \omega\rangle^2\\ &= \alpha\tau^2 + \kappa^2.\end{aligned} \tag{3.8}$$

Alternatively, in terms of T and ω only:

$$\begin{aligned}\langle \Omega, J\Omega\rangle &= \langle \Omega, \Omega\rangle - \langle \Omega, (J-\mathrm{id})\Omega\rangle \\ &= \langle \omega, \omega\rangle + (\alpha-1)\langle T, \omega\rangle^2.\end{aligned} \tag{3.9}$$

For symmetry reasons the Lagrange top has its barycenter on the axis of symmetry, which goes through T. So its potential energy is given by

$$\mathcal{U} = -2\langle a, T\rangle$$

with some $a \in \mathbb{R}^3$.

We obtain the action functional for the Lagrange top

$$\mathcal{S}[\Phi] = \int_0^L \left(\langle \omega, \omega\rangle + (\alpha-1)\langle \omega, T\rangle^2 + 2\langle a, T\rangle\right) \mathrm{d}s. \tag{3.10}$$

Remark 3.14. Note that the functional $\mathcal{S}[\Phi]$ originally depends on $\Phi : I \to \mathbb{H}_1$. In particular it depends on its derivative $\varphi(s) = \Phi'(s) \in \mathrm{T}_{\Phi(s)}\mathbb{H}_1$, or equivalently[19] on $\omega(s) = 2\Phi'(s)\Phi^{-1}(s) \in \mathrm{Im}\mathbb{H}$.
If we want to treat (Φ, φ) as independent variables,[20] we have to impose an additional constraint characterizing the relation $\Phi' = \varphi$. In terms of (Φ, ω) this is $\Phi' = \frac{1}{2}\omega\Phi$. This leads to the phase space $\mathbb{H}_1 \times \mathrm{Im}\mathbb{H}$. Since Φ enters $\mathcal{S}$ only in terms of T we can of course reduce this further, replacing $\mathbb{H}_1$ by $\mathbb{S}^2$.
Finally we end up with a functional $\mathcal{S}[T, \omega]$ on the phase space $\mathbb{S}^2 \times \mathbb{R}^3$ and the additional condition $T' = \omega \times T$.

Remark 3.15. From now on we will not distinguish between $\mathcal{R} \in \mathrm{SO}(3)$ and $\Phi \in \mathbb{H}_1$ anymore.

3.5 Smooth elastic rods

Elastic rods are described by framed curves

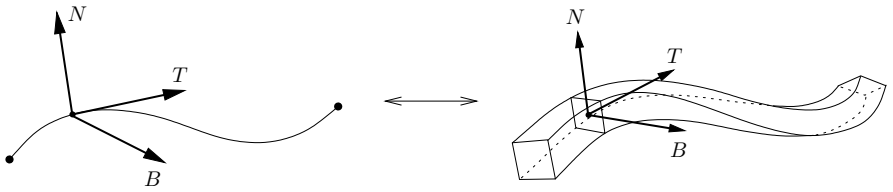

Figure 3.8. Elastic rods as framed curves

We extend variations of the curve $\gamma : [0, L] \to \mathbb{R}^3$ with fixed endpoints and fixed length to the frame $\Phi : [0, L] \to \mathrm{SO}(3)$,

[19] By identifying all tangent spaces of $\mathbb{H}_1$ with $\mathrm{Im}\mathbb{H}$ by right translation.

[20] This means replacing the configuration space SO(3) by the phase space TSO(3) which is the tangent bundle.

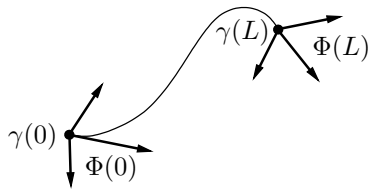

Figure 3.9. Curve with fixed end-frames.

which leads to admissible variations that

- fix $\gamma(0)$, $\gamma(L) \in \mathbb{R}^3$,
- fix $\Phi(0)$, $\Phi(L) \in \mathrm{SO}(3)$,
- preserve orthonormality, i.e. $\Phi(s) \in \mathrm{SO}(3)$ for all $s \in [0, L]$, in particular preserve the arc length parametrization and therefore the length of the curve.

We complement the bending energy of γ by an adjustable torsion energy

$$\mathcal{E}[\Phi] \coloneqq \int_0^L \left(\kappa(s)^2 + \alpha\tau(s)^2\right) \mathrm{d}s$$

with some *torsion coefficient* $\alpha \neq 0$.

Definition 3.6 (Elastic rod)**.** An (isotropic) *elastic rod* is a framed curve (γ, Φ) which is a critical point of the energy functional $\mathcal{E}$ under the described admissible variations.

If we want to formulate the variational problem solely in terms of the moving frame $\Phi : [0, L] \to \mathrm{SO}(3)$, we have to impose the additional constraint

- $\int_0^L T(s)\mathrm{d}s = \gamma(L) - \gamma(L) \in \mathbb{R}^3$

again, to take the fixed endpoints of the curve into account.

We use

$$\kappa^2 + \alpha\tau^2 = \langle\omega, \omega\rangle + (\alpha - 1)\langle\omega, T\rangle^2$$

as follows from (3.8) and (3.9) to express the energy in terms of the angular velocity ω and T only, where $T' = \omega \times T$. Implementing the constraint for the fixed endpoints of the curve $\int_0^L T(s)\mathrm{d}s = const.$ via Lagrange-multiplicators, we finally obtain

$$\mathcal{E}_a[T, \omega] = \int_0^L \left(\langle\omega, \omega\rangle + (\alpha - 1)\langle\omega, T\rangle^2 + 2\langle a, T\rangle\right) \mathrm{d}s.$$

Recognizing the action functional (3.10) of the Lagrange top we formulate the Kirchhoff analogy for elastic rods.

Theorem 3.11 (Kirchhoff analogy for elastic rods)**.** *A arc length parametrized curve $\gamma : [0, L] \to \mathbb{R}^3$ with frame $\Phi : [0, L] \to \mathrm{SO}(3)$ is an elastic rod if and only if its tangent vector $T \coloneqq \gamma' : [0, L] \to \mathbb{S}^2$ describes the evolution of the symmetry axis of the Lagrange top with angular velocity $\omega : [0, L] \to \mathbb{R}^3$ of the frame Φ. The arc length parameter of the framed curve coincides with the time parameter of the top.*

To derive the Euler-Lagrange equations for elastic rods, we investigate how admissible variations of Φ look in terms of ω and T where $T' = \omega \times \Phi$.
Since $\mathbb{H}_1$ is a multiplicative (differentiable) group we can express all variations

$$\tilde{\Phi} : [0, L] \times (-\varepsilon, \varepsilon) \to \mathbb{H}_1$$

as

$$\tilde{\Phi}(s, t) = H(s, t)\Phi(s),$$

where

$$H : [0, L] \times (-\varepsilon, \varepsilon) \to \mathbb{H}_1$$

with $H(s, 0) = 1$, $H(0, t) = H(L, t) = 0$.

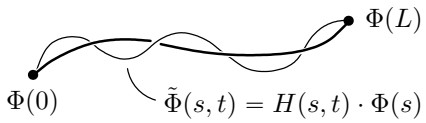

Figure 3.10. Variations of the frame Φ in terms of multiplication by a quaternion.

The variational vector fields along the curve are described by

$$\eta(s) \coloneqq \dot{\eta}(s, 0) = \frac{\partial H}{\partial t}(s, 0) \in \mathrm{Im}\mathbb{H} \qquad \big(\Rightarrow \eta(0) = \eta(L) = 0\big),$$

which build a vector space.[21]

So admissible variations of $\omega(s) = 2\Phi'(s)\Phi^{-1}(s)$ become

$$\begin{aligned}\tilde{\omega}(s, t) &\coloneqq 2\tilde{\Phi}'(s, t)\tilde{\Phi}^{-1}(s, t) = 2(H\Phi)'(H\Phi)^{-1} \\ &= 2(H'\Phi + H\Phi')\Phi^{-1}H^{-1} = 2(H'\Phi + \frac{1}{2}H\omega\Phi)\Phi^{-1}H^{-1} \\ &= 2H'H^{-1} + H\omega H^{-1},\end{aligned}$$

and the corresponding variational vector fields

$$\begin{aligned}\dot{\tilde{\omega}}(s, 0) &= \big(2\eta' H^{-1} - 2H'H^{-1}\eta H^{-1} + \eta\omega H^{-1} - H\omega H^{-1}\eta H^{-1}\big)\big|_{t=0} \\ &= 2\eta' + \eta\omega - \omega\eta = 2\eta' + [\eta, \omega] = 2(\eta' + \eta \times \omega).\end{aligned}$$

With $T(0) = \mathbb{i}$ the integral version of $T' = \omega \times T = \frac{1}{2}[\omega, T]$ is $T = \Phi\mathbb{i}\Phi^{-1}$. So admissible variations of T are

$$\tilde{T}(s, t) \coloneqq \tilde{\Phi}\mathbb{i}\tilde{\Phi}^{-1} = H\Phi\mathbb{i}\Phi^{-1}H^{-1} = HTH^{-1},$$

and the corresponding variational vector fields

$$\begin{aligned}\dot{\tilde{T}}(s, 0) &= \big(\eta TH^{-1} - HTH^{-1}\eta H^{-1}\big)\big|_{t=0} \\ &= \eta T - T\eta = [\eta, T] = 2\eta \times T.\end{aligned}$$

This describes admissible variations of $(T, \omega) : [0, L] \to \mathbb{S}^2 \times \mathbb{R}^3$.

[21] We denote partial derivatives w.r.t. s by $'$ and w.r.t. t by $\dot{}$

For the variation of the energy we obtain

$$\begin{aligned}
\frac{\mathrm{d}}{\mathrm{d}t}\Big|_{t=0} \mathcal{E}_a[\tilde{T},\tilde{\omega}] &= \int_0^L \frac{\partial}{\partial t}\Big|_{t=0} \Big(\langle\tilde{\omega},\tilde{\omega}\rangle + (\alpha-1)\langle\tilde{\omega},\tilde{T}\rangle^2 + 2\langle a,\tilde{T}\rangle\Big)\,\mathrm{d}s \\
&= 4\int_0^L \big(\langle\eta'+\eta\times\omega,\omega\rangle + (\alpha-1)\langle\omega,T\rangle(\langle\eta'+\eta\times\omega,T\rangle + \langle\omega,\eta\times T\rangle) \\
&\qquad + \langle a,\eta\times T\rangle\big)\mathrm{d}s \\
&= 4\int_0^L \big(\langle\eta',\omega\rangle + (\alpha-1)\langle\omega,T\rangle\langle\eta',T\rangle + \langle a,\eta\times T\rangle\big)\,\mathrm{d}s \\
&= 4\int_0^L \big(\langle\eta',-\omega+(1-\alpha)\tau T\rangle + \langle\eta,T\times a\rangle\big)\mathrm{d}s \\
&= 4\int_0^L \langle\eta,-\omega'+(1-\alpha)(\tau' T+\tau T') + T\times a\rangle\mathrm{d}s,
\end{aligned}$$

where we used partial integration with vanishing boundary terms due to $\eta(0) = \eta(L) = 0$. So the Euler-Lagrange equations are given by

$$\begin{cases} T' &= \omega\times T \\ \omega' &= (1-\alpha)(\tau' T+\tau T') + T\times a. \end{cases}$$

Further simplification is still possible by the following Lemma.

Lemma 3.12. *The torsion τ of an elastic rod is constant.*

Proof. We have $\tau = \langle\omega, T\rangle$. So

$$\tau' = \langle\omega', T\rangle + \langle\omega, T'\rangle = (1-\alpha)\tau',$$

where we plugged in the Euler-Lagrange equations for T' and ω'. So we get $\tau' = 0$ since $\alpha \neq 0$ for elastic rods. □

Eventually we arrive at the final version of the Euler-Lagrange equations for elastic rods.

Theorem 3.13 (Euler-Lagrange equations for elastic rods)**.** *An arc length parametrized curve $\gamma : [0, L] \to \mathbb{R}^3$ with frame $\Phi : [0, L] \to \mathbb{R}^3$ is an elastic rod with torsion coefficient α if and only if its torsion τ is constant ($\tau' = 0$) and one of the following conditions is satisfied:*

(i) There is $a \in \mathbb{R}^3$ such that

$$\begin{cases} T' &= \omega\times T \\ \omega' &= (1-\alpha)\tau T' + T\times a, \end{cases}$$

where $T = \gamma'$ is the tangent vector and $\omega = 2\Phi'\Phi^{-1}$ the angular velocity of the frame.

(ii) There is $a, b \in \mathbb{R}^3$ such that

$$\gamma''\times\gamma' + c\gamma' = a\times\gamma + b.$$

(iii) There is $a \in \mathbb{R}^3$ such that

$$T'' \times T + cT = a \times T,$$

where $c \coloneqq -\alpha\tau$.

Proof. We are left to show the equivalence of these three equations.

(ii)⇔(iii) By integration/differentiation.

(i)⇒(ii) Integrating $\omega' = (1-\alpha)\tau T' + T \times a$, we obtain

$$\omega + b = (1-\alpha)\tau T + \gamma \times a.$$

From this and $T' = \omega \times T$ we get

$$\begin{aligned} T' \times T = (\omega \times T) \times T &= \langle \omega, T \rangle T - \omega \\ &= \tau T - \omega = \alpha\tau T + a \times \gamma + b. \end{aligned}$$

(iii)⇒(i) Define ω by $T' = \omega \times T$ and $\langle \omega, T \rangle = \tau$.[22]
Then $T'' = \omega' \times T + \omega \times T'$. So

$$T'' \times T = \langle \omega', T \rangle T - \omega' + \langle \omega, T \rangle T' = \tau T' - \omega'.$$

On the other hand we have

$$T'' \times T = \tau\alpha T' + a \times T.$$

Together this implies

$$\omega' = (1-\alpha)\tau T' + T \times a.$$

□

We identify the left hand sides of (ii) and (iii) as a linear combination of the Heisenberg flow ∂_t and the tangent flow ∂_x, i.e.

$$(\partial_t + c\partial_x)\gamma = a \times \gamma + b$$

and

$$(\partial_t + c\partial_x)T = a \times T.$$

Corollary 3.14. *A framed curve is an elastic rod if and only if a linear combination of the Heisenberg flow and the tangent flow with non-zero coefficients preserves its form, i.e. under the action of this combined flow the curve evolves by an Euclidean motion.*

[22] In quaternions this is $\omega \coloneqq (T' - \tau)T^{-1}$.

Remark 3.16 (anisotropic elastic rods). The theory can be generalized to anisotropic elastic rods by using an anisotropic bending energy

$$\mathcal{E} = \int \left(\alpha_1 \kappa_1^2 + \alpha_2 \kappa_2^2 + \alpha_3 \tau^2\right) \mathrm{d}s.$$

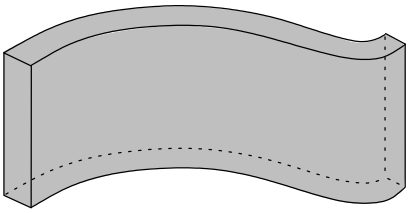

Figure 3.11. Anisotropic rod. The bending energy depends on the cross section.

3.6 Discrete elastic rods

We use the characterization in terms of Heisenberg flow and tangent flow to obtain a definition for discrete elastic rods.

Definition 3.7 (Discrete elastic rods)**.** A discrete arc length parametrized curve $\gamma : I \to \mathbb{R}^3$ is called *discrete elastic rod* if it evolves under a linear combination $(\partial_t + c\partial_x)$, $c \neq 0$ of the discrete Heisenberg flow ∂_t and the discrete tangent flow ∂_x by an Euclidean motion, i.e.

- there is $a, b \in \mathbb{R}^3$ and $c \neq 0$ such that

$$\frac{T_k \times T_{k-1}}{1 + \langle T_k, T_{k-1} \rangle} + c \frac{T_k + T_{k-1}}{1 + \langle T_k, T_{k-1} \rangle} = a \times \gamma_k + b,$$

or equivalently

- there is $a \in \mathbb{R}^3$ and $c \neq 0$ such that

$$\left(\frac{T_{k+1}}{1 + \langle T_{k+1}, T_k \rangle} - \frac{T_{k-1}}{1 + \langle T_k, T_{k-1} \rangle} \right) \times T_k + c \left(\frac{T_{k+1} + T_k}{1 + \langle T_{k+1}, T_k \rangle} + \frac{T_k + T_{k-1}}{1 + \langle T_k, T_{k-1} \rangle} \right) = a \times T_k.$$

Remark 3.17. These equations go to the Euler-Lagrange equations for smooth elastic rods since the discrete Heisenberg flow and discrete tangent flow go to their corresponding smooth counterparts, which we have seen already.

Part II
Discrete Surfaces

We consider discrete surfaces consisting of vertices, edges and faces from the point of view of topology (abstract discrete surfaces), metric geometry (piecewise flat surfaces) and Euclidean geometry (polyhedral surfaces).

4 Abstract discrete surfaces

4.1 Cell decompositions of surfaces

From the topological point of view a discrete surface is a decomposition of a two-dimensional manifold into vertices, edges and faces. This is what we call the *combinatorics* of a discrete surface.

First some preliminary definitions

Definition 4.1 (surface)**.** A *surface* is a real two-dimensional connected manifold, possibly with boundary.

Remark 4.1. We mainly focus on compact surfaces and compact closed surfaces.

Definition 4.2 (n-cell)**.** We denote the open disk in $\mathbb{R}^n$ by

$$D^n \coloneqq \{x \in \mathbb{R}^n \mid \|x\| < 1\}$$

and its boundary by

$$\partial D^n \coloneqq \overline{D^n} \backslash D^n,$$

where the bar denotes the topological closure.
An *n-dimensional cell* or *n-cell* is a topological space homeomorphic to D^n.

Remark 4.2. Note that $D^0 = \{0\}$ is a point and its boundary $\partial D^0 = \varnothing$.

Definition 4.3 (cell decomposition)**.** Let M be a surface and $T = \{U_i\}_{i=1}^N$ a covering of M by pairwise disjoint 0-, 1- and 2-cells.
T is called a finite *cell decomposition* of M if for any n-cell $U_i \in T$ there is a continuous map

$$\varphi_i : \overline{D^n} \to M$$

which maps D^n homeomorphic to U_i and ∂D^n to a union of cells of dimension at most $n-1$, i.e. 1-cells are bounded by 0-cells and 2-cells by 1- and 0-cells.
0-cells are called *vertices*, 1-cells *edges* and 2-cells *faces*.

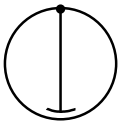

Figure 4.1. This is not a cell decomposition.

Remark 4.3.

- More requirements are needed to define infinite cell decompositions.
- The existence of a finite cell decomposition makes a surface necessarily compact.
- Cell decompositions of surfaces are a special case of *cell complexes*. E.g. a 1-dimensional cell complex is a *graph*.

Example 4.1. A convex polyhedron induces a cell decomposition of $\mathbb{S}^2$.

We introduce some additional properties coming from polyhedra theory but mostly deal with general cell decompositions.

Definition 4.4 (regular and strongly regular)**.** A cell decomposition $T = \{U_i\}_{i=1}^N$ of a surface M is called *regular* if the maps $\varphi_i : \overline{D^n} \to M$ are homeomorphisms.
A regular cell decomposition is called *strongly regular* if for any two cells U_i and U_j the intersection of their closures $\overline{U_i} \cap \overline{U_j}$ is either empty or the closure of *one* cell.

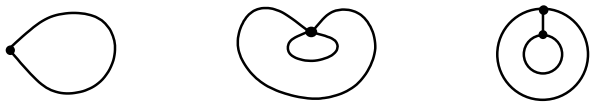

Figure 4.2. Examples of non-regular cell decompositions. Cells with boundary identifications –i.e. self-touching cells– are not allowed. E.g. no loops.

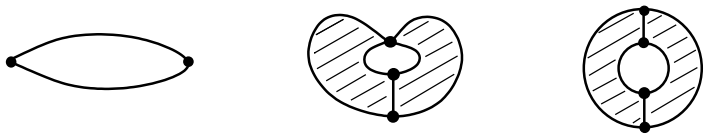

Figure 4.3. Examples of non-strongly regular cell decompositions. Cells with multiple common boundary components are not allowed. E.g. no double edges.

Example 4.2.

(1) The cell decompositions of $\mathbb{S}^2$ induced by convex polyhedra are strongly regular.

(2) Cube with a hole:

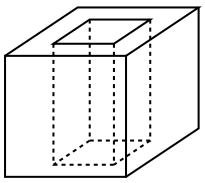

This is not a cell-decomposition of the cube with a hole.

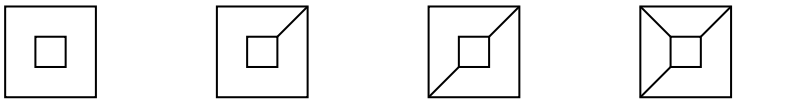

Figure 4.4. Cube with a hole. From "not a cell decomposition" to a strongly regular cell decomposition by adding edges.

Definition 4.5 (abstract discrete surface)**.** Let T be a cell decomposition of a surface M. Then we call the combinatorial data $\mathcal{S} \coloneqq (M, T)$ an *abstract discrete surface* and a homeomorphism $f : M \to \mathbb{R}^n$ its *geometric realization*. We write this as $f : \mathcal{S} \to \mathbb{R}^n$.

Remark 4.4.

- Abstract discrete surfaces are compact.
- We use the terms vertices, edges and faces for the combinatorial cells $U_i \in T$ as well as for the images under the geometric realization $f(U_i) \subset f(M) \subset \mathbb{R}^n$.

Example 4.3 (quad-graph)**.** A *quad-graph* is an abstract discrete surface with all faces being quadrilaterals. A geometric realization with planar faces is called a *Q-net*.

4.2 Topological classification of compact surfaces

We outline the topological classification of compact surfaces. This means that we are interested in topological invariants which uniquely identify a compact surface up to homeomorphisms. A cell decomposition of a surface induces the following topological invariant.

Definition 4.6 (Euler characteristic)**.** Let V, E, F be the sets of vertices, edges and faces of an abstract discrete surface $\mathcal{S} \coloneqq (M, T)$ and $|V|$, $|E|$, $|F|$ their cardinalities. Then

$$\chi(M) \coloneqq |V| - |E| + |F|$$

is called the *Euler characteristic* of M.

Remark 4.5. Since the Euler characteristic is independent of the cell decomposition T of M and every compact surface has a cell decomposition[23], this indeed defines a topological invariant of the surface M.

Example 4.4.

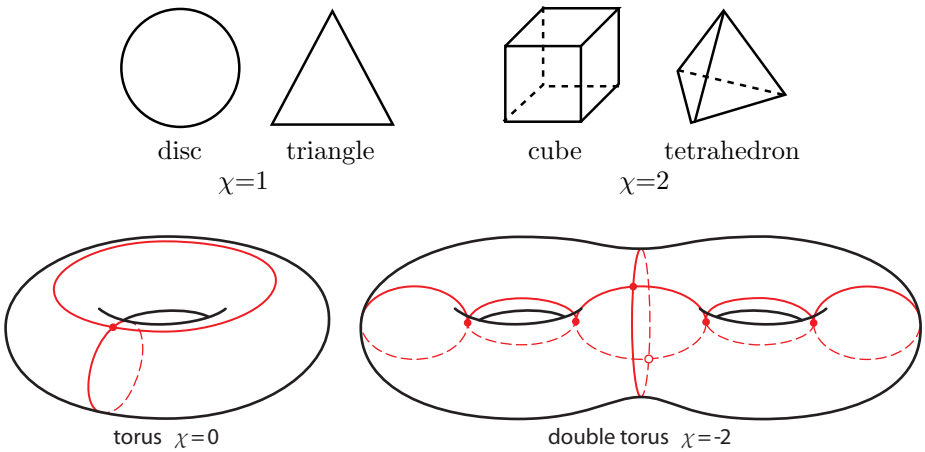

Figure 4.5. Cell decompositions of a disk, sphere, torus and double torus. With Euler characteristic $\chi = |V| - |E| + |F|$.

We describe the construction of closed surfaces by combining some elementary compact closed surfaces of high Euler characteristic using the connected sum. The classification theorem then states that this already yields all possible compact closed surfaces up to homeomorphisms.

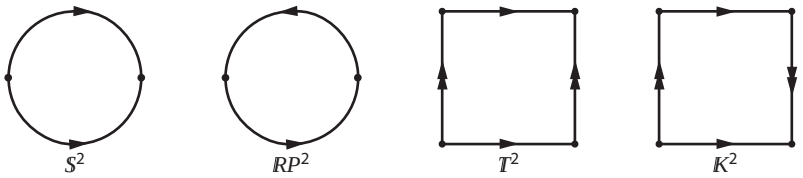

Figure 4.6. Elementary closed surfaces from identifying edges of bigons and quadrilaterals.

There are two essentially different ways of orienting the two edges of a bigon. Identifying the two edges along these orientations yields the *sphere* $\mathbb{S}^2$ and the *real projective plane* $\mathbb{RP}^2$ respectively. The first of which is orientable while the second is not. Counting vertices, edges and faces of the cell decompositions induced by the original bigon we obtain the Euler characteristics

$$\chi(\mathbb{S}^2) = 2 - 1 + 1 = 2, \quad \chi(\mathbb{RP}^2) = 1 - 1 + 1 = 1.$$

Pairwise identifying the four edges of a quadrilateral gives us two additional

[23] Even stronger: Every compact surface has a triangulation.
Note that abstract discrete surfaces –which is our case of interest– are compact and always come with a cell decomposition.

surfaces which are the *torus* $\mathbb{T}^2$ and the *Klein bottle* $\mathbb{K}^2$ with

$$\chi(\mathbb{T}^2) = 1 - 2 + 1 = 0, \quad \chi(\mathbb{K}^2) = 1 - 2 + 1 = 0.$$

We notice that the torus and the Klein bottle can not be distinguished by their Euler characteristic alone. But the torus is orientable while the Klein bottle is not.

For two surfaces M and N their connected sum $M\#N$ is obtained by removing an open disk from each and gluing the resulting surfaces together along the circular boundary components of the missing disks.
This operation is associative, commutative and the sphere is the identity element, i.e.

$$M\#\mathbb{S}^2 = \mathbb{S}^2\#M = M$$

Let us determine the Euler characteristic of the connected sum $M\#N$. Consider a cell decomposition of M and N respectively. A cell decomposition of M° which is the surface M with an open disk removed can be obtained by adding one edge as a loop at one vertex of the cell decomposition of M, so

$$\chi(M^\circ) = \chi(M) - 1.$$

Same for N°. Gluing along the circular boundaries is then equivalent to the identification of these new edges and the adjacent vertex. So we have one edge less and one vertex less in the connected sum which cancel out in the Euler characteristic

$$\chi(M\#N) = \chi(M^\circ) + \chi(N^\circ) - 1 + 1 = \chi(M) + \chi(N) - 2.$$

Starting with a sphere as the identity element we construct surfaces of lower Euler characteristic by connecting tori, projective planes and Klein bottles to it. Connecting g tori to the sphere[24] yields an orientable surface with g holes, i.e.

$$\chi((\mathbb{T}^2)^{\#g}) = \chi(\mathbb{T}^2\#\ldots\#\mathbb{T}^2) = 2 - 2g, \qquad g \geqslant 0,$$

where we define $M^{\#0} \coloneqq \mathbb{S}^2$ by the identity element. g is called the *genus* of the resulting surface.

Building the connected sum of h projective planes we obtain surfaces of odd and even Euler characteristic all of them non-orientable.[25]

$$\chi((\mathbb{RP}^2)^{\#h}) = \chi(\mathbb{RP}^2\#\ldots\#\mathbb{RP}^2) = 2 - h, \qquad h \geqslant 1.$$

Any other combination of connected sums of our elementary surfaces $\mathbb{S}^2$, $\mathbb{T}^2$, $\mathbb{RP}^2$ and $\mathbb{K}^2$ does not yield new surfaces. Indeed building the connected sum of two projective planes already gives us a Klein bottle

$$\mathbb{RP}^2\#\mathbb{RP}^2 = \mathbb{K}.$$

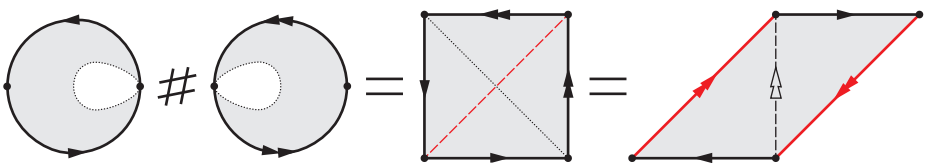

Figure 4.7. The connected sum of two projective planes is a Klein bottle.

[24] Or equivalently to each other.
[25] Any connected sum containing at least one projective plane is non-orientable.

Attaching another projective plane to the Klein bottle is the same as attaching it to a torus[26]

$$\mathbb{K}\#\mathbb{RP}^2 = \mathbb{T}^2\#\mathbb{RP}^2.$$

So any mixed combinations of tori and projective planes are already included.[27]

$\mathbb{T}^2$ and $\mathbb{RP}^2$ together with the connected sum $\#$ generate a monoid of which the classification theorem states that it already includes all compact closed surfaces.

Theorem 4.1 (classification by connected sums)**.** *Any compact closed surface M is either homeomorphic to the connected sum of $g \geqslant 0$ tori*

$$M = (\mathbb{T}^2)^{\#g}$$

or to the connected sum of $h \geqslant 1$ real projective planes

$$M = (\mathbb{RP}^2)^{\#h}.$$

In the first case M is orientable and in the second non-orientable.

And as an immediate consequence of our considerations about the Euler characteristics

Corollary 4.2 (classification by orientability and Euler characteristic)**.** *Any compact closed surface is uniquely determined by its orientability and Euler characteristic up to homeomorphisms.*

Remark 4.6.

- A compact closed orientable surface can be classified by its Euler characteristic only, or equivalently by its genus g since

$$\chi(M) = 2 - 2g.$$

- The classification theorem can be generalized to compact surfaces with boundary by adding another topological invariant which is the number of connected boundary components k. In this case the Euler characteristic for orientable surfaces becomes

$$\chi(M) = 2 - 2g - k.$$

- The easiest and most recent proof of the classification theorem is Conway's ZIP proof which can be found in [FW99].

- The procedure of identifying edges of bigons and quadrilaterals to obtain compact closed surfaces can be generalized to the pairwise identification of edges of even-sided polygons. This leads to other possible ways of classification.

[26] We see that the connected sum has no inverse operation.

[27] This can be restated more general in the following way. On any non-orientable surface there is no way to distinguish a handle from an attached Klein-bottle.

5 Polyhedral surfaces and piecewise flat surfaces

We start with a short presentation of curvature in the classical smooth theory.

5.1 Curvature of smooth surfaces

Extrinsic curvatures of a smooth surface immersed in $\mathbb{R}^3$ are defined as follows. Consider the one parameter family of tangent spheres $S(\kappa)$ with signed curvature κ touching the surface at a point p. κ is positive if the sphere lies at the same side of the tangent plane as the normal vector and negative otherwise. Let M be the set of tangent spheres intersecting any neighborhood U of p in more than one point. The values

$$\kappa_1 \coloneqq \inf_{S\in M} \kappa(S), \quad \kappa_2 \coloneqq \sup_{S\in M} \kappa(S)$$

are called the *principal curvatures* of the surface at p.

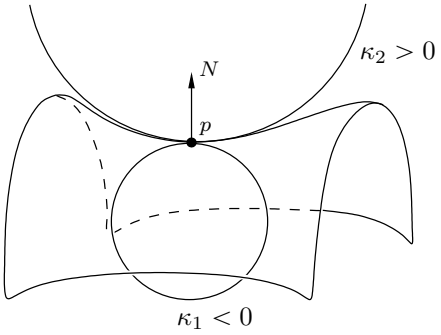

Figure 5.1. The curvature spheres touching the surface in p.

The spheres $S(\kappa_1)$ and $S(\kappa_2)$ are called *principal curvature spheres* and are in second order contact with the surface. The contact directions are called *principal directions* and are orthogonal.

The *Gaussian curvature* and *mean curvature* are defined as

$$K \coloneqq \kappa_1\kappa_2, \quad H \coloneqq \frac{1}{2}(\kappa_1 + \kappa_2).$$

The Gaussian curvature of a surface at a point p is also the quotient of oriented areas $A(\cdot)$:

$$K(p) = \lim_{\varepsilon\to 0} \frac{A(N(U_\varepsilon(p)))}{A(U_\varepsilon(p))},$$

where $U_\varepsilon(p)$ is an ε-neighborhood of p on the surface, and $N(U_\varepsilon(p)) \subset S^2$ is its image under the Gauss map.
The following classical theorems hold.

Theorem 5.1 (Gauss' Theorema Egregium)**.** *The Gaussian curvature of a surface is preserved by isometries.*

Theorem 5.2 (Gauss-Bonnet)**.** *The total Gaussian curvature of a compact closed surface S is given by*

$$\int_S K \mathrm{d}A = 2\pi\chi(S).$$

5.1.1 Steiner's formula

The *normal shift* of a smooth surface S with normal map N is defined as

$$S_\rho := S + \rho N.$$

For sufficiently small ρ the surface S_ρ is also smooth. Interpreting S as an enveloping surface of the principal sphere congruences one can show that the centers of the principal curvature spheres of S and S_ρ coincide. The signed radii are reduced by ρ so the principal curvatures change as

$$\frac{1}{\kappa_{1\rho}} = \frac{1}{\kappa_1} - \rho, \quad \frac{1}{\kappa_{2\rho}} = \frac{1}{\kappa_2} - \rho.$$

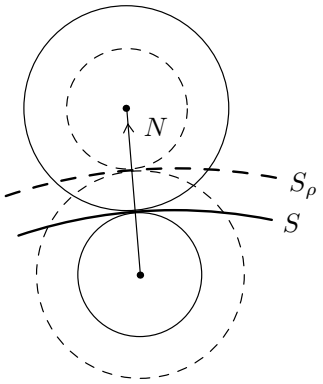

Theorem 5.3 (Steiner's formula)**.** *Let S be a smooth surface and S_ρ its smooth normal shift for sufficiently small ρ. Then the area of S_ρ is a quadratic polynomial in ρ,*

$$A(S_\rho) = A(S) - 2H(S)\rho + K(S)\rho^2,$$

where $K(S) = \int_S K \mathrm{d}A$ and $H(S) = \int_S H \mathrm{d}A$ are the total Gaussian and total mean curvature of S.

Proof. Let $\mathrm{d}A$ and $\mathrm{d}A_\rho$ be the area forms of S and S_ρ. The normal shift preserves the Gauss map, therefore one has

$$K\mathrm{d}A = K_\rho \mathrm{d}A_\rho,$$

where K and K_ρ are the corresponding Gaussian curvatures. For the area this implies

$$\begin{aligned} A(S_\rho) &= \int_{S_\rho} \mathrm{d}A_\rho = \int_S \frac{K}{K_\rho}\mathrm{d}A \\ &= \int_S \kappa_1\kappa_2(\frac{1}{\kappa_1} - \rho)(\frac{1}{\kappa_2} - \rho)\mathrm{d}A \\ &= \int_S \left(1 - (\kappa_1 + \kappa_2)\rho + \kappa_1\kappa_2\rho^2\right)\mathrm{d}A \\ &= A(S) - 2H(S)\rho + K(S)\rho^2. \end{aligned} \tag{5.1}$$

□

Remark 5.1. Equation (5.1) also holds true without integration. We can state Steiner's formula in the differential version

$$\mathrm{d}A_\rho = (1 - 2H(p)\rho + K(p)\rho^2)\mathrm{d}A,$$

where $K(p)$ and $H(p)$ are the (local) Gaussian and mean curvature at p.

5.2 Curvature of polyhedral surfaces

Definition 5.1 (polyhedral surface)**.** A *polyhedral surface* in $\mathbb{R}^n$ is a geometric realization $f : \mathcal{S} \to \mathbb{R}^n$ of an abstract discrete surface $\mathcal{S} = (M, T)$ such that the edges are intervals of straight lines and the faces are planar.
A *simplicial surface* is a polyhedral surface with all faces being triangles.

5.2.1 Discrete Gaussian curvature

For a polyhedral surface the Gaussian curvature is concentrated at vertices in the following sense: The area of $N(U_\varepsilon(p))$ vanishes for all internal points on faces and edges. For a vertex it is equal to the oriented area of the corresponding spherical polygon.

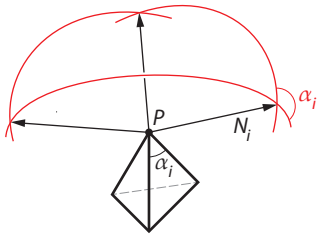

Figure 5.2. The angle α_i at vertex p is the external angle of the spherical polygon at vertex N_i.

Let N_i be the normal vectors of the faces adjacent to the vertex p. Each two neighboring normals define a geodesic line on $\mathbb{S}^2$, which all together constitute a spherical polygon. The angle α_i at vertex p of the face on the polyhedral surface with normal vector N_i is equal to the external angle of the spherical polygon at the vertex N_i. So the angle defect $2\pi - \sum \alpha_i$ at the vertex p is the area of the spherical polygon where $\sum \alpha_i$ is the total angle on the polyhedral surface around the vertex p.[28]

Definition 5.2 (discrete Gaussian curvature)**.** For a closed polyhedral surface S the angle defect

$$K(p) := 2\pi - \sum_i \alpha_i \tag{5.2}$$

at a vertex p is called the *Gaussian curvature* of S at p.
The *total Gaussian curvature* is defined as the sum

$$K(S) := \sum_{p \in V} K(p).$$

The points with $K(p) > 0$, $K(p) = 0$ and $K(p) < 0$ are called *elliptic*, *flat* and *hyperbolic* respectively.

[28] This is an oriented area since the "external angle" depends on the orientation of the polygon.

Remark 5.2. The angle defect at a vertex p is bounded from above by 2π but unbounded from below.

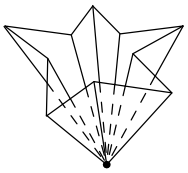

Figure 5.3. The discrete Gaussian curvature at a vertex p can be made arbitrarily low by "folding" a vertex star.

Lemma 5.4. *Let p be an inner point of a polyhedral surface. Then*

$$\begin{aligned} p \text{ convex} &\Rightarrow p \text{ elliptic} \\ p \text{ planar} &\Rightarrow p \text{ flat} \\ p \text{ saddle} &\Rightarrow p \text{ hyperbolic}, \end{aligned}$$

where

$$\begin{aligned} p \text{ convex} &:\Leftrightarrow \text{the spherical polygon of the normal vectors around } p \text{ is convex} \\ p \text{ planar} &:\Leftrightarrow p \text{ and its neighbors lie in a plane} \\ p \text{ saddle} &:\Leftrightarrow p \text{ lies in the convex hull of its neighbors (and } p \text{ not planar).} \end{aligned}$$

Remark 5.3. In general, none of the implications in Lemma 5.4 is reversible.

Since the discrete Gaussian curvature is defined intrinsically[29] we immediately obtain a discrete version of Gauss' Theorema Egregium.

Theorem 5.5 (polyhedral Gauss' Theorema Egregium)**.** *The Gaussian curvature of a polyhedral surface is preserved by isometries, i.e. depends on the polyhedral metric only.*

There also holds a discrete version of the Gauss-Bonnet theorem.

Theorem 5.6 (polyhedral Gauss-Bonnet)**.** *The total Gaussian curvature of a closed polyhedral surface S is given by*

$$K(S) = 2\pi\chi(S).$$

Proof. We have

$$K(S) = \sum_{p \in V} K(p) = 2\pi\,|V| - \sum_{\text{all angles of } S} \alpha_i.$$

The angles $\pi - \alpha_i$ are the (oriented) external angles of a polygon. Their sum is

$$\sum_{\substack{\text{all angles of} \\ \text{one polygon}}} (\pi - \alpha_i) = 2\pi.$$

[29] The cone angle $\sum \alpha_i$ is invariant under isometries. We discuss this and polyhedral metrics in more detail in Section 5.3.

The sum over all faces gives

$$2\pi\,|F| = \sum_{\text{all angles of } S} (\pi - \alpha_i) = 2\pi|E| - \sum_{\text{all angles of } S} \alpha_i,$$

where we used that the number of angles is equal to $2|E|$ (each edge is associated with 4 attached angles but each angle comes with two edges).
Finally

$$K(S) = 2\pi(|V| - |E| + |F|) = 2\pi\chi(S).$$

□

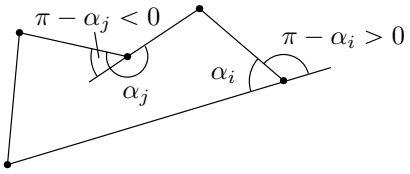

Figure 5.4. Oriented external angles of a polygon.

Example 5.1 (Gaussian curvature of a cube)**.** Consider a standard cube with all vertex angles equal to $\frac{\pi}{2}$. Then the Gaussian curvature at every vertex p is

$$K(p) = 2\pi - 3\frac{\pi}{2} = \frac{\pi}{2}.$$

So the sum over all eight vertices yields $K(S) = 4\pi$.
On the other hand $\chi(S) = \chi(\mathbb{S}^2) = 2$.

Remark 5.4. The polyhedral Gauss-Bonnet theorem can be extended to polyhedral surfaces with boundary. Since the boundary components of a polyhedral surface are piecewise geodesic we only have to add the turning angle of the boundary curve

$$\varphi(p) \coloneqq \pi - \sum_i \alpha_i$$

at each boundary vertex p to the total discrete Gaussian curvature.[30]

5.2.2 Discrete mean curvature

Definition 5.3 (discrete mean curvature)**.** The *discrete mean curvature* of a closed polyhedral surface S at the edge $e \in E$ is defined by

$$H(e) := \frac{1}{2}\theta(e)l(e),$$

where $l(e)$ is the length of e, and $\theta(e)$ is the oriented angle between the normals of the adjacent faces sharing the edge e (the angle is considered to be positive in the convex case and negative otherwise).
The *total mean curvature* is defined as the sum over all edges

$$H(S) := \sum_{e\in E} H(e) = \frac{1}{2}\sum_{e\in E} \theta(e)l(e).$$

[30] Or alternatively define the discrete Gaussian curvature at boundary vertices by the turning angle.

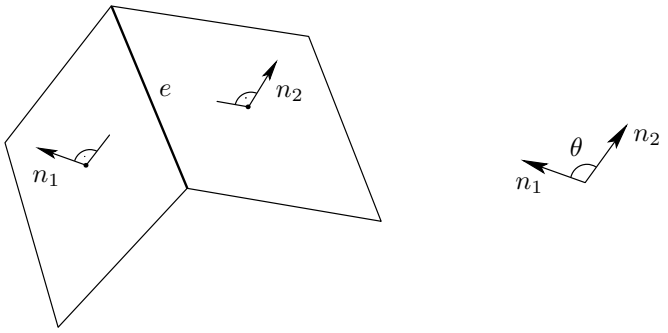

Figure 5.5. Discrete mean curvature for polyhedral surfaces.

With this definition the following discrete version of Steiner's formula holds true.

Theorem 5.7 (Steiner's formula for convex polyhedra)**.** *Let $\mathcal{P}$ be a convex polyhedron with boundary surface $S = \partial\mathcal{P}$. Let $\mathcal{P}_\rho$ be the parallel body at the distance ρ*

$$\mathcal{P}_\rho := \left\{p \in \mathbb{R}^3 \mid d(p, \mathcal{P}) \leqslant \rho\right\}.$$

Then the area of the boundary surface $S_\rho := \partial\mathcal{P}_\rho$ is given by

$$A(S_\rho) = A(S) + 2H(S)\rho + 4\pi\rho^2. \tag{5.3}$$

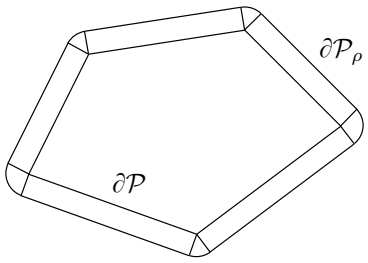

Figure 5.6. Boundary surface S of a convex polyhedron and S_ρ of its parallel body at distance ρ.

Proof. The parallel surface S_ρ consists of three parts:

- Plane pieces congruent to the faces of S.
  Their areas sum up to $A(S)$.
- Cylindrical pieces of radius ρ, angle $\theta(e)$ and length $l(e)$ along the edges e of S with area $\theta(e)l(e)\rho = 2H(e)\rho$.
- Spherical pieces at the vertices p of S with area $K(p)\rho^2$. Since a convex polyhedron is a topological sphere the Gaussian curvature sums up to $K(S) = 4\pi$, i.e. merged together by parallel translation the spherical pieces comprise a round sphere of radius ρ.

□

Remark 5.5 (Steiner's formula for polyhedral surfaces). At non-convex edges and vertices we can define the parallel surface as depicted in Figure 5.7

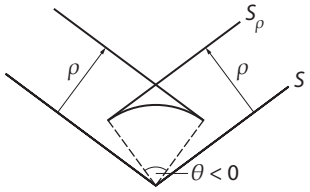

Figure 5.7. On the definition of the parallel surface S_ρ in the non-convex case.

and take the area of the corresponding cylindrical and spherical pieces as negative. Then Steiner's formula for an arbitrary closed polyhedral surface S reads as follows:

$$A(S_\rho) = A(S) + 2H(S)\rho + K(S)\rho^2,$$

where $K(S) = 2\pi\chi(S)$ is the total Gaussian curvature.

5.3 Polyhedral Metrics

We want to investigate the intrinsic geometry induced by polyhedral surfaces.

Definition 5.4. A *metric* on a set M is a map

$$d : M \times M \to \mathbb{R}$$

such that for any $x, y, z \in M$

(i) $d(x, y) \geqslant 0$

(ii) $d(x, y) = 0 \Leftrightarrow x = y$

(iii) $d(x, y) = d(y, x)$

(iv) $d(x, y) + d(y, z) \geqslant d(x, z)$

The pair (M, d) is called a *metric space*.
Let (M, d) and $(\tilde{M}, \tilde{d})$ be two metric spaces. Then a map $f : M \to \tilde{M}$ such that for any $x, y \in M$

$$\tilde{d}(f(x), f(y)) = d(x, y)$$

is called an *isometry*.
(M, d) and $(\tilde{M}, \tilde{d})$ are called *isometric* if there exists a bijective isometry $f : M \to \tilde{M}$ called a *global isometry*.
(M, d) is called *locally isometric* to $(\tilde{M}, \tilde{d})$ at a point $x \in M$ if there exists a neighborhood U of x and a neighborhood $\tilde{U} \subset \tilde{M}$ such that (U, d) is isometric to $(\tilde{U}, \tilde{d})$.

Remark 5.6.

- Every isometry is continuous and every global isometry a homeomorphism.
- An abstract discrete surface $\mathcal{S} = (M, T)$ equipped with a metric becomes a *metric space* (M, d).
- For a geometric realization $f : \mathcal{S} \to \mathbb{R}^n$ the Euclidean metric on $\mathbb{R}^n$ induces a metric on $f(M) \subset \mathbb{R}^n$. To study this metric intrinsically on the corresponding abstract discrete surface $\mathcal{S}$ we pull it back, i.e. we define the metric on $\mathcal{S}$ such that f is an isometry.

Let $f : \mathcal{S} \to \mathbb{R}^n$ be a polyhedral surface. We examine the metric induced by the Euclidean metric of $\mathbb{R}^n$. For two points $x, y \in f(M)$ we are interested in the length $L(\gamma)$ of the shortest curve γ lying on $f(M)$ connecting x and y:

$$d(x, y) = \inf_{\gamma} \{L(\gamma) \mid \gamma : [0, 1] \to f(M), \gamma(0) = x, \gamma(1) = y\} .$$

Example 5.2 (shortest paths on a polyhedral surface)**.** Isometrically unfolding a cube to a plane we see that connecting two points by a straight line might not always constitute a shortest path.

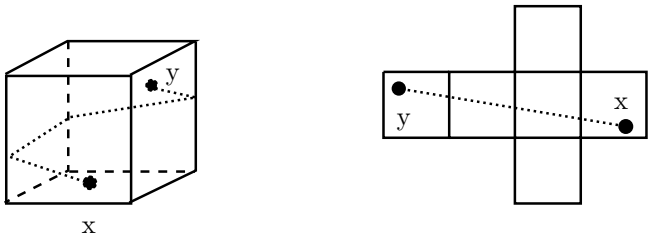

Figure 5.8. Straight line on a cube which is not the shortest path connecting x and y.

Shortest paths are a global property of the metric.

We start by investigating locally shortest paths which are called geodesics. We look for local isometries to some planar domain where we already know the geodesics.

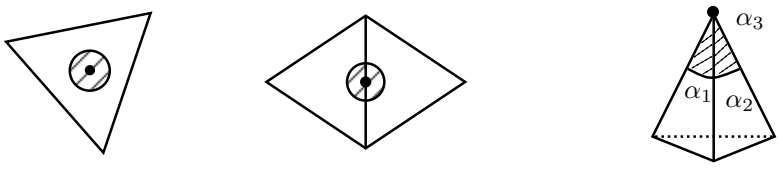

Figure 5.9. Neighborhoods of a point on a face, edge and vertex of a polyhedral surface.

Consider a point $p \in M$ on a face $A \in F$. Then a small enough neighborhood of $f(p)$ on $f(M)$ is entirely contained in the planar face $f(A)$. So the neighborhood can be mapped isometrically to a disk D^2.

For points on edges a small neighborhood intersects the interior of two planar faces. Isometrically unfolding those two faces to a plane we find that the neighborhood is also isometric to a disk.
For points on a vertex we could also unfold the adjacent faces to a plane. But this leaves a cut in the neighborhood. What we can do isometrically is map the small neighborhood to the tip of a cone characterized by the angle θ which is the sum of angles α_i between the edges adjacent to the vertex. The *angle defect*

$$K(p) \coloneqq 2\pi - \theta$$

is a measure for the non-flatness of the metric at p.
In general θ can be greater than 2π in which case the cone becomes a saddle. We make the following classification

$K > 0$ elliptic point, locally isometric to a cone.

$K = 0$ flat point, locally isometric to a disk,
i.e. the vertex and its adjacent edges could be completely removed from the combinatorics without changing the polyhedral surface.

$K < 0$ hyperbolic point, locally isometric to a saddle.

We find that the metric induced on the polyhedral surface $f(M)$ by the Euclidean metric in $\mathbb{R}^n$ is locally equivalent to the Euclidean metric of $\mathbb{R}^2$ everywhere except for the vertices.

Pulling back the metric with the map f to the abstract discrete surface $\mathcal{S}$ we obtain a metric with the same properties, i.e. a small neighborhood of a point $p \in M$ on a

- face is isometric to a disk D^2.
- edge is isometric to a disk D^2.
- vertex is isometric to the tip of a cone.

We can now forget about the combinatorics and obtain an abstract surface M with a polyhedral metric which we call piecewise flat surface.

Definition 5.5 (piecewise flat surface)**.** A metric d on a surface M is called a *polyhedral metric* if (M, d) is locally isometric to a cone at finitely many points $V = \{P_1, \dots, P_N\} \subset M$ (*conical singularities* of the metric) and locally isometric to a plane elsewhere.
The pair (M, d) of a surface and a polyhedral metric is called a *piecewise flat surface.*

Remark 5.7. A polyhedral metric d on a surface M carries no obvious information about edges and faces, only about the vertices.

How to prescribe a polyhedral metric?

We investigate how the information about the metric gets transferred from a polyhedral surface to its corresponding piecewise flat surface (w.l.o.g. we consider simplicial surfaces).
A simplicial surface induces a piecewise flat surface (M, d) together with a triangulation T such that the vertex set includes the conical singularities and all edges are geodesics on (M, d).

Definition 5.6 (geodesic triangulation)**.** Let (M, d) be a piecewise flat surface with conical singularities V_0.
Then a *geodesic triangulation* of (M, d) is a triangulation of M such that its vertex set includes the conical singularities $V_0 \subset V$ and all edges are geodesics on (M, d).

Remark 5.8. In general a geodesic triangulation on a piecewise flat surface does not have to come from a polyhedral surface.

The geodesic triangulation fixes the polyhedral metric of the piecewise flat surface. Its triangles are isometric to Euclidean triangles with straight edges and the polyhedral metric is determined by the lengths of the edges.
The Euclidean triangles on the other hand are uniquely determined by the lengths of its edges if and only if these satisfy the triangle-inequality.
We obtain the following general construction on how to prescribe a polyhedral metric.[31]

- Start with an abstract discrete surface $\mathcal{S} = (M, T)$ where T is a triangulation.
- Define a length function $l : E \to \mathbb{R}_+$ on the edges E of T such that on every face the triangle-inequality is satisfied.

From this data we can construct unique Euclidean triangles which fit together along corresponding edges of T. We can always glue the obtained Euclidean triangles together along the edges around one common vertex –thus obtaining a polyhedral metric on the abstract surface $\mathcal{S}$– but we cannot be sure that they will fit together to constitute a whole polyhedral surface. Summing up the angles at corresponding vertices we obtain the angle defect of the conical singularities of the polyhedral metric.

We get closer to the answer of the questions:

> Is a piecewise flat surface always realizable as a polyhedral surface?
> And is the corresponding polyhedral surface uniquely determined?

Isometric deformations of a simplicial surface preserve its polyhedral metric and therefore the corresponding piecewise flat surface.

Example 5.3 (pushing a vertex in)**.** If all neighbors of a vertex p are coplanar we can reflect the whole vertex star in this plane without changing any angles.

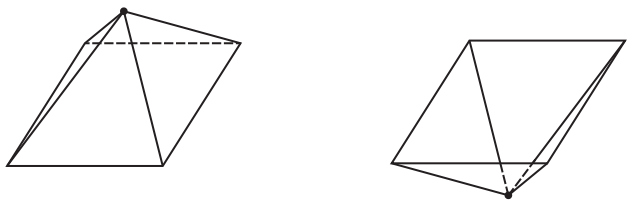

Figure 5.10. Pushing a vertex in does not change the metric.

We obtain the same piecewise flat surface with the same geodesic triangulation. So the polyhedral surface generating a piecewise flat surface is in general not unique.

[31] Note that choosing a triangulation of M –i.e. gluing M together from triangles– to prescribe the polyhedral metric is still eminent in this construction.

Example 5.4 (isometric bending of a polyhedral quadrilateral and edge flipping)**.** Consider two planar triangles with a common edge. Isometrically unfolding the two triangles along the common edge we obtain a planar quadrilateral. If the quadrilateral is convex we can replace the edge by the other diagonal and fold the quadrilateral along this new edge.

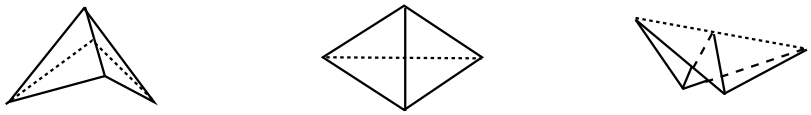

Figure 5.11. Edge flip. Isometrically unfold a quadrilateral to a plane and fold it along the other diagonal.

The edge flip can be done directly on the polyhedral surface without any folding by introducing a non-straight edge.
We obtain a different geodesic triangulation on the same piecewise flat surface which does not necessarily come from a polyhedral surface anymore.

Lemma 5.8 (Possibility of an edge-flip)**.** *Let (M, d) be a piecewise flat surface with a geodesic triangulation T.*
Then an edge e of T can be flipped if its two neighboring triangles are distinct and unfolding them into a plane yields a convex quadrilateral.

Remark 5.9. Since we admit non-regular triangulations we need the condition of the two triangles to be distinct to make the edge flip combinatorially possible.

Example 5.5 (tetrahedron)**.** Four congruent equilateral triangles can be glued together to obtain a tetrahedron.

Figure 5.12. Two geodesic triangulations of the piecewise flat surface given by a tetrahedron.

An edge-flip of one of their edges constitute four triangles which do not fit together as a whole polyhedral surface with the given combinatorics.

We have seen that not every geodesic triangulation of a piecewise flat surface is realizable as a polyhedral surface. Nor is the polyhedral surface we seek uniquely determined even if we know the combinatorics.

We finish this section by stating two classical theorems.

Theorem 5.9 (Burago-Zalgaller, 1960)**.** *Every piecewise flat surface can be realized as a polyhedral surface embedded in* $\mathbb{R}^3$*.*

Remark 5.10*.*

- Note that the ambient space can always be taken to be $\mathbb{R}^3$.
- This is a pure existence statement and the proof gives no indication on how to construct the polyhedral surface.

For convex polyhedral metrics the corresponding polyhedral surface which is convex is unique and can be obtained via a construction algorithm.

Theorem 5.10 (Alexandrov)**.** *Let* (M, d) *be a piecewise flat sphere with a convex polyhedral metric* d*. Then there exists a convex polytope* $\mathcal{P} \subset \mathbb{R}^3$ *such that the boundary of* $\mathcal{P}$ *is isometric to* (M, d)*. Besides,* $\mathcal{P}$ *is unique up to a rigid motion.*

Remark 5.11*.*

- A polyhedral metric d with conical singularities $P_1, \ldots, P_N$ is called convex if all its conical singularities are elliptic, i.e. $K(P_i) \geqslant 0$.
- The edges of $\mathcal{P}$ are a complicated functions of d, since the metric does not distinguish points on edges from points on faces.
- For a proof of this theorem with a construction algorithm see [BI08].
- An implementation of the algorithm can be found at [Sec].

6 Discrete cotan Laplace operator

We introduce a discrete Laplace operator naturally induced by a simplicial surface (or more general by a geodesic triangulation of a piecewise flat surface).

6.1 Smooth Laplace operator in $\mathbb{R}^N$

Let $\Omega \subset \mathbb{R}^N$ be an open set with boundary $\partial\Omega$. We denote the coordinates in $\mathbb{R}^N$ by $x = (x_1, ..., x_N)$. The Laplace operator of a function $f : \Omega \to \mathbb{R}$ is defined by

$$\Delta f = \sum_{i=1}^{N} \frac{\partial^2 f}{\partial x_i^2}$$

A function with $\Delta f = 0$ is called *harmonic*.
The problem of finding a harmonic function with prescribed boundary data $g : \partial\Omega \to \mathbb{R}$

$$\Delta f|_\Omega = 0, \quad f|_{\partial\Omega} = g \tag{DBVP}$$

is known as the *Dirichlet boundary value problem*.
The *Dirichlet energy* is given by

$$E(f) = \frac{1}{2} \int_\Omega |\nabla f|^2 \, \mathrm{d}A,$$

where ∇f is the gradient of f.
Let $\varphi \in \mathcal{C}_0^1(\Omega)$ be a continuously differentiable function with compact support on Ω. Then due to Green's formula

$$\frac{d}{dt} E(f + t\varphi)|_{t=0} = \int_\Omega \langle \nabla f, \nabla \varphi \rangle \mathrm{d}A = \int_\Omega \varphi(\Delta f) \mathrm{d}A.$$

This integral vanishes for arbitrary φ if and only if f is harmonic. So harmonic functions are the critical points of the Dirichlet energy.
For sufficient smooth boundary[32] one can prove the existence and uniqueness of solutions of the Dirichlet boundary value problem (DBVP) for arbitrary continuous $g \in \mathcal{C}(\partial\Omega)$. This solution minimizes the Dirichlet energy.

Remark 6.1. Sometimes the Laplace operator is defined with minus sign to obtain a positive definite operator.

[32] For example of Hölder class $\partial\Omega \in \mathcal{C}^{1+a}$, with some $a > 0$.

6.2 Laplace operator on graphs

Definition 6.1 (Laplace operator and Dirichlet energy on graphs)**.** Let $G = (V, E)$ be a finite graph with vertices V and edges E. Let $\nu : E \to \mathbb{R}$ be a *weight function* defined on the edges of G.
Then the *discrete Laplace operator* on G with weights ν is defined by

$$(\Delta f)(i) = \sum_{j:(ij)=e\in E} \nu(e)(f(i) - f(j))$$

for all $i \in V$ and all functions $f : V \to \mathbb{R}$ on vertices.
The *Dirichlet energy* of f is defined by

$$E(f) = \frac{1}{2} \sum_{(ij)=e\in E} \nu(e)(f(i) - f(j))^2.$$

A function $f : V \to \mathbb{R}$ satisfying $\Delta f = 0$ is called *discrete harmonic*.

Example 6.1. By setting $\nu(e) = 1$ for all $e \in E$ one obtains the *combinatorial Laplace operator*

$$(\Delta f)(i) = \sum_{j:(ij)\in E} (f(i) - f(j))$$

on any graph G.
In the case $G = \mathbb{Z}$ we obtain

$$(\Delta f)(n) = 2f(n) - f(n + 1) - f(n - 1),$$

and for $G = \mathbb{Z}^2$

$$(\Delta f)(n, m) = 4f(m, n) - f(m - 1, n) - f(m + 1, n) - f(m, n - 1) - f(m, n + 1).$$

Let $V_0 \subset V$ (treated as the "boundary" of G).

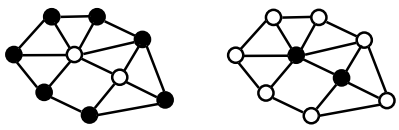

Figure 6.1. The set V_0 of "boundary" vertices on a graph (black vertices in the figure) is arbitrary.

Given some $c : V_0 \to \mathbb{R}$ consider the space of functions with prescribed values on the boundary

$$\mathcal{F}_{V_0,c} = \left\{ f : V \to \mathbb{R} \mid \ f|_{V_0} = c|_{V_0} \right\}.$$

This is an affine space over the vector space $\mathcal{F}_{V_0,0}$.

Theorem 6.1. *A function $f : V \to \mathbb{R}$ is a critical point of the Dirichlet energy $E(f)$ on $\mathcal{F}_{V_0,c}$ if and only if it is harmonic on $V\backslash V_0$, i.e.*

$$\Delta f(i) = 0 \quad \forall i \in V\backslash V_0.$$

Proof. Consider a variation $f + t\varphi \in \mathcal{F}_{V_0,c}$ of $f \in \mathcal{F}_{V_0,c}$, i.e. $\varphi \in \mathcal{F}_{V_0,0}$. We have

$$\begin{aligned} E(f + t\varphi) &= E(f) + t^2 E(\varphi) + t \sum_{(ij)\in E} \nu(ij)(f(i) - f(j))(\varphi(i) - \varphi(j)) \\ &= E(f) + t^2 E(\varphi) + t \sum_{i\in V} \varphi(i) \sum_{j:(ij)\in E} \nu(ij)(f(i) - f(j)) \\ &= E(f) + t^2 E(\varphi) + t \sum_{i\in V} \varphi(i)(\Delta f)(i). \end{aligned}$$

So

$$\left.\frac{\mathrm{d}}{\mathrm{d}t}\right|_{t=0} E(f + t\varphi) = \sum_{i\in V} \varphi(i)(\Delta f)(i)$$

vanishes for all $\varphi \in \mathcal{F}_{V_0,0}$ if and only if $\Delta f(i) = 0$ for all $i \in V\backslash V_0$. □

If all the weights are positive $\nu : E \to \mathbb{R}_+$ then the discrete harmonic functions have properties familiar from the smooth case.

Theorem 6.2 (maximum principle)**.** *Let $G = (V, E)$ be a connected graph and $V_0 \subset V$. Let Δ be a discrete Laplace operator on G with positive weights. Then a function $f : V \to \mathbb{R}$ which is harmonic on $V\backslash V_0$ can not attain its maximum (and minimum) on $V\backslash V_0$.*

Proof. At a local maximum $i \in V \subset V_0$ of f one has $\Delta f(i) = \sum_{j:(ij)\in E} \nu(ij)(f(i) - f(j)) > 0$, therefore f cannot be harmonic. □

For $V_0 = \varnothing$ this implies:

Corollary 6.3 (discrete Liouville theorem)**.** *A harmonic function on a connected graph is constant.*

and for $V_0 \neq \varnothing$:

Corollary 6.4 (dDBVP, uniqueness)**.** *The solution of the discrete Dirichlet boundary value problem*

$$\Delta f|_{V\backslash V_0} = 0, \quad f|_{V_0} = c \tag{dDBVP}$$

is unique.

Proof. Let $f, \tilde{f}$ be two solutions of (dDBVP). Then $\varphi \coloneqq \tilde{f} - f \in \mathcal{F}_{V_0,0}$ for which the maximum principle implies $\varphi|_V = 0$. □

Theorem 6.5. *Let $G = (E, V)$ be a finite connected graph with positive weights $\nu : E \to \mathbb{R}_+$ and $\varnothing \neq V_0 \subset V$. Given some $c : V_0 \to \mathbb{R}$ there exists a unique minimum $f : V \to \mathbb{R}$ of the Dirichlet energy on $\mathcal{F}_{V_0,c}$.*
This minimum is the unique solution of the discrete Dirichlet boundary value problem (dDBVP).

Proof. The Dirichlet energy is a function on $\mathcal{F}_{V_0,c} \cong \mathbb{R}^{|V\setminus V_0|}$. We investigate its behavior for $\left\| f|_{V\setminus V_0} \right\| \to \infty$. Define

$$\nu_0 := \min_E\{\nu(e)\}, \quad c_0 := \max_{i\in V_0}\{c(i)\}.$$

For $R > c_0$ let $f(k) > R$ at some vertex $k \in V\setminus V_0$. Let $\gamma_k \subset E$ be a path connecting k to some vertex in V_0. It has at most $|E|$ edges. For the Dirichlet energy this gives the following rough estimate:[33]

$$\begin{aligned} E(f) &\geqslant \frac{1}{2}\nu_0 \sum_{(ij)\in\gamma_k} (f(i) - f(j))^2 \\ &\geqslant \frac{1}{2}\nu_0 \frac{(R - c_0)}{|E|} \to \infty \quad (R \to \infty). \end{aligned}$$

Thus the minimum of the Dirichlet energy is attained on a compact set $\{f \in \mathcal{F}_{V_0,c} \mid |f(i)| < R \ \forall i\}$ with some $R \in \mathbb{R}$.
The uniqueness has already been shown in Corollary 6.4. □

Summarizing we have the following equivalent statements:

- $f \in \mathcal{F}_{V_0,c}$ harmonic, i.e. $\Delta f|_{V\setminus V_0} = 0$, $f|_{V_0} = c$.
- f is a critical point of the Dirichlet energy on $\mathcal{F}_{V_0,c}$, i.e. $\nabla_f E = 0$.
- f is the unique minimum of the Dirichlet energy E on $\mathcal{F}_{V_0,c}$.

[33] Where we use $\sum_{i=1}^n a_i^2 \geqslant \frac{1}{n}\left(\sum_{i=1}^n a_i\right)^2$.

6.3 Dirichlet energy of piecewise affine functions

We compute the Dirichlet energy of an affine function on a triangle.
Denote by 1, 2, 3 the vertices of a triangle F and by $\varphi_1, \varphi_2, \varphi_3$ the basis of affine functions on F given by

$$\varphi_j(i) = \delta_{ij}, \quad i, j = 1, 2, 3.$$

Then $\varphi_1 + \varphi_2 + \varphi_3 = 1$ and an affine function $f : F \to \mathbb{R}$ on the triangle F is determined by its values $f_i = f(i)$ at the vertices:

$$f = \sum_{i=1}^{3} f_i \varphi_i.$$

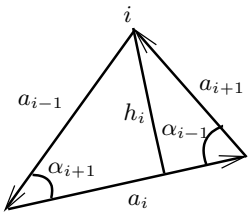

Figure 6.2. Triangle F with vertices i, sides a_i, angles α_i and heights h_i.

For gradient of f we get

$$|\nabla f|^2 = \left| \sum_{i=1}^{3} f_i^2 \nabla \varphi_i \right|^2 = \sum_{i=1}^{3} f_i \left|\nabla \varphi_i\right|^2 + 2 \sum_{i=1}^{3} f_i f_{i+1} \langle \nabla \varphi_i, \nabla \varphi_{i+1} \rangle, \tag{6.1}$$

where the indices are considered modulo 3.
For the gradient $\nabla \varphi_i$ we calculate further

$$\begin{aligned} \left|\nabla \varphi_i\right|^2 &= \frac{1}{h_i^2} = \frac{1}{2A(F)} \frac{|a_i|}{h_i} = \frac{1}{2A(F)} (\cot \alpha_{i-1} + \cot \alpha_{i+1}), \\ \langle \nabla \varphi_i, \nabla \varphi_{i+1} \rangle &= \frac{\langle a_i, a_{i+1} \rangle}{4A(F)^2} = \frac{|a_i|\,|a_{i+1}| \cos \alpha_{i-1}}{4A(F)^2} = -\frac{\cot \alpha_{i-1}}{2A(F)}, \end{aligned}$$

where $a_i \in \mathbb{R}^2$ is the side opposite i and h_i the height at the vertex i. The area of the triangle is $A(F) = \frac{1}{2} h_i \, |a_i|$.
For the gradient (6.1) of f this implies

$$|\nabla f|^2 = \frac{1}{2A(F)} \sum_{i=1}^{3} (f_{i+1} - f_{i-1})^2 \cot \alpha_i.$$

Multiplying by $\frac{1}{2} A(F)$ we obtain the Dirichlet energy of f on F:

$$E(f) = \frac{1}{2} \int_F |\nabla f|^2 \, \mathrm{d}A = \frac{1}{4} \sum_{i=1}^{3} (f_{i+1} - f_{i-1})^2 \cot \alpha_i.$$

Theorem 6.6. *Let S be a simplicial surface and $f : S \to \mathbb{R}$ a continuous and piecewise affine function (affine on each face of S).*
Then its Dirichlet energy is

$$E(f) = \frac{1}{2} \sum_{(ij)\in E} \nu(ij)(f(i) - f(j))^2,$$

with weights

$$\nu(ij) = \begin{cases} \frac{1}{2} \ (\cot \alpha_{ij} + \cot \alpha_{ji}) & \textit{for internal edges} \\ \frac{1}{2} \ \cot \alpha_{ij} & \textit{for external edges} \end{cases} \tag{6.2}$$

called cotan-weights.

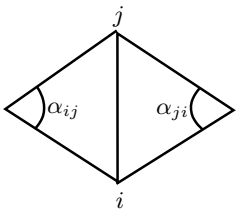

Figure 6.3. α_{ij} and α_{ji} are the angles opposite the edge (ij).

A discrete function $f : V \to \mathbb{R}$ defined at the vertices of a simplicial surface S uniquely extends to a piecewise affine function $f : S \to \mathbb{R}$.
Even more for a discrete function $f : V \to \mathbb{R}$ defined at the vertices of a geodesic triangulation of a piecewise flat surface (M, d) we can unfold each triangle to the Euclidean plane and define its Dirichlet energy by the affine extension to this triangle in the same way. We define the corresponding discrete Laplace operator on triangulated piecewise flat surfaces.

Definition 6.2 (discrete cotan Laplace operator)**.** Let (M, d) be a piecewise flat surface, $V \subset M$ a finite set of points that contains all conical singularities. Let $T \in \mathcal{T}_{M,V}$ be a geodesic triangulation of M.
Then we define the *discrete cotan Laplace operator* of T by

$$(\Delta f)(i) \coloneqq \sum_{j:(ij)\in E} \nu(ij)(f(i) - f(j))$$

for all $i \in V$ and all discrete functions $f : V \to \mathbb{R}$, with cotan-weights as defined in (6.2).

6.4 Simplicial minimal surfaces (I)

The area of simplicial surfaces can be represented as a Dirichlet energy.
The area of the triangle ABC with angles α, β, γ and edge lengths a, b, c is equal to

$$\frac{1}{4}(a^2 \cot\alpha + b^2 \cot\beta + c^2 \cot\gamma).$$

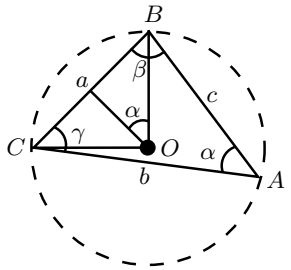

Figure 6.4. Subdivide the triangle ABC into three triangles by connecting the center O of the circumcircle to its vertices. The area of the triangle OBC is $\frac{1}{4}a^2 \cot\alpha$

Let $f : \mathcal{S} \to \mathbb{R}^N$ be a simplicial surface $S \coloneqq f(\mathcal{S})$. Then its total area is given by

$$A(S) = \frac{1}{2} \sum_{(i,j)\in E} \nu(ij)\|f(i) - f(j)\|^2$$

with cotan-weights ν as defined in (6.2). The square of the edge lengths is

$$\|f(i) - f(j)\|^2 = \sum_{k=1}^{N} |f_k(i) - f_k(j)|^2.$$

Theorem 6.7. *Let $f : \mathcal{S} \to \mathbb{R}^N$, $S \coloneqq f(\mathcal{S})$ be a simplicial surface. It is completely determined by its vertices $f : V \to \mathbb{R}^N$. Its area is given by*

$$A(S) = \sum_{k=1}^{N} E(f_k),$$

where $E(f_k)$ is the Dirichlet energy of the k-th coordinate function.
The area gradient at the vertex $f(i)$ is equal to the discrete cotan Laplace operator of f at i

$$\nabla_{f(i)} A(S) = (\Delta f)(i) = \sum_{j:(i,j)\in E} \nu(ij)(f(i) - f(j)).$$

Proof. Consider a variation $f + t\varphi$ of the vertex $i \in V$ only, i.e.

$$\varphi(j) = y\delta_{ij}$$

for all $j \in V$ with some $y \in \mathbb{R}^N$. Then

$$\begin{aligned}\left.\frac{\mathrm{d}}{\mathrm{d}t}\right|_{t=0} A(f + t\varphi) &= \sum_{k=1}^{N} \left.\frac{\mathrm{d}}{\mathrm{d}t}\right|_{t=0} E(f_k + t\varphi_k) \\ &= \sum_{k=1}^{N} y_k \Delta f_k(i) = \langle y, \Delta f(i)\rangle,\end{aligned}$$

which is

$$\nabla_{f(i)} A(S) = (\Delta f)(i).$$

□

Remark 6.2.

- Note that f is involved in the definition of Δ since the weights are determined by the geometry of the simplicial surface.
- For $u : V \to \mathbb{R}^N$ the equation $\Delta u = 0$ is to be understood component-wise, i.e.
$$\Delta u = 0 \;\Leftrightarrow\; \Delta u_k = 0 \;\forall k = 1, \ldots, N.$$

We have

f harmonic (w.r.t. cotan Laplace) $\;\Leftrightarrow\;$ S critical for the area functional.

So we might define *simplicial minimal surfaces* as suggested in [PP93] by

$$S \text{ discrete minimal surface } :\Leftrightarrow\; \Delta f = 0,$$

which immediately comes with a computation algorithm.

Data: Simplicial surface $f : \mathcal{S} \to S \subset \mathbb{R}^N$
Result: Simplicial minimal surface (w.r.t. cotan Laplace operator).
while *S is not critical for the area functional* **do**
  Compute $\tilde{f}$ such that
  $$\Delta \tilde{f} = 0$$
  which defines a new simplicial surface $\tilde{S}$;
  Replace S by the new surface $\tilde{S}$;
end

Figure 6.5. Simplicial minimal surface algorithm (with cotan Laplace operator).

Remark 6.3. In each step a new simplicial surface is generated which carries a new cotan Laplace operator.

The weights ν of the discrete cotan Laplace operator can be negative. So it lacks the following property which is a reformulation of the maximum principle for $\mathbb{R}^N$-valued functions.

Proposition 6.8 (local maximum principle)**.** *Let Δ be a discrete Laplace operator on a graph G with positive weights. Let $u : V \to \mathbb{R}^N$ be a map which is harmonic at a vertex $i \in V$.*
Then the value $u(i)$ at the vertex i lies in the convex hull of the values of its neighbors.

Proof. With

$$C \coloneqq \sum_{j:(ij)\in E} \nu(ij)$$

we have

$$(\Delta f)(i) = \sum_{j:(ij)\in E} \nu(ij)\,(f(i) - f(j)) = 0$$

$$\Leftrightarrow\ f(i) = \sum_{j:(ij)\in E} \frac{\nu(ij)}{C} f(j).$$

□

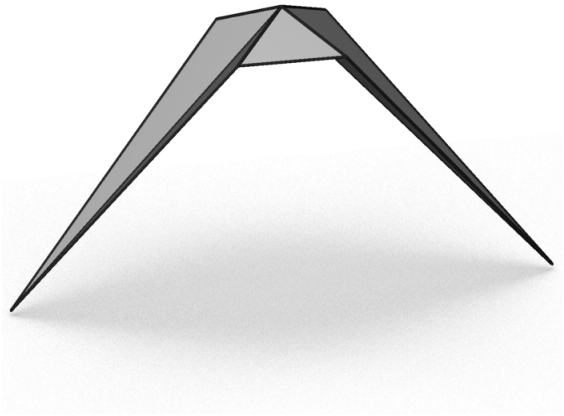

Figure 6.6. Simplicial minimal surface violating the maximum principle. One vertex does not lie in the convex hull of its neighbors.

The maximum principle is a desirable feature analogous to the smooth property of all points of a minimal surface being hyperbolic. So we ask the question

When does the cotan Laplace operator have positive weights?

For an edge $(ij) \in E$ we have

$$\begin{aligned} \nu(ij) &= \frac{1}{2}(\cot\alpha_{ij} + \cot\alpha_{ji}) \\ &= \frac{1}{2}\left(\frac{\cos\alpha_{ij}\sin\alpha_{ji} + \cos\alpha_{ji}\sin\alpha_{ij}}{\sin\alpha_{ij}\sin\alpha_{ji}}\right) \\ &= \frac{\sin(\alpha_{ij}+\alpha_{ji})}{\sin\alpha_{ij}\sin\alpha_{ji}} \geqslant 0 \ \Leftrightarrow\ \alpha_{ij}+\alpha_{ji} \leqslant \pi, \end{aligned} \tag{6.3}$$

which is not satisfied for the long edges in Figure 6.6. We will come back to this when introducing the discrete Laplace-Beltrami operator.

7 Delaunay tessellations

We have noted that the polyhedral metric of a piecewise flat surface (M, d) carries no obvious information about edges and faces. In the following we show how to use the metric to obtain a distinguished geodesic tessellation of (M, d). After recalling the notion of Delaunay tessellations of the plane we demonstrate how to generalize it to piecewise flat surfaces.

7.1 Delaunay tessellations of the plane

7.1.1 Delaunay tessellations from Voronoi tessellations

Consider n distinct points in the plane $V = \{P_1, \dots, P_n\} \subset \mathbb{R}^2$. For each $P_i \in V$ one defines the *Voronoi region*

$$W_{P_i} := \left\{P \in \mathbb{R}^2 \mid |PP_i| < |PP_j| \ \forall j \neq i\right\}.$$

With $H_{ij} := \left\{P \in \mathbb{R}^2 \mid |PP_i| < |PP_j|\right\}$ we have $W_{P_i} = \bigcap_{j \neq i} H_{ij}$. Thus Voronoi regions are convex polygons.

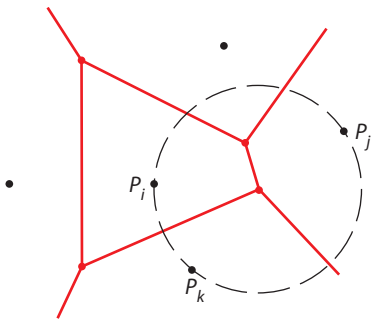

Figure 7.1. Voronoi tessellation for some given points $V = \{P_1, \dots, P_n\}$ in the plane. A vertex Q of the Voronoi tessellation has equal shortest distance to at least three points of V.

Voronoi regions are the 2-cells of the *Voronoi tessellation.*[34]
For $P \in \mathbb{R}^2$ consider

$$\Gamma_{P,V} := \left\{P_j \in V \mid |PP_j| = \min_{P_k \in V} |PP_k|\right\}.$$

We can identify points of 2-cells, 1-cells and 0-cells of the Voronoi tessellation by counting points in V that have equal shortest distance to P.
The 2-cells of the Voronoi tessellation are the connected components of

$$\left\{P \in \mathbb{R}^2 \mid \#\Gamma_{P,V} = 1\right\},$$

the 1-cells are the connected components of

$$\left\{P \in \mathbb{R}^2 \mid \#\Gamma_{P,V} = 2\right\},$$

[34] A tessellation is a cell-decomposition with polygonal 2-cells.

and the 0-cells are the points in

$$\left\{P \in \mathbb{R}^2 \mid \#\Gamma_{P,V} \geqslant 3\right\}.$$

For $P' \in \mathbb{R}^2$ with $\#\Gamma_{P',V} = 2$, $P_i, P_j \in \Gamma_{P',V}$, $P_i \neq P_j$ the corresponding 1-cell is given by

$$\left\{P \in \mathbb{R}^2 \mid |PP_i| = |PP_j| < |PP_k| \ \forall k \neq i,j\right\},$$

and for $P \in \mathbb{R}^2$ with $\#\Gamma_P \geqslant 3$, $P_i, P_j, P_k \in \Gamma_{P,V}$ different, the corresponding 0-cell is given by

$$\left\{P \in \mathbb{R}^2 \mid |PP_i| = |PP_j| = |PP_k| \leqslant |PP_m| \ \forall m\right\}.$$

Let Q be a vertex of the Voronoi tessellation, i.e.

$$\exists i,j,k \ \forall m: \ r_Q \coloneqq |PP_i| = |PP_j| = |PP_k| \leqslant |PP_m|.$$

Define the disk

$$D_Q \coloneqq \left\{P \in \mathbb{R}^2 \mid |PQ| < r_Q\right\}.$$

It contains no points of V. But its closure $\bar{D}_Q$ contains at least three. Thus

$$H_Q \coloneqq \operatorname{conv}\left\{P_i \in V \mid |QP_i| = r_Q\right\}$$

is a convex circular polygon.

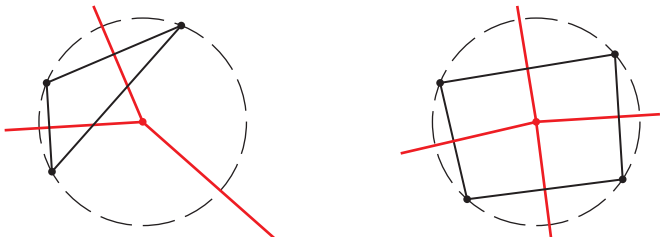

Figure 7.2. Delaunay cells are convex circular polygons. They are triangles in the generic case.

The H_Q are the 2-cells of the *Delaunay tessellation*.
The vertices of this tessellation are V and the edges (P_iP_j) where i,j are indices of neighboring Voronoi cells, i.e. there exists a corresponding Voronoi edge.

Remark 7.1.

- Voronoi and Delaunay tessellations are dual cell-decompositions.
- Corresponding edges of the Voronoi and Delaunay tessellation are orthogonal but do not necessarily intersect (see Figure 7.2). The Voronoi edge bisects the corresponding Delaunay edge.
- Voronoi and Delaunay tessellations of the plane are strongly regular.

- One can also introduce a Delaunay-Voronoi quad-tessellation as a composition of both:

Figure 7.3. Voronoi-Delaunay quad tessellation. Faces (dotted lines) are convex or non-convex kites.

Vertices are the union of Voronoi and Delaunay vertices.
Edges are the intervals connecting the centers of Voronoi cells with their vertices or alternatively the centers of Delaunay cells with their vertices.
Faces are embedded quads with orthogonal diagonals and the diagonal which is a Delaunay-edge is bisected into two equal intervals by the line through the orthogonal Voronoi-edge.

Theorem 7.1. *Given a set of distinct points $V = \{P_1, \ldots, P_n\} \in \mathbb{R}^2$ there exists a unique Voronoi and Delaunay tessellation.*
These tessellations are dual to each other: The Delaunay vertices V are the generating points of the Voronoi tessellation. The Delaunay faces are convex circular polygons centered at Voronoi vertices. The corresponding edges of the Voronoi and Delaunay tessellations are orthogonal.

7.1.2 Delaunay tessellations in terms of the empty disk property

How to define Delaunay tessellations without referring to Voronoi?
We noticed that:

All faces of a Delaunay tessellation are convex circular polygons.
The corresponding Delaunay open disks D_Q contain no vertices.

and call this the *empty disk property*.

Definition 7.1. A tessellation of a planar domain is called *Delaunay* if it possesses the empty disk property.
An edge of a tessellation is called *Delaunay edge* if two faces sharing this edge do not have any of their vertices in the interior of their disks.

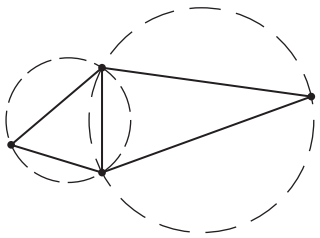

Figure 7.4. Empty disk property of Delaunay tessellations.

Theorem 7.2. *The property of being a Delaunay tessellation is invariant under Möbius transformations.*

Proof. Follows directly from the empty disk property being Möbius invariant. □

Remark 7.2. Delaunay tessellations on $\mathbb{S}^2$ can be obtained by stereographic projection.

Lemma 7.3 (angle criterion for circular quadrilaterals)**.** *Let $P_1, P_2, P_3, P_4 \in \mathbb{R}^2$ be four points in the plane cyclically ordered. Let C be the circle through P_1, P_2, P_3,*

$$\alpha \coloneqq \measuredangle P_1P_2P_3, \quad \beta \coloneqq \measuredangle P_3P_4P_1.$$

Then

$$\begin{aligned} P_4 \text{ lies outside } C &\Leftrightarrow \alpha + \beta < \pi \\ P_4 \text{ lies on } C &\Leftrightarrow \alpha + \beta = \pi \\ P_4 \text{ lies inside } C &\Leftrightarrow \alpha + \beta > \pi. \end{aligned}$$

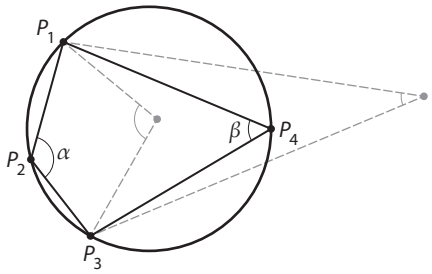

Figure 7.5. Angle criterion for circular quadrilaterals.

Proposition 7.4 (angle criterion for Delaunay triangulations)**.** *A triangulation of the plane is Delaunay if and only if for each edge the sum of the two angles opposite to this edge is less than or equal to π.*

7.2 Delaunay tessellations of piecewise flat surfaces

7.2.1 Delaunay tessellations from Voronoi tessellations

Let (M, d) be a piecewise flat surface. Let $V = \{P_1, \ldots, P_n\}$ be points on M such that $V \supset \{\text{conical singularities of } (M, d)\}$.
On M –in contrast to the planar case– it can happen that the distance between two points is realized by more than one geodesic. The suitable generalization of counting points of equal shortest distance to V is counting geodesics that realize this distance. For $P \in M$ we define

$$\Gamma_{P,V} \coloneqq \{\gamma : [0,1] \to M \text{ geodesic} \mid \gamma(0) = P,\ \gamma(1) \in V,\ \mathrm{L}(\gamma) = d(P,V)\}.$$

The 2-cells of the *Voronoi tessellation* of M with vertex set V are the connected components of

$$\{P \in M \mid \#\Gamma_{P,V} = 1\},$$

the 1-cells are the connected components of

$$\{P \in M \mid \#\Gamma_{P,V} = 2\},$$

and the 0-cells are the points in

$$\{P \in M \mid \#\Gamma_{P,V} \geqslant 3\}.$$

We can try to describe the cells in a similar manner as in the planar case. E.g. for $P' \in M$ with $\#\Gamma_{P',V} = 2$, $\gamma_1, \gamma_2 \in \Gamma_{P'}$, $\gamma_1 \neq \gamma_2$, $P_i = \gamma_1(1), P_j = \gamma_2(1) \in V$ (possibly $i = j$) the corresponding 1-cell is given by

$$\left\{P \in M \mid d(P, P_i) = d(P, P_j) < d(P, P_k)\ \forall k \neq i, j \text{ (and } \#\Gamma_{P,\{P_i,P_j\}} = 2)\right\}.$$

Example 7.1 (Voronoi tessellation of a cube)**.** Let V be the set of vertices of a cube.

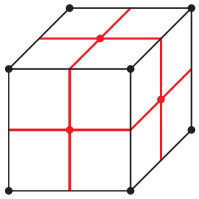

Figure 7.6. Voronoi tessellation of a cube.

Let P be an internal point of a Voronoi edge. Then there is $P_i, P_j \in V$ (possibly $i = j$) such that

$$d(P, P_i) = d(P, P_j) < d(P, P_k)\ \forall k \neq i, j.$$

This describes an *empty immersed disk* centered at P with exactly two elements of V on the boundary.[35]
The endpoints of Voronoi edges are Voronoi vertices. Let Q be such a point. Then there is $P_i, P_j, P_k \in V$ such that

$$d(Q, P_i) = d(Q, P_j) = d(Q, P_k) \leqslant d(Q, P_l)\ \forall l.$$

This describes an empty immersed disk centered at Q with at least three elements of V on the boundary.[36]
As in the plane the Delaunay tessellation is defined as dual to the Voronoi tessellation.

[35] Or one element but two different geodesics minimizing the distance to P.
[36] Or less but with at least three different geodesics minimizing the distance to P.

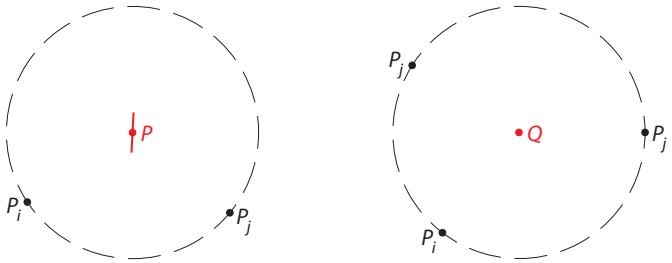

Figure 7.7. (left) An internal point P of a Voronoi edge. (right) A Voronoi vertex Q. Both are the center of an empty immersed disk on M with vertices on the boundary. The Delaunay edges are geodesic arcs connecting the points of V on the boundary, i.e. the Delaunay faces are flat circular polygons.

Remark 7.3. A *geodesic tessellation* of a piecewise flat surface (M, d) is a tessellation with flat polygonal 2-cells (compare Definition 5.6).
Delaunay tessellations are geodesic tessellations on M. The edges of Voronoi tessellations are geodesic arcs but it is not a geodesic tessellation since the faces are not flat.

Theorem 7.5. *Let (M, d) be a piecewise flat surface without boundary, $V \subset M$ a finite set of points that contains all conical singularities.*
Then there exists a unique Delaunay tessellation of M.

Remark 7.4.

- The proof via construction of the Voronoi tessellation can be found in [MS91].
- If one triangulates all Delaunay faces by triangulating the corresponding circular polygons in the corresponding empty immersed disks one can obtain *Delaunay triangulations*.[37]
  On the contrary, the unique Delaunay tessellation can be recovered from any Delaunay triangulation by deleting edges.
- We will show later how to construct a Delaunay triangulation starting from an arbitrary triangulation by applying an algorithm of consecutive edge flips.

7.2.2 Delaunay tessellations in terms of the empty disk property

We define Delaunay tessellations on a piecewise flat surface in a selfcontained way without referring to Voronoi.

Definition 7.2 (empty immersed disk)**.** Let (M, d) be a piecewise flat surface without boundary, $V \subset M$ a finite set of points that contains all conical singularities.
Then an *immersed empty disk* is a continuous map $\varphi : \bar{D} \to M$ such that $\varphi|_D$ is an isometric immersion[38] and $\varphi(D) \cap V = \varnothing$.

[37] In contrast to the Delaunay tessellation the Delaunay triangulation is not unique as soon as one has circular polygons which are not triangles.

[38] An isometric immersion is a local isometry, i.e. each $P \in D$ has a neighborhood which is mapped to M isometrically.

Definition 7.3 (Delaunay tessellation)**.** Let (M, d) be a piecewise flat surface without boundary, $V \subset M$ a finite set of points that contains all conical singularities.
The *Delaunay tessellation* of M with vertex set V is a cell-decomposition with the following cells:
$C \subset M$ is a closed cell of the Delaunay tessellation if there exists an immersed empty disk $\varphi : \bar{D} \to M$ such that $\varphi^{-1}(D) \neq \varnothing$ and $C = \varphi(\text{conv}\varphi^{-1}(V))$.
The cell is a 0-, 1-, 2-cell if $\varphi^{-1}(V)$ contains 1, 2, or more points respectively.

Claim 7.6. *This is indeed a tessellation.*

Remark 7.5. For the proof see [BS07].

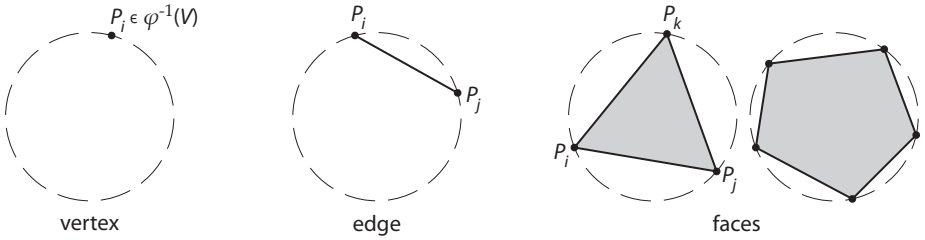

Figure 7.8. Delaunay cells and their corresponding empty immersed disks.

We characterize Delaunay triangulations in terms of a local edge property.

Definition 7.4 (Delaunay edge)**.** Let T be a geodesic triangulation of a piecewise flat surface (M, d). Let e be an interior edge of T. We can isometrically unfold the two triangles of T that are adjacent to e. e is called a *Delaunay edge* if the vertices of these unfolded triangles are not contained inside the circumcircles of the triangles.

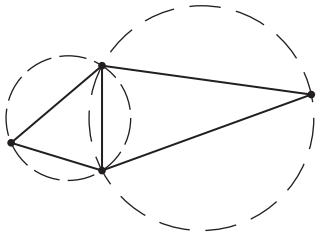

Figure 7.9. Unfolded triangles adjacent to a Delaunay edge. The inside of the circumcircles contain no vertices.

Theorem 7.7 (Characterization of Delaunay triangulations in terms of Delaunay edges)**.** *Let (M, d) be a piecewise flat surface without boundary, $V \subset M$ a finite set of points that contains all conical singularities.*
A geodesic triangulation $T \in \mathcal{T}_{M,V}$ of (M, d) is Delaunay if and only if all of its edges are Delaunay edges.

Remark 7.6. We first explain the general scheme used in the proof to obtain a locally isometric model in the Euclidean plane for parts of our surface M. We do some notably identifications on the way.

- For any face $\Delta \in F(T)$ there is a triangle in the Euclidean plane which can be isometrically immersed into the piecewise flat surface M (continuous on the boundary) such that its image corresponds to the face.
  Notationally we identify the combinatorial/metrical face on M and the unfolded Euclidean triangle.
- We extend the isometric immersion such that it stays an isometric immersion in the interior and continuous on the boundary.
  E.g. by some circular piece or a neighboring triangle.
- Note that we might not be able to extend it to the circumcircle of the unfolded triangle in the plane.
  That is why it is not obvious whether Delaunay edges imply the existence of empty immersed disks for their adjacent faces.
- Only inside the domain of this extended immersion can we be sure to draw straight lines and obtain geodesics on M and measure lengths and angles as they are on M, i.e. measure quantities in our planar isometric model that are well-defined by the piecewise flat surface.

Proof. If T is Delaunay obviously all edges are Delaunay edges.
Assume that all edges are Delaunay but the triangulation is not.

Any face $\Delta \in F(T)$ can be isometrically unfolded into the plane. We denote its circumcircle in the plane by D_Δ.
For an edge a of Δ consider the one-parameter family of circles in the plane through its endpoints. a divides the corresponding open disks into two parts of which we take the one that does not intersect Δ. We call them disk segments which fit to Δ along a.

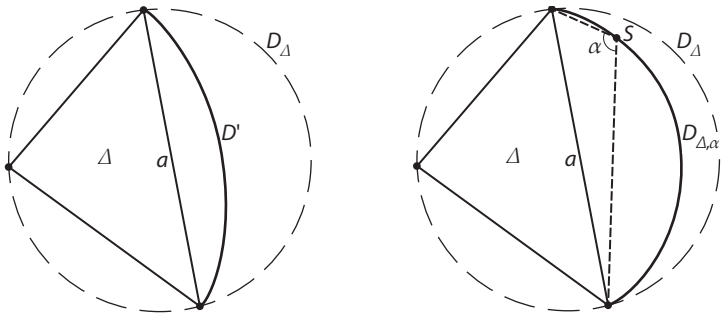

Figure 7.10. (left) Unfolded face Δ with circumcircle D_Δ and disk segment D' fitting to Δ along a. (right) We extend the isometric immersion of Δ behind the edge a to the largest possible disk segment $D_{\Delta,a}$. To every $(\Delta, a, S) \in \mathcal{A}$ we associate an angle α.

$$\mathcal{D}_{\Delta,a} \coloneqq \{D' \mid \text{disk segment fitting to } \Delta \text{ along } a,\\ \text{the isometric immersion of } \Delta \text{ can be extended to } D'\\ \text{(continuously to } \bar{D}'),\\ D' \cap V = \varnothing\}$$

For any edge a of a face Δ we denote the largest such disk segment by

$$D_{\Delta,a} \coloneqq \bigcup_{D' \in \mathcal{D}_{\Delta,a}} D'.$$

If $\mathcal{D}_{\Delta,a}$ is bounded, then $D_{\Delta,a} \in \mathcal{D}_{\Delta,a}$ and there has to be a vertex on the circular arc bounding $D_{\Delta,a}$, i.e.

$$(\partial D_{\Delta,a} \backslash \bar{a}) \cap V \neq \varnothing.$$

Otherwise we could enlarge $D_{\Delta,a}$.

A face Δ which has no empty immersed disk must have an edge a such that $(\bar{D}_{\Delta,a} \backslash \bar{a}) \subset D_\Delta$. Thus the set

$$\mathcal{A} \coloneqq \{(\Delta, a, S) \in F \times E \times V \mid \Delta \text{ has no empty immersed disk},\\ a \text{ is edge of } \Delta \text{ with } (\bar{D}_{\Delta,a} \backslash \bar{a}) \subset D_\Delta,\\ S \in (\partial D_{\Delta,a} \backslash \bar{a}) \cap V\}$$

is not empty.

We introduce the angle $\alpha : \mathcal{A} \to (0, \pi)$,

$$\alpha\,(\Delta, (BC), S) \coloneqq \sphericalangle BSC.$$

Let $(\Delta, a, S) \in \mathcal{D}$ such that

$$\alpha(\Delta, a, S) = \max_{(\tilde{\Delta}, \tilde{a}, \tilde{S}) \in \mathcal{A}} \alpha(\tilde{\Delta}, \tilde{a}, \tilde{S}). \tag{7.1}$$

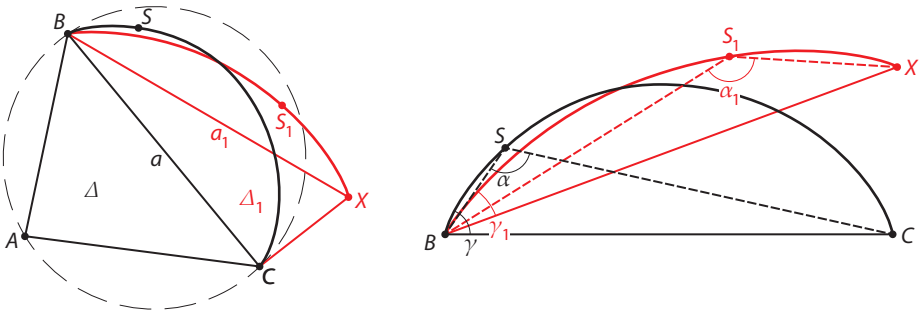

Figure 7.11. (left) For $(\Delta, a, S) \in \mathcal{A}$ we obtain a neighboring element $(\Delta_1, a_1, S_1 \in \mathcal{A}$. (right) We find $\alpha(\Delta_1, a_1, S_1) > \alpha(\Delta, a, S)$ since $\gamma_1 < \gamma$ in contradiction to the assumption.

Let Δ_1 be the face sharing the edge a with Δ. We can isometrically unfold it to the same plane as Δ. Let B, C be the endpoints of a and X the opposite vertex of Δ_1.

$$a \text{ Delaunay edge } \Rightarrow X \notin D_\Delta.$$

Since no triangle may contain any vertices we also have $S \notin \Delta_1$.
Let a_1 be the edge of Δ_1 closest to S, say $a_1 = (BX)$. Then there is $S_1 \in V$ (possibly $S_1 = S$) such that

$$(\Delta_1, a_1, S_1) \in \mathcal{A}.$$

Let us denote the corresponding angles by $\alpha \coloneqq \alpha(\Delta, a, S)$ and $\alpha_1 \coloneqq \alpha(\Delta_1, a_1, S_1)$. Due to Lemma 7.8 the angle $\gamma \coloneqq \pi - \alpha$ is the intersection angle of the circular arc of $\partial D_{\Delta,a}$ with a at B. Similarly γ_1.
Clearly, $\gamma > \gamma_1$ which implies

$$\alpha < \alpha_1$$

in contradiction to (7.1). □

Lemma 7.8. *Let B, S, C be three points on a circle, $\alpha \coloneqq \sphericalangle BSC$. Then the intersection angle between the tangent to the circle at B and the secant (BC) as depicted in Figure 7.12 is equal to α.*

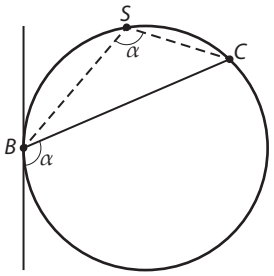

Figure 7.12. Angle in a circular arc.

Proof. While moving S along the circular arc the angle $\alpha = \sphericalangle BSC$ stays constant. In the limit $S \to B$ the edge (BS) becomes the tangent at B and $(SC) \to (BC)$. □

The characterization of Delaunay triangulations in terms of Delaunay edges allows us to formulate an angle criterion as in the planar case.

Proposition 7.9 (Angle criterion for Delaunay triangulations)**.** *A geodesic triangulation of a piecewise flat surface is Delaunay if and only if for every edge the sum of the two angles opposite to this edge is less than or equal to π.*

This is a practical geometric characterization since angles can be measured directly on the piecewise flat surface without any need to find empty immersed disks. Recalling (6.3) we notice at this point

Proposition 7.10. *The discrete cotan Laplace operator of a geodesic triangulation T of a piecewise flat surface (M, d) has non-negative weights if and only if T is Delaunay.*

7.3 The edge-flip algorithm

Let T be a geodesic triangulation of a piecewise flat surface (M, d).
If we unfold two adjacent triangles of T into the plane, we obtain a quadrilateral Q, where one of its diagonals e corresponds to the shared edge of the triangles and the other one e^* corresponds to the edge resulting in an edge flip of e if possible.

Lemma 7.11. *Every non-Delaunay edge of T can be flipped and the flipped edge is then Delaunay.*

Proof. Let e be a non-Delaunay edge.
We use Lemma 5.8 to characterize whether e can be flipped. The sum of the angles opposite to e in the adjacent triangles is greater than π. Therefore the two triangles have to be different since the sum of all angles in a triangle is equal to π. The two triangles form a convex quadrilateral as can be seen e.g. from Figure 7.5. So e can be flipped and the sum of the angles opposite to the flipped edge e^* is less than or equal to π. □

The following question emerges.

> Can any given triangulation be made Delaunay by consecutive edge-flips?

Definition 7.5. We denote the set of all geodesic triangulations of a given piecewise flat surface (M, d) with vertex set V by $\mathcal{T}_{M,V}$.

The edge-flip algorithm acts on $\mathcal{T}_{M,V}$ in the following way.

Data: Some $T \in \mathcal{T}_{M,V}$.
Result: A Delaunay triangulation $T \in \mathcal{T}_{M,V}$.
while T *is not Delaunay* **do**
  Take any non-Delaunay edge e of T;
  Flip e in T;
end

Figure 7.13. Edge-flip algorithm.

Example 7.2. We make the triangulation of the tetrahedron shown in Figure 7.14 Delaunay by applying the edge-flip algorithm.

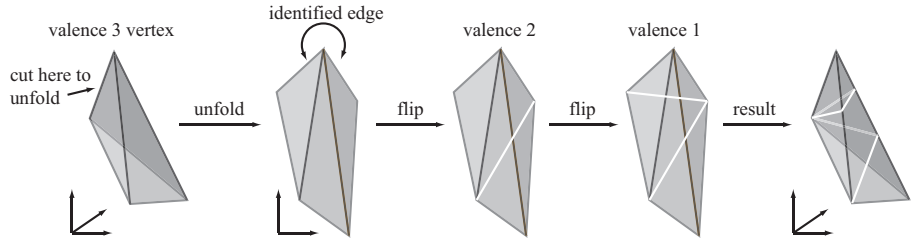

Figure 7.14. Making a given triangulation Delaunay.

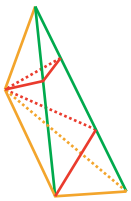

Figure 7.15. Result with colored edges. Green and yellow edges are original edges. Red and yellow edges are Delaunay edges.

Note that the resulting triangulation is not regular and has a vertex of valence one.

Theorem 7.12. *The edge-flip algorithm terminates for any start triangulation $T \in \mathcal{T}_{M,V}$ after a finite number of steps.*

Remark 7.7. Removing all edges which would stay Delaunay upon an edge-flip we obtain the unique Delaunay tessellation. Claiming the existence of some geodesic triangulation on any piecewise flat surface this implies Theorem 7.5. In practice having some start triangulation is not an issue since the standard ways of prescribing a piecewise flat surface already includes a triangulation.

The state of the algorithm is determined by the current triangulation in $\mathcal{T}_{M,V}$. We address the question of possible loops in the algorithm later by means of a function $f : \mathcal{T}_{M,V} \to \mathbb{R}$ that decreases on each step.

For a piecewise flat surface –in contrast to triangulations of a finite set of points in the plane– the set of all triangulations $\mathcal{T}_{M,V}$ is an infinite set in general.

Example 7.3 (infinitely many triangulations of the cube with arbitrary long edges)**.** Consider a standard cube with vertex set V. Unwrapping the cube as in Figure 5.8 suggests how to create an arbitrary long edge between two vertices of V. Completing to a triangulation we conclude that there are infinitely many triangulations of the cube.

So even with the exclusion of loops the algorithm might not terminate.

Definition 7.6 (proper function)**.** We call a function $f : \mathcal{T}_{M,V} \to \mathbb{R}$ proper if for each $c \in \mathbb{R}$ the sublevel set $\{T \in \mathcal{T}_{M,V} \mid f(T) \leqslant c\}$ is finite.

Having a proper decreasing function we can ensure termination after a finite number of steps.

Example 7.4 (edge length function)**.** For an edge e of a triangulation T we denote its length by $l(e)$. Consider the function $l : \mathcal{T}_{M,V} \to \mathbb{R}$ which assigns to each triangulation its maximal edge length

$$l(T) \coloneqq \max_{e \in E(T)} l(e).$$

As we have seen in Example 7.3 the function l might be unbound on $\mathcal{T}_{M,V}$. Nonetheless bounding l only leaves a finite number of triangulations.

Claim 7.13. *The edge length function l is proper.*

7.3.1 Dirichlet energy and edge-flips

Let T be a geodesic triangulation of a piecewise flat surface (M, d). We investigate the local change in the Dirichlet energy of a discrete function $u : V(T) \to \mathbb{R}$ upon an edge-flip.

The geometry of a convex non-degenerate quadrilateral Q with vertices $1, 2, 3, 4$ denoted in counter-clockwise direction is completely determined by the values of $r_1, r_2, r_3, r_4 > 0$ and $\theta \in (0, \pi)$ as depicted in Figure 7.16. We denote such a quadrilateral by $Q(r_1, r_2, r_3, r_4, \theta)$.

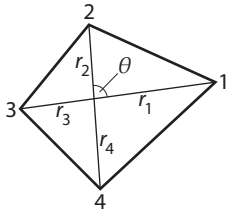

Figure 7.16. A convex non-degenerate quadrilateral $Q(r_1, r_2, r_3, r_4, \theta)$.

Lemma 7.14 (Rippa's Lemma)**.** *Let u_1, u_2, u_3, u_4 be the values of a function on the vertices of the convex non-degenerate quadrilateral $Q(r_1, r_2, r_3, r_4, \theta)$. Let $u_{13} : Q \to \mathbb{R}$ and be the linear interpolation which is affine on the triangles* (123) *and* (134) *whereas $u_{24} : Q \to \mathbb{R}$ is the linear interpolation affine on* (234) *and* (241)*. Let u_0 and u_0^* be the values at the intersection point of the diagonals of u_{13} and u_{24} respectively.*
Then the difference of the corresponding Dirichlet energies is

$$E(u_{13}) - E(u_{24}) = \frac{1}{4} \frac{(u_0 - u_0^*)^2}{\sin\theta} \frac{(r_1 + r_3)(r_2 + r_4)}{r_1 r_2 r_3 r_4} (r_1 r_3 - r_2 r_4). \tag{7.2}$$

Proof. The diagonals of Q separate the quadrilateral into four triangles Δ_1, Δ_2, Δ_3, Δ_4. Both linear interpolations are affine on each of these triangles while the Dirichlet energy of any affine function $u : \Delta_i \to \mathbb{R}$ on the triangle Δ_i is given by

$$E_{\Delta_i}(u) = \frac{1}{2} \int_{\Delta_i} |\nabla u|^2 \, \mathrm{d}A = \frac{1}{2}(u_x^2 + u_y^2) A(\Delta_i).$$

Consider the triangle Δ_1. The interpolation $u \coloneqq u_{13}$ is determined by the values u_0, u_1, u_2 and the geometric data r_1, r_2, θ of the triangle. Choosing a coordinate system such that the x-axis is aligned with the edge r_1 of Δ_1

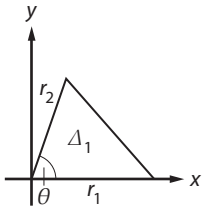

Figure 7.17. Triangle Δ_1 in suitable coordinate system.

we find

$$\begin{aligned} u_1 - u_0 &= u_x r_1 \\ u_2 - u_0 &= u_x r_2 \cos\theta + u_y r_2 \sin\theta, \end{aligned}$$

from which we obtain the partial derivatives u_x and u_y of u on Δ_1

$$\begin{aligned} u_x &= \frac{u_1 - u_0}{r_1} \\ u_y &= \frac{1}{\sin\theta}\left(\frac{u_2 - u_0}{r_2} - \frac{u_1 - u_0}{r_1}\cos\theta\right). \end{aligned}$$

For the gradient we get

$$|\nabla u|^2 = u_x^2 + u_y^2 = \frac{1}{\sin^2\theta}\left(\left(\frac{u_1 - u_0}{r_1}\right)^2 + \left(\frac{u_2 - u_0}{r_2}\right)^2 - 2\frac{(u_1 - u_0)(u_2 - u_0)\cos\theta}{r_1 r_2}\right).$$

The gradient of the interpolation $u^* \coloneqq u_{24}$ on Δ_1 is obtained by replacing u_0 by u_0^*. With $A(\Delta_1) = \frac{1}{2} r_1 r_2 \sin\theta$ the difference of the Dirichlet energies on Δ_1 is

$$\begin{aligned} E_{\Delta_1}(u) - E_{\Delta_1}(u^*) &= \frac{1}{2}\Big(|\nabla u|^2 - |\nabla u^*|^2\Big) A(\Delta_1) \\ &= \frac{r_1 r_2}{4\sin\theta}\Bigg((u_0^2 - u_0^{*2})\left(\frac{1}{r_1^2} + \frac{1}{r_2^2} - \frac{2\cos\theta}{r_1 r_2}\right) \\ &\quad + 2(u_0 - u_0^*)\left(-\frac{u_1}{r_1^2} - \frac{u_2}{r_2^2} + \frac{(u_1 + u_2)\cos\theta}{r_1 r_2}\right)\Bigg) \\ &= \frac{u_0 - u_0^*}{4\sin\theta}\Bigg((u_0 + u_0^*)\left(\frac{r_2}{r_1} + \frac{r_1}{r_2} - 2\cos\theta\right) \\ &\quad + 2\left(-u_1\frac{r_2}{r_1} - u_2\frac{r_1}{r_2} + (u_1 + u_2)\cos\theta\right)\Bigg). \end{aligned}$$

For the difference on Δ_2 we replace $r_1 \to r_2$, $r_2 \to r_3$, $\theta \to \pi - \theta$ and obtain

$$\begin{aligned} E_{\Delta_2}(u) - E_{\Delta_2}(u^*) = \frac{u_0 - u_0^*}{4\sin\theta}\Bigg((u_0 + u_0^*)\left(\frac{r_3}{r_2} + \frac{r_2}{r_3} + 2\cos\theta\right) \\ + 2\left(-u_2\frac{r_3}{r_2} - u_3\frac{r_2}{r_3} - (u_2 + u_3)\cos\theta\right)\Bigg). \end{aligned}$$

Similarly for Δ_3 and Δ_4.

We sum up over all four triangles obtaining the difference of the Dirichlet energies on the whole quadrilateral

$$\begin{aligned}
E(u) - E(u^*) &= \sum_{i=1}^{4} \Big(E_{\Delta_i}(u) - E_{\Delta_i}(u^*) \Big) \\
&= \frac{u_0 - u_0^*}{4 \sin\theta} \Bigg((u_0 + u_0^*) \Big(\frac{r_1}{r_2} + \frac{r_2}{r_3} + \frac{r_3}{r_4} + \frac{r_4}{r_1} + \frac{r_2}{r_1} + \frac{r_3}{r_2} + \frac{r_4}{r_3} + \frac{r_1}{r_4} \Big) \\
&\quad - 2 \Big(u_1 \Big(\frac{r_2}{r_1} + \frac{r_4}{r_1} \Big) + u_2 \Big(\frac{r_3}{r_2} + \frac{r_1}{r_2} \Big) + u_3 \Big(\frac{r_4}{r_3} + \frac{r_2}{r_3} \Big) + u_4 \Big(\frac{r_1}{r_4} + \frac{r_3}{r_4} \Big) \Big) \Bigg) \\
&= \frac{u_0 - u_0^*}{4 \sin\theta} \Bigg((u_0 + u_0^*) \Big((r_2 + r_4) \Big(\frac{1}{r_1} + \frac{1}{r_3} \Big) + (r_1 + r_3) \Big(\frac{1}{r_2} + \frac{1}{r_4} \Big) \Big) \\
&\quad - 2 \Big((r_2 + r_4) \Big(\frac{u_1}{r_1} + \frac{u_3}{r_3} \Big) \Big) + (r_1 + r_3) \Big(\frac{u_2}{r_2} + \frac{u_4}{r_4} \Big) \Big) \Bigg).
\end{aligned}$$

The values u_0 and u_0^* come from the different linear interpolations along the diagonals (13) and (24) respectively.

$$\begin{aligned}
u_0 &= \frac{r_3 u_1 + r_1 u_3}{r_1 + r_3} \\
u_0^* &= \frac{r_4 u_2 + r_2 u_4}{r_2 + r_4}
\end{aligned}$$

Using

$$\begin{aligned}
\frac{u_1}{r_1} + \frac{u_3}{r_3} &= u_0 \frac{r_1 + r_3}{r_1 r_3} \\
\frac{u_2}{r_2} + \frac{u_4}{r_4} &= u_0 \frac{r_2 + r_4}{r_2 r_4}
\end{aligned}$$

we can eliminate all dependence of the vertex values from the difference of the Dirichlet energies

$$\begin{aligned}
E(u) - E(u^*) &= \frac{u_0 - u_0^*}{4 \sin\theta} (r_1 + r_3)(r_2 + r_4) \left((u_0 + u_0^*) \left(\frac{1}{r_1 r_3} + \frac{1}{r_2 r_4} \right) - 2 \left(\frac{u_0}{r_1 r_3} + \frac{u_0^*}{r_2 r_4} \right) \right) \\
&= \frac{u_0 - u_0^*}{4 \sin\theta} (r_1 + r_3)(r_2 + r_4) \left(u_0 \left(\frac{1}{r_2 r_4} - \frac{1}{r_1 r_3} \right) + u_0^* \left(\frac{1}{r_1 r_3} - \frac{1}{r_2 r_4} \right) \right) \\
&= \frac{(u_0 - u_0^*)^2}{4 \sin\theta} (r_1 + r_3)(r_2 + r_4) \frac{r_1 r_3 - r_2 r_4}{r_1 r_2 r_3 r_4}.
\end{aligned}$$

□

We notice that all factors in (7.2) but the last are positive.[39] The sign of the last factor determines which edge is Delaunay.

[39] Note that for $u_0 - u_0^* \neq 0$ we require that not all of u_1, u_2, u_3, u_4 are equal.

Lemma 7.15 (circular quadrilaterals)**.** *The quadrilateral $Q(r_1, r_2, r_3, r_4, \theta)$ is circular if and only if $r_1 r_3 = r_2 r_4$.*
Furthermore

$$r_1 r_3 > r_2 r_4 \Leftrightarrow (24) \text{ Delaunay}$$
$$r_1 r_3 < r_2 r_4 \Leftrightarrow (13) \text{ Delaunay.}$$

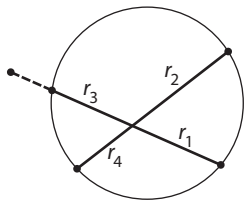

Figure 7.18. Circularity criterion for a convex quadrilateral in terms of lengths of diagonal segments.

Corollary 7.16. *Suppose that not all of the vertex values u_1, u_2, u_3, u_4 are equal. Then*

$$E(u_{13}) = E(u_{24}) \Leftrightarrow Q \text{ circular, i.e. both edges are Delaunay}$$
$$E(u_{13}) > E(u_{24}) \Leftrightarrow (24) \text{ Delaunay}$$
$$E(u_{13}) < E(u_{24}) \Leftrightarrow (13) \text{ Delaunay.}$$

So an edge-flip from a non-Delaunay edge to a Delaunay edge decreases the Dirichlet energy.

Remark 7.8. Note that the Dirichlet energy depends on the triangulation T as well as on the function $u : V(T) \to \mathbb{R}$. To ensure that the Dirichlet energy decreases upon an edge-flip u is required to be non-constant close to the edge.

7.3.2 Harmonic index

We introduce a related function that decreases on each step of the edge-flip algorithm and only depends on the triangulation.

Definition 7.7 (harmonic index)**.** For a triangle Δ with side-lengths a, b, c we define its *harmonic index* to be

$$h(\Delta) \coloneqq \frac{a^2 + b^2 + c^2}{A(\Delta)},$$

and for a geodesic triangulation $T \in \mathcal{T}_{M,V}$ of a piecewise flat surface

$$h(T) \coloneqq \sum_{\Delta \in F(T)} h(\Delta).$$

Lemma 7.17. *Let Δ be a triangle with angles α, β, γ. Then*

$$h(\Delta) = 4(\cot\alpha + \cot\beta + \cot\gamma).$$

Proof. Denote by a, b, c the lengths of the sides of Δ opposite α, β, γ respectively. Consider the height h_a on a.

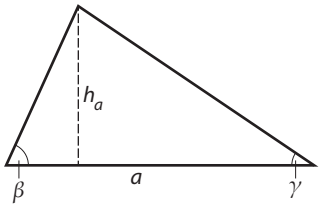

Figure 7.19. Triangle with side lengths a, b, c, corresponding heights h_a, h_b, h_c and angles α, β, γ.

Then

$$a = h_a(\cot\beta + \cot\gamma),$$

and therefore

$$a^2 = 2A(\Delta)(\cot\beta + \cot\gamma).$$

Adding this up with the corresponding formulas for the remaining edge lengths we obtain

$$a^2 + b^2 + c^2 = 4A(\Delta)(\cot\alpha + \cot\beta + \cot\gamma).$$

□

What has the harmonic index of a triangulation T to do with the Dirichlet energy?

Lemma 7.18. *Let T be a geodesic triangulation of a piecewise flat surface, $\varphi_i : V(T) \to \mathbb{R}$, $\varphi_i(j) \coloneqq \delta_{ij}$ the basis functions on T. Then*

$$h(T) = 8 \sum_{i \in V(T)} E(\varphi_i).$$

Proof. The Dirichlet energy of φ_i is given by

$$E(\varphi_i) = \frac{1}{4} \sum_{j \in V : (ij) \in E} (\cot\alpha_{ij} + \cot\alpha_{ji}).$$

Summing along all vertices $i \in V$ amounts in counting every angle twice

$$\sum_{i \in V} E(\varphi_i) = \frac{1}{2} \sum_{(ij) \in E} (\cot\alpha_{ij} + \cot\alpha_{ji}).$$

□

Corollary 7.19. *The harmonic index decreases on each step of the edge-flip algorithm.*

Lemma 7.20. *The harmonic index $h : \mathcal{T}_{M,V} \to \mathbb{R}$ is a proper function.*

Proof. Denote by A the total area of the surface M. We do a very coarse estimation using the maximal edge length $l : \mathcal{T}_{M,V} \to \mathbb{R}$ introduced in Example 7.4:

$$h(T) = \sum_{\Delta \in F(T)} h(\Delta) \geqslant \frac{l(T)}{A}.$$

So for $c \in \mathbb{R}$

$$h(T) \leqslant c \;\Rightarrow\; l(T) \leqslant \sqrt{h(T)A} = \sqrt{cA},$$

and we know that l is proper. □

We conclude that the edge-flip algorithm terminates after a finite number of steps. We have therefore proven Theorem 7.12. But even more

Theorem 7.21. *Let (M, d) be a piecewise flat surface without boundary, $V \subset M$ a finite set of points that contains all conical singularities.*
Let $f : V \to \mathbb{R}$. For each triangulation $T \in \mathcal{T}_{M,V}$ let $f_T : M \to \mathbb{R}$ be the piecewise linear interpolation of f which is affine on the faces of T.
Then the minimum of the Dirichlet energy $E(f_T) = \int_M |\nabla f_T|^2 \, \mathrm{d}A$ among all possible triangulations is attained on a Delaunay triangulation $T_D^\Delta \in \mathcal{T}_{M,V}$ of (M, d):

$$\min_{T \in \mathcal{T}_{M,V}} E(f_T) = E(f_{T_D^\Delta}).$$

7.4 Discrete Laplace-Beltrami operator

Let (M, d) be a piecewise flat surface without boundary, $V \subset M$ a finite set of points that contains all conical singularities.
Let T_D be the Delaunay tessellation of M and $T_D^\Delta \in \mathcal{T}_{M,V}$ some Delaunay triangulation of T_D. Recalling (6.3) we see that for an edge $(ij) \in E$ we have

$$\nu(ij) = 0 \;\Leftrightarrow\; \alpha_{ij} + \alpha_{ji} = \pi,$$

which is the case for circular quadrilaterals. So the edges in T_D^Δ coming from triangulating circular polygons of the Delaunay tessellation T_D have zero weights. The weights of edges on the boundary of circular polygons of T_D are independent of the chosen triangulation as can be seen in Figure 7.20.

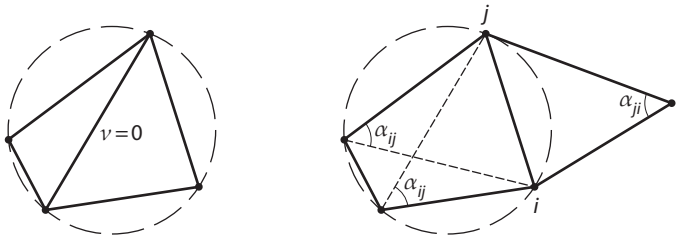

Figure 7.20. Cotan-weights of the Delaunay tessellation. (left) An edge coming from triangulating circular polygons has zero cotan-weight. (right) The cotan-weight of an edge on the boundary of a circular polygon does not depend on the triangulation.

So the cotan-weights are well-defined on the edges of the Delaunay tessellation.

Definition 7.8 (discrete Laplace-Beltrami operator)**.** Let (M, d) be a piecewise flat surface without boundary, $V \subset M$ a finite set of points that contains all conical singularities.
Let T_D be the Delaunay tessellation of M.
Then the *discrete Laplace-Beltrami operator* of (M, d) is defined by

$$\Delta f(i) = \sum_{e=(ij)\in E(T_D)} \nu(e)\,(f(i) - f(j))$$

for any function $f : V \to \mathbb{R}$.
The corresponding Dirichlet energy on (M, d) is defined by

$$E(f) \coloneqq \frac{1}{2} \sum_{e=(ij)\in E(T_D)} \nu(e)\,(f(i) - f(j))^2\,,$$

where ν are the cotan-weights as defined in (6.2) coming from any Delaunay triangulation $T_D^\Delta \in \mathcal{T}_{M,V}$ of T_D.

Remark 7.9.

- The sum can be taken over all edges of any Delaunay triangulation as we have seen above.
  The notion of neighboring vertices might differ from the one given by the "extrinsic triangulation" of a polyhedral surface in $\mathbb{R}^N$. Also triangles of a Delaunay triangulation are not necessarily planar in $\mathbb{R}^N$ anymore.

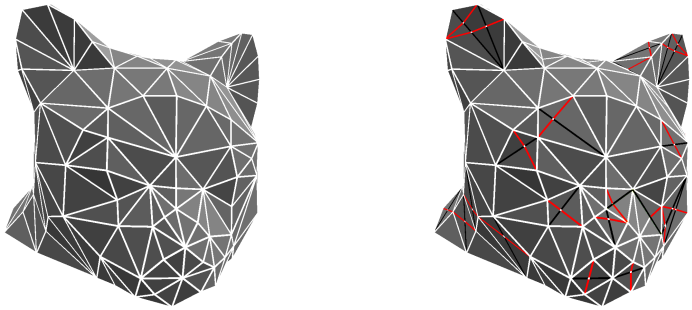

Figure 7.21. Simplicial cat. (left) Triangulation coming from the simplicial surface. (right) Delaunay triangulation (white and red edges).

- The Laplace-Beltrami operator is a well-defined property of the Delaunay tessellation T_D which is uniquely determined by (M, d) and the vertex set V. So we have defined a unique discrete Laplace-Beltrami operator of the piecewise flat surface (M, d), which is determined by the polyhedral metric only, i.e. invariant w.r.t. isometries.
- In Proposition 7.10 we have seen that all weights of the Delaunay triangulation are non-negative. With above considerations we can now conclude that all weights of the Delaunay tessellation are positive. So for the discrete Laplace-Beltrami operator we can apply the results of the theory of discrete Laplace operators with positive weights. We are assured to have the maximum principle and unique minima of the Dirichlet energy.

7.5 Simplicial minimal surfaces (II)

Having the discrete Laplace-Beltrami operator we can improve the definition of simplicial minimal surfaces of Section 6.4.

Definition 7.9 (simplicial minimal surface)**.** Let $f : \mathcal{S} \to S \subset \mathbb{R}^N$ be a simplicial surface and T its triangulation. Then

$$\begin{aligned} S \text{ minimal (in the wide sense)} &:\Leftrightarrow \Delta f = 0 \\ S \text{ minimal (in the narrow sense)} &:\Leftrightarrow \Delta f = 0 \text{ and } T \text{ is Delaunay,} \end{aligned}$$

where in both cases Δ is the discrete Laplace-Beltrami operator of S.

Remark 7.10.

- The Laplace-Beltrami operator coincides with the cotan-Laplace operator only in the narrow definition. So only in this case the surface is actually a critical point of the area functional.
- The Laplace-Beltrami operator has all positive weights. If f is harmonic the maximum principle (Proposition 6.8) implies that any vertex point $f(i)$ lies in the convex hull of its neighbors:

  $$f(i) \in \operatorname{conv}\{f(j) \in \mathbb{R}^n \mid (ij) \in E(T_D)\},$$

  where neighbors are determined by the Delaunay tessellation T_D of S.

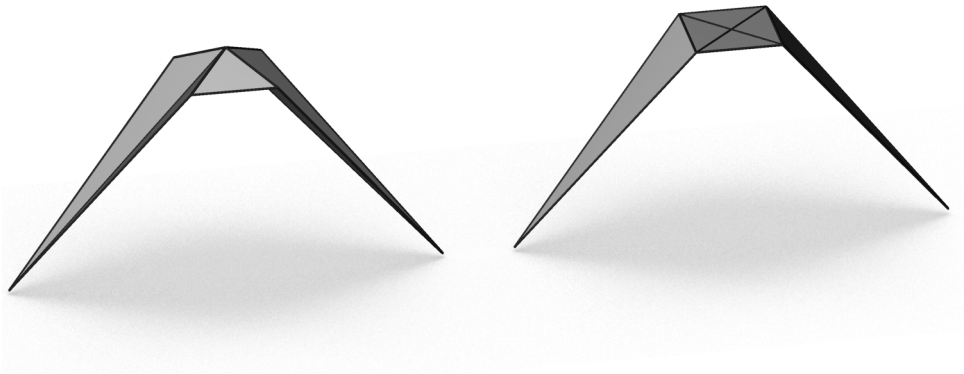

Figure 7.22. (left) Simplicial surface which is minimal with respect to the definition of Section 6.4. It violates the maximum principle. (right) Corresponding minimal surface (in the narrow sense) with respect to Definition 7.9. It satisfies the maximum principle. By "corresponding" we mean that it is obtained by applying Algorithm 7.23 to the left surface.

In the wide definition the neighbors satisfying the maximum principle might be different from the ones given by the triangulation of S, where in the narrow definition they coincide.

This new definition leads to the following algorithm producing minimal surfaces in the narrow sense, if it converges.

Data: Simplicial surface $f : \mathcal{S} \to S \subset \mathbb{R}^N$ with triangulation T.
Result: Simplicial minimal surface in the narrow sense.
while S *is not minimal in the narrow sense* **do**
  Compute Delaunay triangulation $\tilde{T}$ of S (use Algorithm 7.13);
  Compute $\tilde{f}$ such that
$$\Delta_{(S,\tilde{T})}\tilde{f} = 0,$$
  which defines a new simplicial surface $\tilde{S}$;
  Replace S by the new surface $\tilde{S}$;
  Replace T by $\tilde{T}$;
end

Figure 7.23. Simplicial minimal surface algorithm (with intrinsic discrete Laplace-Beltrami-operator and change of combinatorics).

Remark 7.11. The state of the algorithm is determined by the simplicial surface S and its triangulation T.
In each step of the while-loop we replace

$$(S, T) \leftarrow (\tilde{S}, \tilde{T}),$$

where $\tilde{T}$ is the Delaunay triangulation of S which might not be Delaunay anymore for $\tilde{S}$.
Besides using the intrinsic Laplace-Beltrami operator the fundamental difference to Algorithm 6.5 is the change of combinatorics in each step.

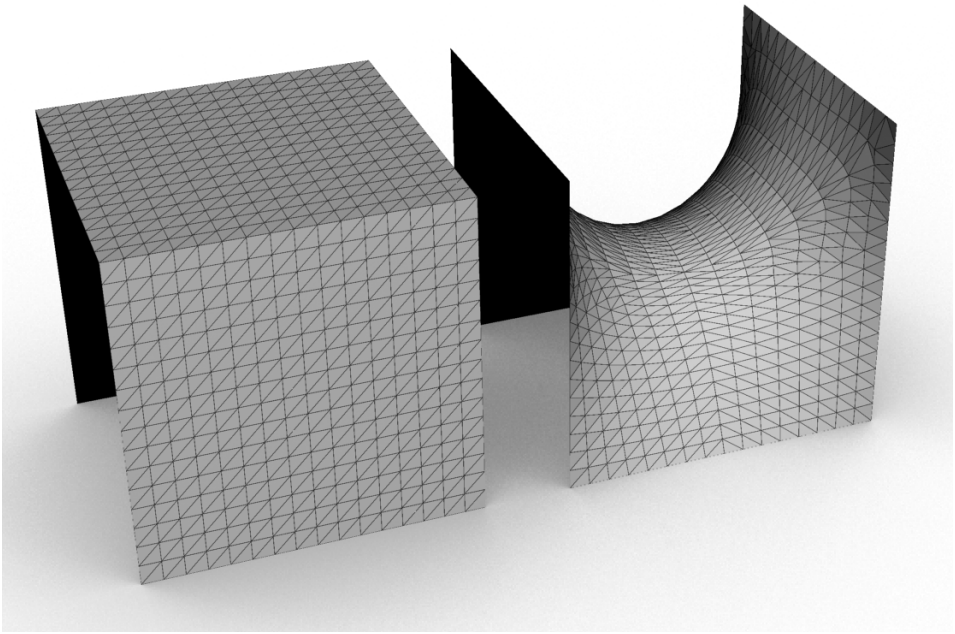

Figure 7.24. Simplicial minimal surface from Algorithm 7.23.

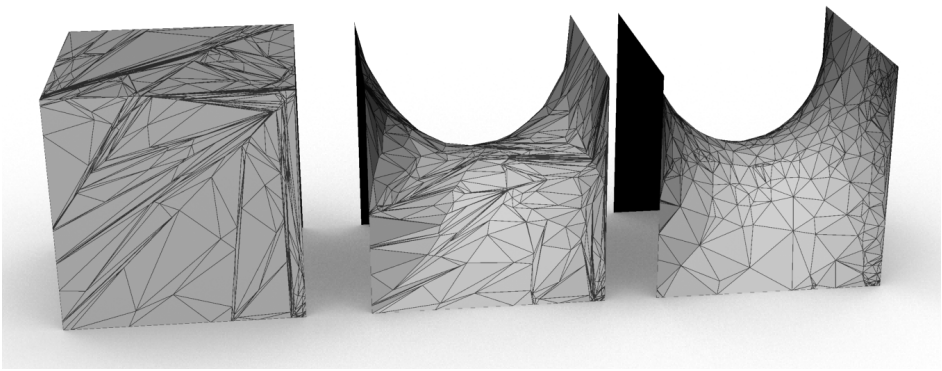

Figure 7.25. Using the intrinsic Laplace-Beltrami operator with and without change of combinatorics. Starting with a random triangulation the change becomes particularly eminent. (left) Random start triangulation. (middle) Result of Algorithm 7.23 without change of combinatorics. (right) Result of Algorithm 7.23 with change of combinatorics.

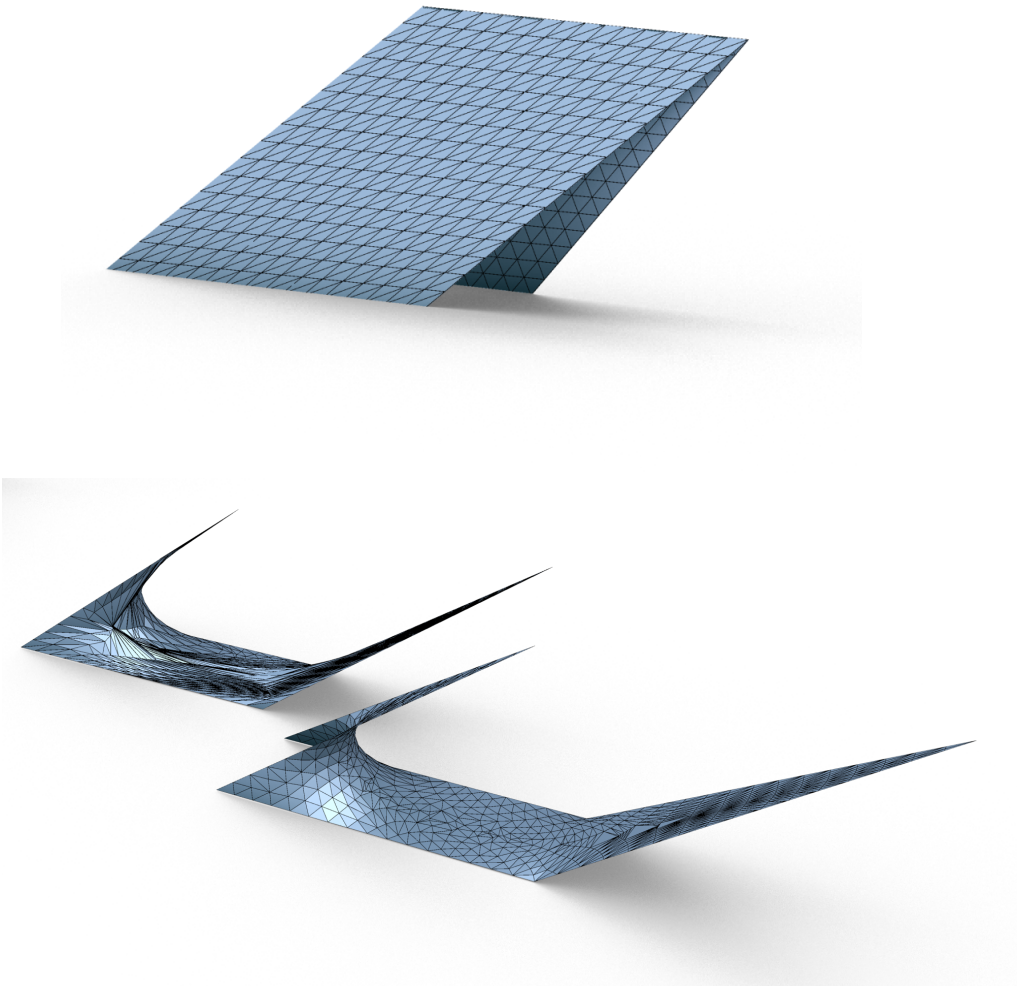

Figure 7.26. Comparing intrinsic and extrinsic Laplace-Beltrami operator. We start with a triangulation which is not suitable for the resulting minimal surface. (top) Start triangulation. (bottom left) Result of applying Algorithm 6.5 for some time. No convergence! (bottom right) Result of Algorithm 7.23.

Part III
Appendix

A The Heisenberg magnet model

We have seen the Heisenberg flow playing an important role in the characterization of elastica (in the smooth and in the discrete case, see Section 3).
The Heisenberg flow (2.4) as it acts on the tangent vectors

$$\partial_t T = (\partial_t \gamma)' = (\gamma'' \times \gamma')' = \gamma''' \times \gamma' = T'' \times T \tag{A.1}$$

is also obtained as the equation of motion in the continuous *Heisenberg magnet model* also known as the continuous *Heisenberg chain*.

Although later seen to be a rather naive discretization the following discrete model might motivate the continuous Heisenberg chain. Consider a system of N classical spins $S_k = (S_k^1, S_k^2, S_k^3) \in \mathbb{S}^2$ on a (closed) chain, i.e. $S : \mathbb{Z}_N \to \mathbb{S}^2$. We introduce isotropic nearest neighbor interactions by defining the Hamilton function

$$H(S_1, \ldots, S_N) = -J \sum_{i=1}^{N} \langle S_i, S_{i+1} \rangle,$$

with interaction coefficient $J \neq 0$.[40] So a configuration with many aligned neighboring spins has low energy while a configuration with many anti-parallel next neighbors has high energy. To make each spin behave like a magnetic momentum we introduce an angular momentum-like Poisson structure by the following relations:

$$\{S_i^\alpha, S_j^\beta\} = \sum_\gamma \varepsilon^{\alpha\beta\gamma} \delta_{ij} S_j^\gamma$$

for $\alpha, \beta = 1, 2, 3$, $i, j = 1, \ldots, N$, where $\varepsilon_\gamma^{\alpha\beta}$ and δ_{ij} are the Levi-Civita and Kronecker symbols.
Let us compute the time flow of this Hamiltonian system.

$$\partial_t S_i^\alpha = \{S_i^\alpha, H\} = -J \sum_{j,\beta} \{S_i^\alpha, S_j^\beta S_{j+1}^\beta\}.$$

With

$$\begin{aligned} \{S_i^\alpha, S_j^\beta S_{j+1}^\beta\} &= \{S_i^\alpha, S_j^\beta\} S_{j+1}^\beta + S_j^\beta \{S_i^\alpha, S_{j+1}^\beta\} \\ &= \sum_\gamma (\varepsilon^{\alpha\beta\gamma} \delta_{ij} S_i^\gamma S_{j+1}^\beta + \varepsilon^{\alpha\beta\gamma} \delta_{i,j+1} S_i^\gamma S_j^\beta) \end{aligned}$$

we obtain

$$\partial_t S_i^\alpha = -J \sum_{\beta,\gamma} \varepsilon^{\alpha\beta\gamma} S_i^\gamma (S_{i+1}^\beta + S_{i-1}^\beta),$$

so for the spin vectors S_i

$$\partial_t S_i = \{S_i, H\} = J S_i \times (S_{i+1} + S_{i-1}). \tag{A.2}$$

[40] Notice that we introduced periodic boundary conditions when setting $N + 1 = 1$.

Uniformly refining the chain on the interval $[0, N]$ while keeping the length of the spins unit, the smooth limit is a continuous chain of spins $S : [0, N] \to \mathbb{S}^2$ with periodicity $S(x + N) = S(x)$.
Introducing appropriate scaling the smooth limit of the equations of motion (A.2) is

$$\partial_t S = JS \times S'', \tag{A.3}$$

which is the Heisenberg flow as seen in (A.1) with $J = -1$. A corresponding Hamilton function is

$$H[S] = \frac{J}{2} \int_0^L \left\|S'(x)\right\|^2 \mathrm{d}x,$$

with Poisson structure given by

$$\{S^\alpha(x), S^\beta(y)\} = \sum_\gamma \varepsilon^{\alpha\beta\gamma} \delta(x - y) S^\gamma(x),$$

where δ denotes the delta-distribution.

These all are smooth limits of the discrete equations above.
Indeed, let us start with the Hamilton function. Taking $x = \varepsilon i$ we get

$$\begin{aligned}\langle S_i, S_{i+1}\rangle &= \langle S(x), S(x + \varepsilon)\rangle \\ &= \langle S(x), S(x), \varepsilon S'(x) + \frac{1}{2}\varepsilon^2 S''(x) + o(\varepsilon^2)\rangle \\ &= 1 + \frac{1}{2}\varepsilon^2 \langle S(x), S''(x)\rangle + o(\varepsilon^2).\end{aligned}$$

From the orthogonality of $S(x)$ and $S'(x)$ we get

$$0 = \frac{\mathrm{d}}{\mathrm{d}x}\langle S(x), S'(x)\rangle = \left\|S'(x)\right\|^2 + \langle S(x), S''(x)\rangle.$$

Altogether while replacing H by $H + N$ we obtain[41]

$$\begin{aligned}H &= \frac{J}{2}\varepsilon^2 \sum \left\|S'(x)\right\|^2 + o(\varepsilon^2) \\ &= \frac{J}{2}\varepsilon \int \left\|S'(x)\right\|^2 \mathrm{d}x + o(\varepsilon).\end{aligned}$$

So we have to scale the Hamilton function by $\frac{1}{\varepsilon}$ upon taking the limit.
The scaling of the Hamilton function corresponds to replacing the equations of motion (A.2) by

$$\partial_t S_i = \left\{S_i, \frac{1}{\varepsilon} H\right\} = \frac{J}{\varepsilon} S_i \times (S_{i+1} + S_{i-1}).$$

So we get

$$\begin{aligned}\partial_t S(x) &= \frac{J}{\varepsilon} S(x) \times (S(x + \varepsilon) + S(x - \varepsilon)) \\ &= \frac{J}{\varepsilon} S(x) \times (2S(x) + \varepsilon^2 S''(x) + o(\varepsilon^2)) \\ &= J\varepsilon S(x) \times S''(x) + o(\varepsilon),\end{aligned}$$

[41] Already knowing the result we might get this immediately from observing

$$1 - \langle S_i, S_{i+1}\rangle = \frac{1}{2}\langle S_{i+1} - S_i, S_{i+1} - S_i\rangle = \frac{1}{2}\varepsilon^2 \left\|S'(x)\right\|^2 + o(\varepsilon^2).$$

which still needs rescaling to get a non-trivial limit. Since the Hamilton function is already fixed this can be achieved by rescaling the time. Replacing t by εt we obtain (A.3).
The limit of the Poisson structure can be obtained similarly.

Remark A.1. The continuous Heisenberg chain is integrable, see e.g. [FT87]. In Proposition 2.2 we see that the discrete flow (A.2) does not commute with the tangent flow which indicates that the naive discrete model we used to motivate the continuous Heisenberg chain might actually not be an appropriate discretization rather than (2.14) which is discrete integrable.
With the notation from this chapter this is

$$\partial_t S_i = 2JS_i \times \left(\frac{S_{k+1}}{1 + \langle S_{k+1}, S_k \rangle} + \frac{S_{k-1}}{1 + \langle S_k, S_{k-1} \rangle} \right),$$

which is associated with the Hamilton function

$$H = -2 \sum_i \log \left(\frac{1 + \langle S_i, S_{i+1} \rangle}{2} \right).$$

Acknowledgements

Many thanks to

- Alexander Bobenko for his advice and support.
- Thilo Rörig, Stefan Sechelmann, Emanuel Huhnen-Venedey, Lara Skuppin and Boris Springborn for discussions and answering questions.
- Alexandra Haack for producing beautiful vector graphics as well as Emanuel Huhnen-Venedey for providing some of his old ones.
- Kristoffer Josefsson and Stefan Sechelmann for provinding the rendered graphics showing results of the simplicial minimal surface algorithms.
- Max. Techter, Lara Skuppin, Isabella Thiesen and Jim Lobsien for proof-reading.

References

[Arn89] Vladimir I. Arnol'd. *Mathematical Methods of Classical Mechanics*. Graduate Texts in Mathematics. Springer, 1989. ISBN: 9780387968902.

[BI08] Alexander I. Bobenko and Ivan Izmestiev. "Alexandrov's theorem, weighted Delaunay triangulations, and mixed volumes". In: *Annales de l'Institut Fourier* 58.2 (2008), pp. 447–505. DOI: 10.5802/aif.2358.

[Bob14] Alexander I. Bobenko. "Geometry 2 - Variational Principles in Discrete Differential Geometry". University Lecture. 2014.

[BS07] Alexander I. Bobenko and Boris A. Springborn. "A Discrete Laplace-Beltrami Operator for Simplicial Surfaces". English. In: *Discrete and Computational Geometry* 38.4 (2007), pp. 740–756. ISSN: 0179-5376. DOI: 10.1007/s00454-007-9006-1.

[FT87] Ludwig D. Faddeev and Leon A. Takhtajan. *Hamiltonian Methods in the Theory of Solitons*. English. Springer Series in Soviet Mathematics. Springer Berlin Heidelberg, 1987. ISBN: 978-3-540-69843-2. DOI: 10.1007/978-3-540-69969-9.

[FW99] George K. Francis and Jeffrey R. Weeks. "Conway's ZIP Proof". In: *The American Mathematical Monthly* 106.5 (May 1999), pp. 393–399. URL: http://www.jstor.org/stable/2589143.

[Hof08] Tim Hoffmann. *Discrete Differential Geometry of Curves and Surfaces*. Vol. 18. COE Lecture Note. Faculty of Mathematics, Kyushu University, 2008.

[MS91] Howard Masur and John Smillie. "Hausdorff Dimension of Sets of Nonergodic Measured Foliations". In: *Annals of Mathematics* 134.3 (Nov. 1991), pp. 455–543. ISSN: 0003-486X. DOI: 10.2307/2944356.

[PP93] Ulrich Pinkall and Konrad Polthier. "Computing discrete minimal surfaces and their conjugates". In: *Experiment. Math.* 2.1 (1993), pp. 15–36. URL: http://projecteuclid.org/euclid.em/1062620735.

[Sec] Stefan Sechelmann. *Homepage*. URL: http://www.sechel.de.

[Tur81] Lukasz A. Turski. "Hydrodynamical description of the continuous Heisenberg chain". In: *Canadian Journal of Physics* 59.4 (1981), pp. 511–514. DOI: 10.1139/p81-065.